

8-2012

TRANSCRIPTIONAL AND POST- TRANSLATIONAL MECHANISMS CONTRIBUTE TO MAINTENANCE OF REST IN NEURAL TUMORS

Akanksha Singh

Follow this and additional works at: http://digitalcommons.library.tmc.edu/utgsbs_dissertations

 Part of the [Medicine and Health Sciences Commons](#)

Recommended Citation

Singh, Akanksha, "TRANSCRIPTIONAL AND POST-TRANSLATIONAL MECHANISMS CONTRIBUTE TO MAINTENANCE OF REST IN NEURAL TUMORS" (2012). *UT GSBS Dissertations and Theses (Open Access)*. Paper 289.

This Dissertation (PhD) is brought to you for free and open access by the Graduate School of Biomedical Sciences at DigitalCommons@The Texas Medical Center. It has been accepted for inclusion in UT GSBS Dissertations and Theses (Open Access) by an authorized administrator of DigitalCommons@The Texas Medical Center. For more information, please contact laurel.sanders@library.tmc.edu.

**TRANSCRIPTIONAL AND POST-TRANSLATIONAL MECHANISMS CONTRIBUTE
TO MAINTENANCE OF REST IN NEURAL TUMORS**

by

Akanksha Singh, B.A.

APPROVED:

Vidya Gopalakrishnan, Ph.D., Supervisory Professor

Jaroslav Aronowski, Ph.D.

Andrew Bean, Ph.D.

Oliver Bogler, Ph.D.

Patrick Zweidler-McKay, M.D., Ph.D.

APPROVED:

George M. Stancel, Ph.D., Dean, The University of Texas
Graduate School of Biomedical Sciences at Houston

**TRANSCRIPTIONAL AND POST-TRANSLATIONAL MECHANISMS CONTRIBUTE
TO MAINTENANCE OF REST IN NEURAL TUMORS**

A

DISSERTATION

Presented to the Faculty of
The University of Texas
Health Science Center at Houston
and
The University of Texas
M. D. Anderson Cancer Center
Graduate School of Biomedical Sciences
in Partial Fulfillment

of the Requirements

for the Degree of

DOCTOR OF PHILOSOPHY

By

Akanksha Singh, B.A.

Houston, Texas

August 2012

Dedication

To my mom...

An example of integrity and resilience, who has supported me in everything that I wanted to accomplish, and taught me to work hard and reach for the stars... and that life may get me down, but what counts is that I get back up and try again...

Acknowledgements

First and foremost, I would like to thank my advisor, Dr. Vidya Gopalakrishnan, for allowing me to work in her lab and supporting me all these years. I am grateful for her input and encouragement through the years. I have learned a lot from her, and feel prepared for what lies ahead. Even during her grant submissions, she has always managed to be available if I needed her. Thanks Vidya!

I would also like to thank all my committee members, Dr. Jaroslaw Aronowski, Dr. Andrew Bean, Dr. Oliver Bogler, and Dr. Patrick Zweidler-Mckay, for their invaluable support and insight into my project. Thank you for taking the time to serve on my committee, and helping me grow. Big thanks to Dr. Zweidler-McKay for his willingness to share reagents, constructs, and ideas, as well as to Dr. Bogler for allowing me the use of his equipment for experiments and personnel (Laura Gibson, B.S.) for technical advice. I would also like to thank my past committee members, Dr. Sharon Dent, Dr. Joseph McCarty, Dr. Thomas Westbrook, and Dr. Peter Zage, for serving on my committee and for their guidance.

Gopalakrishnan lab has been my home for the past few years, and all the members of the lab have been great to work with. Each one has taught me something new, and I have truly enjoyed our interactions through these past years. I would especially like to thank Dr. Pete Taylor for answering my endless questions every day, for training me with such patience and diligence, and for being my go-to person for all things science related. I could not have done it without him! Monica Gireud allowed me the opportunity to train her when she first joined the lab, and it was a great learning experience for me as well. I would also like to thank Dr. Pete Taylor and Dr. Chris Rokes for their contributions to the work presented in this dissertation. It has been a pleasure working with both of them.

Of course, a big thanks to the Pediatrics department! Everyone has been incredibly helpful and friendly. Here, a special thanks to Dr. Sankaranarayanan Kannan and Dr. Srinivias Somanchi for all the technical advice and reagents they have provided over the years. I would also like to acknowledge all my friends in the fellows office who have been have been a constant source of companionship and support (especially Dr. Krithi Rao-Bindal and Dr. Mandy Hall).

Finally, I would like to thank my family and friends, especially Jonathan Verma for his constant support and encouraging words. I am forever grateful to my parents for their selfless

and tireless effort in raising me, and providing me with the confidence and the means to strive to be the best that I can be while staying honest and true to myself. My brother... my partner in crime...has always been available when I really needed someone to talk to and spend time with.

**TRANSCRIPTIONAL AND POST-TRANSLATIONAL MECHANISMS CONTRIBUTE
TO MAINTENANCE OF REST IN NEURAL TUMORS**

Publication No._____

Akanksha Singh, B.A.

Supervisory Professor: Vidya Gopalakrishnan, Ph.D.

The *RE-1* silencing transcription factor (REST) is an important regulator of normal nervous system development. It negatively regulates neuronal lineage specification in neural progenitors by binding to its consensus *RE-1* element(s) located in the regulatory region of its target neuronal differentiation genes. The developmentally coordinated down-regulation of REST mRNA and protein in neural progenitors triggers terminal neurogenesis.

REST is overexpressed in pediatric neural tumors such as medulloblastoma and neuroblastoma and is associated with poor neuronal differentiation. High REST protein correlate with poor prognosis for patients with medulloblastoma, however similar studies have not been done with neuroblastoma patients. Mechanism(s) underlying elevated REST levels medulloblastoma and neuroblastoma are unclear, and is the focus of this thesis project. We discovered that transcriptional and post-translational mechanisms govern REST mis-regulation in medulloblastoma and neuroblastoma. In medulloblastoma, *REST* transcript is aberrantly elevated in a subset of patient samples. Using loss of function and gain of function experiments, we provide evidence that the Hairy Enhancer of Split (HES1) protein represses *REST* transcription in medulloblastoma cell lines, modulates the expression of neuronal differentiation genes, and alters the survival potential of these cells *in vitro*.

We also show that REST directly represses its own expression in an auto-regulatory feedback loop. Interestingly, our studies identified a novel interaction between REST and HES1. We also observed their co-occupancy at the *RE-1* sites, thereby suggesting potential for co-regulation of *REST* expression.

Our pharmacological studies in neuroblastoma using retinoic acid revealed that REST levels are controlled by transcriptional and post-transcriptional mechanisms. Post-transcriptional mechanisms are mediated by modulation of E3 ligase or REST, SCF^{β-TRCP}, and contribute to resistance of some cells to retinoic acid treatment.

Table of Contents

Approval Signatures.....	i
Title Page.....	ii
Dedication.....	iii
Acknowledgements.....	iv
Abstract.....	vi
Table of Contents.....	vii
List of Figures.....	xi
List of Tables.....	xiv
Chapter 1: Introduction	1
Medulloblastoma	2
Classification.....	2
Origin.....	3
Genetic vs epigenetic mechanisms in medulloblastoma etiology.....	4
Mouse models.....	6
Neuroblastoma	8
Classification.....	9
Origin.....	9
REST	11
Discovery.....	11
Structure.....	12
Mechanism of REST mediated repression.....	12
Target genes and function.....	15
Expression.....	17
Regulation.....	18
REST in neural tumors.....	19
REST in non-neural tumors.....	20
Aim of the Study	22
Chapter 2: <i>REST</i> is transcriptionally mis-regulated in medulloblastoma patient samples	23
Rationale	24

Results	25
Summary	29
Chapter 3: HES1 regulates <i>REST</i> expression	30
Rationale	31
HES1 background	33
Structure.....	33
Mode of repression.....	33
Function in the brain.....	35
Cross-talk between HES1 and other pathways.....	35
HES1 and medulloblastoma.....	36
Results	38
HES1 levels in medulloblastoma tumor samples and cell lines.....	38
HES1 binds to <i>REST</i> 5' upstream region.....	39
HES1 represses <i>REST</i> expression in medulloblastoma cells.....	40
HES1-dependent modulation of <i>REST</i> transcription alters <i>REST</i> target gene expression.....	43
Interference with HES1 activity provides a survival advantage to DAOY cells....	45
Anchorage independent growth assay.....	47
Summary	50
Chapter 4: <i>REST</i> regulates its own transcription by an auto-regulatory loop	51
Rationale	52
Results	53
<i>REST</i> binds to the <i>RE-1</i> site in the <i>REST</i> 5' upstream region.....	53
<i>REST</i> directly represses its own expression via an auto-regulatory feedback loop.....	54
Interference with <i>REST</i> activity does not provide a survival advantage to DAOY cells.....	58
Summary	60
Chapter 5: HES1 and <i>REST</i> co-regulate of <i>REST</i> transcription	61
Rationale	62
Results	63
HES1 and <i>REST</i> bind to <i>RE-1</i> sites in <i>REST</i> 5' upstream region.....	63

HES1 and REST co-occupy <i>RE-1</i> sites of <i>REST</i> 5' upstream region.....	66
HES1 and REST interact in DAOY cells.....	67
Interfering with REST activity in the absence of HES1 increases <i>REST</i> transcription.....	69
REST does not bind to <i>REST</i> in the absence of HES1.....	70
HES1 and REST co-repress <i>REST</i> transcription.....	72
Summary	75
Chapter 6: Retinoic acid regulates REST protein by modulation of SCF^{β-TRCP}	76
Rationale	77
Results	78
Maintenance REST protein in neuroblastoma patient samples and cell lines.....	78
Differential expression of REST is observed in retinoic acid sensitive, SK-N-SH, versus retinoic acid insensitive, SK-N-AS, cells.....	80
Retinoic acid treatment leads to decreased REST protein levels in SK-N-SH, but not SK-N-AS cells.....	82
REST transcription increases upon retinoic acid treatment in both SK-N-SH and SK-N-AS cells.....	86
Retinoic acid treatment leads to an increase in SCF ^{β-TRCP} mRNA and protein in SK-N-SH cells, but not SK-N-AS cells.....	89
SCF ^{β-TRCP} protein is maintained in a subset of neuroblastoma patient samples.....	90
Ectopic expression of SCF ^{β-TRCP} in SK-N-AS cells leads to increased interaction with REST, REST ubiquitination, and decreased REST protein.....	91
Summary	95
Chapter 7: Discussion, conclusions, and future directions	96
Discussion	97
REST is important for normal neurogenesis and medulloblastoma pathology.....	97
<i>REST</i> is transcriptionally mis-regulated in medulloblastoma patient samples.....	97
HES1 represses <i>REST</i> expression.....	98
REST represses its own transcription in an auto-regulatory loop.....	101
REST-HES1 co-repress <i>REST</i> transcription.....	103
Retinoic acid regulates REST protein via modulation of SCF ^{β-TRCP}	106
Conclusions	110

Future Directions	113
Chapter 8: Materials and Methods	117
References	139
Vita	152

List of Figures

Figure1: Structure of REST.....	12
Figure2: REST repression complex.....	13
Figure3: <i>REST</i> expression is aberrant in medulloblastoma patient samples.....	26
Figure 4: Location of <i>N-boxes</i> on the 5' upstream region of <i>REST</i>	32
Figure 5: Structure of HES1.....	33
Figure 6: Two modes by which HES1 represses its target gene expression.....	34
Figure 7: HES1 mRNA and protein levels in medulloblastoma cells compared to normal cerebellum.....	38
Figure 8: HES1 binds to 5' upstream region of <i>REST</i> in medulloblastoma cells.....	40
Figure 9: Structure of HES1 constructs.....	41
Figure 10: Modulation of HES1 affects <i>REST</i> transcription in medulloblastoma cells.....	42
Figure 11: Modulation of <i>REST</i> via HES1 affects expression of differentiation genes in medulloblastoma cells.....	44
Figure 12: HES1 interference provides a survival advantage, while HES1 overexpression is disadvantageous to cell survival.....	47
Figure 13: Treatment with reagents lead to a decrease in anchorage independent growth potential of MB01110 cells.....	48
Figure 14: <i>RE-1</i> sites on the 5' upstream region of <i>REST</i>	52
Figure 15: REST binds to the 5' upstream region of <i>REST</i> in medulloblastoma cells.....	53
Figure 16: Structure of full-length REST and REST-DBD.....	55
Figure 17: Countering REST activity represses <i>REST</i> transcription in medulloblastoma cells..	56
Figure 18: Structure of the <i>REST</i> luciferase construct.....	57
Figure 19: Mutating <i>RE-1</i> sites leads to increased luciferase activity	58
Figure 20: No change in cell survival is observed upon REST interference.....	59
Figure 21: <i>RE-1</i> sites and <i>N-box</i> on the 5' upstream region of <i>REST</i>	62
Figure 22: HES1 binds to the <i>RE-1</i> sites in 5' upstream region of <i>REST</i> in medulloblastoma cells.....	63
Figure 23: HDAC1 and HDAC2 bind to the <i>RE-1</i> sites in 5' upstream region of <i>REST</i> in medulloblastomas cells.....	66
Figure 24: HES1 and REST co-occupy <i>RE-1</i> sites in DAOY cells.....	67

Figure 25: HES1 and REST interact in DAOY cells.....	68
Figure 26: Countering REST activity represses <i>REST</i> transcription in the absence of HES1...	70
Figure 27: REST does not bind to 5' upstream region of <i>REST</i> in the absence of HES1.....	71
Figure 28: Structure of the <i>REST</i> luciferase constructs.....	73
Figure 29: Mutating <i>N-box</i> and <i>RE-1</i> sites leads to increased luciferase activity as compared to either mutation alone.....	74
Figure 30: REST protein is overexpressed in neuroblastoma patient samples and cell lines.....	79
Figure 31: SK-N-SH cells have lower levels of REST mRNA and protein as compared to SK-N-AS cells.....	81
Figure 32: Differentiation like morphological changes observed in retinoic acid treated SK-N-SH but not SK-N-AS cells.....	83
Figure 33: No significant changes in Sub-G1 DNA content of retinoic acid treated SK-N-SH and SK-N-AS cells.....	84
Figure 34: Retinoic acid treatment leads to decline in REST protein and increased differentiation in SK-N-SH, but not SK-N-AS cells.....	85
Figure 35: Retinoic acid treatment leads to up-regulation of <i>REST</i> transcription in both SK-N-SH and SK-N-AS cells.....	87
Figure 36: MG-132 treatment in the presence of retinoic acid leads to an accumulation of REST protein in SK-N-SH and SK-N-AS cells.....	88
Figure 37: Retinoic acid treatment leads to increased SCF ^{β-TRCP} mRNA and protein in SK-N-SH, but not SK-N-AS cells.....	89
Figure 38: SCF ^{β-TRCP} protein is overexpressed in a subset of neuroblastoma patient samples.....	90
Figure 39: Ectopic expression of SCF ^{β-TRCP} in SK-N-AS cells leads to decreased REST levels.....	92
Figure 40: Ectopic expression of SCF ^{β-TRCP} leads to increased ubiquitination of REST in SK-N-AS cells.....	93
Figure 41: Ectopic expression of SCF ^{β-TRCP} leads to increased SCF ^{β-TRCP} -REST interaction in SK-N-AS cells.....	94
Figure 42: Model of HES1 and REST co-repression of <i>REST</i> expression.....	106

List of Tables

Table 1: Sequence of <i>RE-1</i> sites and mutated <i>RE-1</i>	57
Table 2: Syber Green PCR mix.....	123
Table 3: List of qRT-PCR primers.....	125
Table 4: List of ChIP Primers.....	128
Table 6: List of Cloning Primers.....	134

Chapter 1: Introduction

Medulloblastoma

Medulloblastoma is the most common pediatric malignant brain cancer, with an incidence of ~0.6 per 100 000 children every year in the United States (1, 2). It is a primitive neuroectodermal tumor (PNET) that occurs in the cerebellum as well as the fourth ventricle and dorsal brainstem (3, 4). The standard treatment remains a combination of surgery, chemotherapy, and cranio-spinal radiation. The overall 5 year survival rate is 75-85%, however in high-risk cases survival is lowered to between 50-70% (5). Recurrence of the tumor is noted in 30% of the cases (5). Furthermore, because the cerebellum is still developing at the time of tumor presentation and treatment, neuro-cognitive problems arise and quality of life issues can continue even after the original tumor is resolved. The need for more targeted therapeutics with lower toxicity is apparent. Specific markers to better assess the aggressiveness of each individual patient's disease are also necessary to ensure the delivery of more targeted therapeutics while avoiding unnecessary exposure to overly invasive and aggressive treatments.

Classification

Original classification of medulloblastoma was based on histopathological analysis that divided the tumors into 4 general groups: classic, nodular/desmoplastic, anaplastic, and large cell anaplastic (LCA) (3). Although histologically distinct, these subgroups did not reliably predict presentation, prognosis, treatment, and deregulated pathways. Recent efforts by several groups towards molecular classification using high throughput DNA and RNA microarray analyses of medulloblastoma tumors have yielded four classes of medulloblastoma as well: WNT activation, SHH mutations, MYC overexpression, and undefined genetic anomalies, ranging from the best to the worst prognosis (2, 6-10). These classes correlate loosely to classic, desmoplastic, nodular, anaplastic, and large cell anaplastic histopathologic subtypes respectively although overlap across the histopathological classes still remains (2, 6-10). Since each of the molecular classes is different from the other in terms of presentation, prognosis, survival, and invasiveness, perhaps the molecular signature for each tumor can potentially be used to determine the type and aggressiveness of the treatment, thereby leading to a more targeted and personalized therapy for each patient. Mechanisms contributing to deregulation of

the pathways implicated in each of the molecular classes remain to be elucidated and provide an active area of research.

Origin

Although granule precursor cells (GPC) that comprise the external granule layer (EGL) of the cerebellum are canonically considered the cells of origin of medulloblastoma, recent studies have shown that they account for only the sonic hedgehog (SHH) medulloblastoma subtype (3, 9, 11, 12). The WNT subtype arises from the progenitor cells in the lower rhombic lip (LRL) and the dorsal brain stem (4). Not much is known about the origin of the other medulloblastoma subtypes, although recently the progenitors from the white matter have been suggested to give rise to the MYC subtype (3). Because the role of GPCs and SHH is extensively studied in medulloblastoma and normal brain development, it will dominate most of this section, followed by a brief description of the WNT subtype of medulloblastoma.

Discovery of the germline mutation of *PTCH* that is implicated in medulloblastoma, as well as the critical role of SHH in cerebellar development has sparked extensive research to study this pathway in the context of medulloblastoma pathology. Understanding the contribution of this pathway in normal cerebellar development is important for assessing the implications of its deregulation to medulloblastoma. In mice, cerebellar development begins during embryogenesis around E10 (approximately E20-22 in humans) and continues postnatally until P15 (second year of life in humans) (3, 11, 12). There are three germinal zones that give rise to distinct populations of cells in the cerebellum, with the second germinal zone in the upper rhombic lip (URL) producing the GPCs that form the EGL of the cerebellum (3). At birth, the EGL of the cerebellum is composed of GPCs that proliferate in response to the mitogen SHH, secreted by the Purkinje cells located in the layer beneath the EGL. Decline of the SHH pathway activity signals GPCs to stop proliferating and induces cell cycle exit. The GPCs then start differentiating and migrating down to the inner layers of the cerebellum to form the internal granule layer (IGL). As a result, the developed cerebellum does not contain an EGL, but a molecular layer which contains the axons of the differentiated neurons that migrated to the IGL, a Purkinje cell layer, and an IGL that is composed of the cell bodies of the differentiated neurons (11). However, the maintenance of EGL in a mouse model of medulloblastoma with constitutively active SHH signaling suggests that the failure to down-regulate SHH signaling in a developmentally appropriate manner leads to a bypass of the

normal differentiation program as well as continued proliferation EGL, which that may contribute to tumor formation (3, 11, 13).

WNT subtype of medulloblastoma arises from the progenitor cells in the LRL and the dorsal brain stem, and has genetic features and presentation that are distinct as compared to the SHH subtype (3). Whereas the SHH subtype mainly infiltrate the cerebellar hemispheres, WNT medulloblastomas are noted largely in the fourth ventricle infiltrating the dorsal brainstem (3). Furthermore, mutations in WNT pathway effector *catenin (cadherin-associated protein) beta 1 (Ctnnb1)* led to an aberrant collection of progenitor cells that migrated preferentially to the dorsal brainstem, thereby differentiating the normal differentiation program (3). However, no change was observed in GPC proliferation, cell cycle regulation, differentiation, or apoptosis in the URL, thereby highlighting the distinct origins and molecular pathways of the two tumor subtypes (3, 14). Disruption of p53 in the background of mutations in the SHH pathway has been previously shown to increase the tumor incidence with an earlier onset (14). Similarly, concurrent mutations of *p53* and *Ctnnb1* leads to tumor formation, but only in the fourth ventricle and dorsal brainstem, and not the cerebellum (3). Furthermore, these tumors matched WNT pathway human medulloblastoma tumors in mRNA and DNA microarray analyses (3).

Genetic vs. epigenetic mechanisms in medulloblastoma etiology

Genetic mutations that may contribute to medulloblastoma were established with the discovery of the germline *PTCH* mutation and mutations in adenomatous polyposis coli (APC) in patients with Gorlin syndrome and Turcot syndrome respectively, for in both of these diseases the patients have an increased incidence of medulloblastoma as compared to the general population (3, 11). However, these genetic mutations account for only 20-30% of the cases (3, 15, 16). Observed in 30-40% of medulloblastoma patients, deletion of *17p13.2* and *isochromosome 17q (i17q)* is the most common cytogenetic abnormalities reported (2, 15). Aberrant regulation and expression of many other molecules such as Notch, c-met, ERB-B, IGF, Gli, Mad3, Math1, BMI1 to name a few, have been reported, but exactly how these mechanisms contribute to medulloblastoma pathology remains unclear (1). The latter highlights the need to better delineate the individual roles of these molecules as well as their combined contribution to medulloblastoma pathogenesis.

Several molecules implicated in medulloblastoma have also been shown to be epigenetically deregulated. Epigenetic changes are alterations in gene expression in the absence of changes in DNA sequence. Chromatin consists of repeating nucleosomes, which are units of DNA wrapped around proteins known as histones (17). Nucleosomes can be arranged in an open conformation, called euchromatin, where DNA is accessible for transcription, or a closed conformation, known as heterochromatin, which is associated with gene silencing for the DNA is not available for active transcription (18, 19). Chromatin can be modified in many different mechanisms, for example via the addition or removal of acetyl and methyl groups from histones and/or DNA, and the type of modification as well as where the modification occurs determines whether it is an active or a repressive mark (18, 19). In general, acetylation is associated with euchromatin, while deacetylation is observed in heterochromatin. Types of histone methylation and demethylation, as well as the residues that are methylated and demethylated in a cell specific context indicates whether the modification signals active, repressive, or poised for transcription (18, 20). DNA methylation is usually associated with gene silencing (18, 20). Methylation, demethylation, acetylation, and deacetylation are some of the most commonly investigated modifications in cancer. Overall, hypomethylation of the genome of a cancer cell is observed as compared to a normal cell, which contributes to general genomic instability (21). In addition, promoter hypermethylation of specific genes (several tumor suppressors) occurs, which usually translates into silencing of these genes (21). Indeed altered methylation of 6% of CpG islands have been reported in medulloblastoma (21). Commonly hypermethylated genes in medulloblastoma tumors and cell lines include *HIC1*, *RAASF1A*, *CASP8*, *p16^{INK4a}*, and *MGMT* to name a few (21). Research is currently underway to determine if these epigenetic modifications can be potentially targeted therapeutically using histone deacetylase inhibitors and demethylating agents that have been approved as therapy for other cancers as well as novel compounds (22-24).

Although several genes have been shown to be epigenetically deregulated in medulloblastoma, not much is known about epigenetic regulators of gene expression in the brain or their contribution to medulloblastoma. Research in our laboratory is focused on this aspect of medulloblastoma biology, and especially on one specific epigenetic modulator of neurogenesis that also plays a role in medulloblastoma pathology called Repressor element-1 silencing transcription factor or neuron restrictive silencing factor (REST or NRSF) (25-28).

The current state of our understanding of REST in normal brain development and its role in medulloblastomagenesis is discussed in greater detail in **Chapter 1, Section 3**.

Mouse models

Since SHH remains the most extensively studied pathway in the context of medulloblastoma, most models of this disease are based on deregulated SHH signaling either by mutagenizing the components of SHH pathway itself, or by introducing other genetic alterations. The degree of penetrance of each model is different as they develop the tumor at different ages and rates. *Ptch* and *ND2:SmoA1*, both of which contain mutations in the SHH pathway, are the most widely used transgenic models of medulloblastoma.

The *Ptch* mouse model involves a heterozygous *Ptch* deletion, because homozygous deletion of *Ptch* is embryonic lethal. 14-19% of *Ptch*^{+/-} mice develop medulloblastoma by 5 weeks to 10 months of age (14, 29, 30). Furthermore, crossing *Ptch*^{+/-} mice with *p53*^{-/-} mice increases the incidence of medulloblastoma to 95%-100% by 4 weeks to 3 months. Although a *p53* mutation is not common in medulloblastoma, mis-regulation and/or mis-expression *p53* can lead to accumulation of cytogenetic abnormalities, which can synergize with the *Ptch* mutation to create a greater vulnerability for a higher tumor incidence as well as a more aggressive tumor.

ND2:SmoA1 mouse model was created by mutating *Smo* so that it is constitutively expressed under a cerebellar GPC specific *NeuroD2* (*ND2*) promoter, SHH signaling is thereby rendered constitutively active independent of the presence of the ligand (31). Most of these mice (80%) displayed granule cell hyperproliferation by 8 weeks, and 48% developed tumors by 6-12 months (31). Recently, a homozygous *Smo/Smo* model has also been developed where the mutagenic *Smo* is regulated by *ND2* promoter, but has a tumor incidence of 94% by 2 months and is the first model to also show leptomeningeal spread (32).

In light of the new molecular subgroups, two models of MYC driven medulloblastomas in the absence or interference with *p53* have been recently developed (33, 34). These tumors have similar gene expression analysis as human *MYC* medulloblastomas, and differ greatly from the other subgroups (33, 34). Furthermore, SHH antagonists do not affect proliferation and tumor forming potential *in vitro* or *in vivo*, whereas inhibitors of the PI3K pathway show a marked effect, again suggesting that these tumors are indeed distinct from other subtypes of medulloblastoma. This model also highlights the interactions between other molecular

pathways underscoring the complexity of medulloblastoma pathology (33, 34). As described previously, concurrent disruption of *Ctnnb1* and *p53* also give rise to a distinct WNT subtype of medulloblastoma that is different from other tumors in its presentation as well as its molecular signature (4).

The mouse models described above highlight the complicated cross-talk between major developmental pathways, for perturbations of components Notch and Wnt signaling are observed in SHH mouse models of medulloblastoma (31, 35). For example, up-regulation of Notch2 and HES5, which are components of the Notch pathway, was observed in the cerebella of *ND2:SmoA1* mice relative to control mice (31). Similarly, cerebella of *Ptch*^{+/-} mice displayed up-regulation of Wnt pathway components, including *Wnt1*, *Wnt8*, *mFrz3*, *mFrz4*, *mFrz7*, *mSfrp1*, *mSfrp2* and *Lef1*, relative to control cerebella (35). Brains of *Nestin*^{Cre};*Smo*^{n/c} mice, a model in which SHH signaling is down-regulated, also showed decreased expression of *Notch2*, *Jagged1*, *HES1*, *mSfrp1*, and *mFrz7* (Notch and Wnt signaling) relative to control brains (35). Since our lab focuses on the role of REST in medulloblastoma pathology, it would be interesting to study the interactions between REST and SHH, Notch, and WNT. The presence of such cross-talk suggests that targeting multiple pathways may be necessary for therapy.

Neuroblastoma

Neuroblastoma is the most common pediatric extra-cranial solid tumor. With an incidence of 10.2 cases per 1 million children under 15 years of age every year in the United States, it is responsible for 15% of childhood mortality, and has the highest mortality rate for infants with cancer (36-38). These tumors are found in the sympathetic nervous system tissues, usually in the adrenal medulla and paraspinal ganglia. With a very varied presentation, ranging from essentially asymptomatic tumors that spontaneously regress to severe and metastatic disease, the median age of diagnosis is 17 months (37). Standard of treatment varies over a wide range, reflecting the broad range of disease presentation, and includes surgical resection and chemotherapy, with the aggressiveness of chemotherapy regimen depending on the severity of the disease (36). The overall 5-year survival has improved with current therapies to 74%, but appreciable improvement has not been noted in patients with high risk disease (37).

Neuroblastoma has been associated with many chromosomal abnormalities, including which gain of chromosomes 2, parts of 17q, deletions of parts of the chromosomes 1p and 11q, and triploidy (39, 40). V-myc myelocytomatosis viral related oncogene, neuroblastoma derived (avian) (*MYCN*) amplification on chromosome 2 remains one of the most significant prognostic indicators (39, 41). Found in 25% of cases, it is a very poor prognostic indicator of the disease, correlating with survival rates of only 15-35% even in the presence of other positive prognostic indicators (36, 38). *MYCN* transgenic mice have been shown to spontaneously develop neuroblastoma, but variability in tumor incidence exists depending on the promoter used and the site of random integration (42). Interestingly, retinoic acid, used as maintenance treatment for high-risk patients, down-regulates *MYCN* expression and leads to neuronal differentiation in neuroblastoma cell line (38, 41). However, the mechanism underlying retinoic acid mediated differentiation of neuroblastoma remains unknown.

Activating mutations in *Anaplastic lymphoma kinase (Alk)* also have been shown to have prognostic value in neuroblastoma (41). Found in all cases of familial neuroblastoma and 8% of sporadic cases, *ALK*^{F1174L} is described as the most aggressive activating mutation. Interestingly, 8.9% of *MYCN* amplified tumors also display an activating ALK mutation, correlating with very poor survival (41). Wild-type as well as mutant ALK has been shown to increase *MYCN* transcription in neural and neuroblastoma cells (43). Furthermore,

overexpression of *MYCN* and *ALK*^{F1174L} in immortalized neural crest cultures are shown to cause tumors *in vivo* (44).

Classification

Current classification of neuroblastoma is based on histological subtypes that fall into four of peripheral neuroblastic tumors: neuroblastoma, ganglio-neuroblastoma intermixed, ganglioneuroma, nodular ganglioneuroblastoma (36, 37, 45). Neuroblastoma is Schwannian stroma poor, ganglioneuroblastoma intermixed is Schwannian stroma rich (36). Ganglioneuroma is Schwannian stroma dominant, and ganglioneuroblastoma is a composite of Schwannian stroma rich and poor regions (36). As with many other cancers, histological subtypes alone do not predict the prognosis, survival, or course of the disease, but complemented with other factors such as age of diagnosis, degree of differentiation, Schwannian stroma content, and mitosis-karyorrhexis index (MKI), they provide more predictive value (36). Degree of differentiation and a younger age of diagnosis are positive prognostic factors for neuroblastoma, ganglio-neuroblastoma intermixed, and ganglioneuroma (36, 45). Low to intermediate MKIs are associated with good prognosis, whereas high MKIs along with an undifferentiated status predict poor prognosis (36). Diagnosis under 18 months of age is also associated with good prognostic predictors with high overall survival and lower rates of remission, whereas tumors diagnosed in older children tend to be more aggressive with a worse prognosis (36). As mentioned above, *MYCN* is one of the few molecular markers that reliably correlates with poor prognosis in neuroblastoma, and is taken into account when determining the risk stratification of the patient (36).

Origin

Although neuroblastoma tumors can occur anywhere along the sympathetic axis, adrenal medulla is the most common site of occurrence, accounting for 50% of all tumors, while the rest are found in the chest, abdomen, and pelvis (37). Several lines of evidence have implicated neural crest cells as the origin of neuroblastoma. It occurs at the sites of sympatho-adrenal lineage specificity of neural crest cells (37, 46). Tumors that spontaneously regress are similar to sympathogonia, and finally, patterns of gene expression of the tumor are consistent with those of neural crest cells (37, 46, 47).

Neural crest cells are a transient multipotent population of progenitors located at the border between the neural plate and the non-neural ectoderm (47). As the neural plate closes, and the neural crest cells form the dorsal end of the neural plate, these cells go through epidermal to mesenchymal transition (EMT), where they detach from the neuroepithelium and migrate away from the in a rostro-caudal wave throughout the embryo (47). Neural tube induction is tightly regulated by critical developmental pathways such as fibroblast growth factor (FGF), WNT, Notch, and bone morphogenic protein (BMP) signaling (47). Once these cells migrate to their final destination, they give rise to a variety of different types of tissues depending on their location along the neuraxis, including dorsal root ganglia, sympathetic ganglia, adrenal medulla, cranio-facial cartilage, bone, connective tissue, cranial ganglia, pigment cells, enteric ganglia, and smooth muscle cells (47). The above mentioned developmental pathways, along with SHH, NGF mediated Trk receptor signaling, and several chromosomal abnormalities have been implicated in neuroblastoma, although the exact mechanism as to how these pathways converge to contribute to tumorigenesis remains unknown (47).

Additionally, as with most cancers, epigenetic modulation of 75 genes has been described in primary neuroblastoma as well as cell lines (48). Altered methylation of several genes such as RASSF1A, CASP8, TNFRS10D, HOX1A to name a few have been reported in primary neuroblastoma tumors (48). Several studies have attempted to correlate the presence of these epigenetic marks with other markers of prognosis discussed above to better predict the therapeutic potential and survival, but the results are far from conclusive (48).

REST

The repressor element-1 silencing transcription factor (REST), also known as neuron restrictive silencing factor (NRSF), has been described as the master regulator of neuronal gene expression (49-53). It is highly expressed in embryonic stem cells (ESCs) and neural progenitor cells (NPCs), where it silences the transcription of neuronal genes, thus inhibiting neuronal differentiation (52, 53). REST also represses expression of neuronal genes in non-neural cells. The importance of REST in normal brain development is highlighted by the finding that homozygous deletion of *REST* has been shown to be embryonic lethal at E11.5, with gross changes in morphology and apoptosis observed beginning at E9.5 (53). Interestingly, REST is overexpressed in medulloblastoma, and has been shown to play an oncogenic role. The overall goal of our laboratory is to understand the molecular mechanisms associated with medulloblastoma pathology, with a specific focus on the contribution of REST.

Discovery

The neuron-restrictive binding factor/repressor element-1 silencing factor (NRSF/REST) was first discovered in non-neuronal cells as a DNA binding protein and transcriptional repressor (49, 50). It was shown to bind to a previously described silencer region termed *neuron restrictive silencer element/repressor element-1 (NRSE/RE-1)* that is located upstream of the neuronal genes (49, 50). The *RE-1* region was previously described to have cell specific repressive activity of neuronal genes, such as such as *sodium channel II (NaChII)*, *superior cervical ganglion-10 (SCG10)*, and *synapsin1 (SYN1)* noted in non-neuronal cells (L6, rat myoblasts), but not in neural cells (PC12, rat) (50, 54-57). Consistent with this cell-type specific repressive function of REST, higher levels of REST protein were observed in non-neuronal cells (HeLa, 10T1/2, 393T, L6 cells, and dorsal root ganglion cultures (DRG) established from newborn rats) while the protein was undetected or present at very low levels in neural cells (MAH, SY5Y, PC12) (49, 50). The ectopic expression of REST in PC12 cells conferred a similar repression of the *RE-1* driven CAT promoter reporter construct as that observed in non-neuronal L6 cells (49). The latter suggests that while REST is present in non-neuronal cells, and can therefore bind to *RE-1* sites and repress expression of the *RE-1* reporter construct, REST is absent in neuronal cells, and thus cannot bind to the *RE-1* sites and repress

reporter activity. Finally, ectopic expression of the dominant negative form of REST, comprising only of the DNA binding domain (REST-DBD), interfered with the normal activity of REST as de-repression of the reporter was noted in L6 cells upon transfection of the mutant construct (49). As expected, no changes were noted in the reporter activity in PC12 cells since the protein is absent in these cells (49). Based on this early seminal work, the canonical role of REST is to function as a repressor of neuronal genes in non-neural cells.

Structure

REST is a 116 kilodalton (kDa) zinc finger protein that belongs to krüppel like family of transcription factors (49, 51). It contains 9 zinc fingers, 8 of which comprise its DNA binding domain (DBD), while the last one is located near the carboxy (C-) terminus (52) (Fig. 1) (52, 58). REST also has two repression domains located at the amino- (N-) and carboxy (C-) termini that associate with two independent chromatin remodeling complexes: the mSin3 and Co-REST complexes, respectively (Fig. 1, 2) (58). Together, the two repression complexes allow REST to modify chromatin and epigenetically modulate gene expression of its target genes as detailed below (Fig. 2) (58). The C-terminus also contains two degron sequences that lead to proteasomal degradation of REST (Fig. 1) (59, 60). REST also contains lysine and proline rich domains, but their functions are not clear (Fig. 1) (52). There are two nuclear localization signals (NLS), one of which is contained in the lysine-rich region, while the other is located in zinc finger 5 (Fig. 1) (61-63).

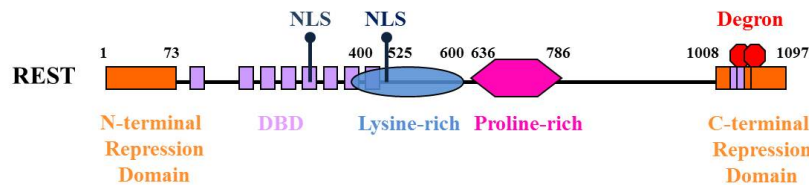
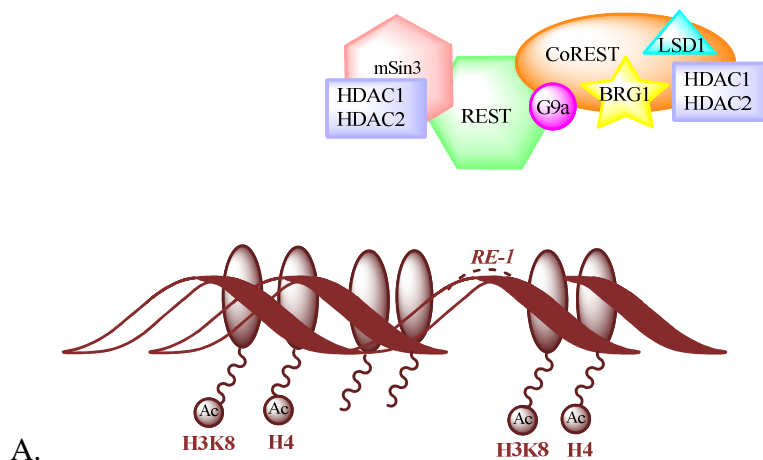


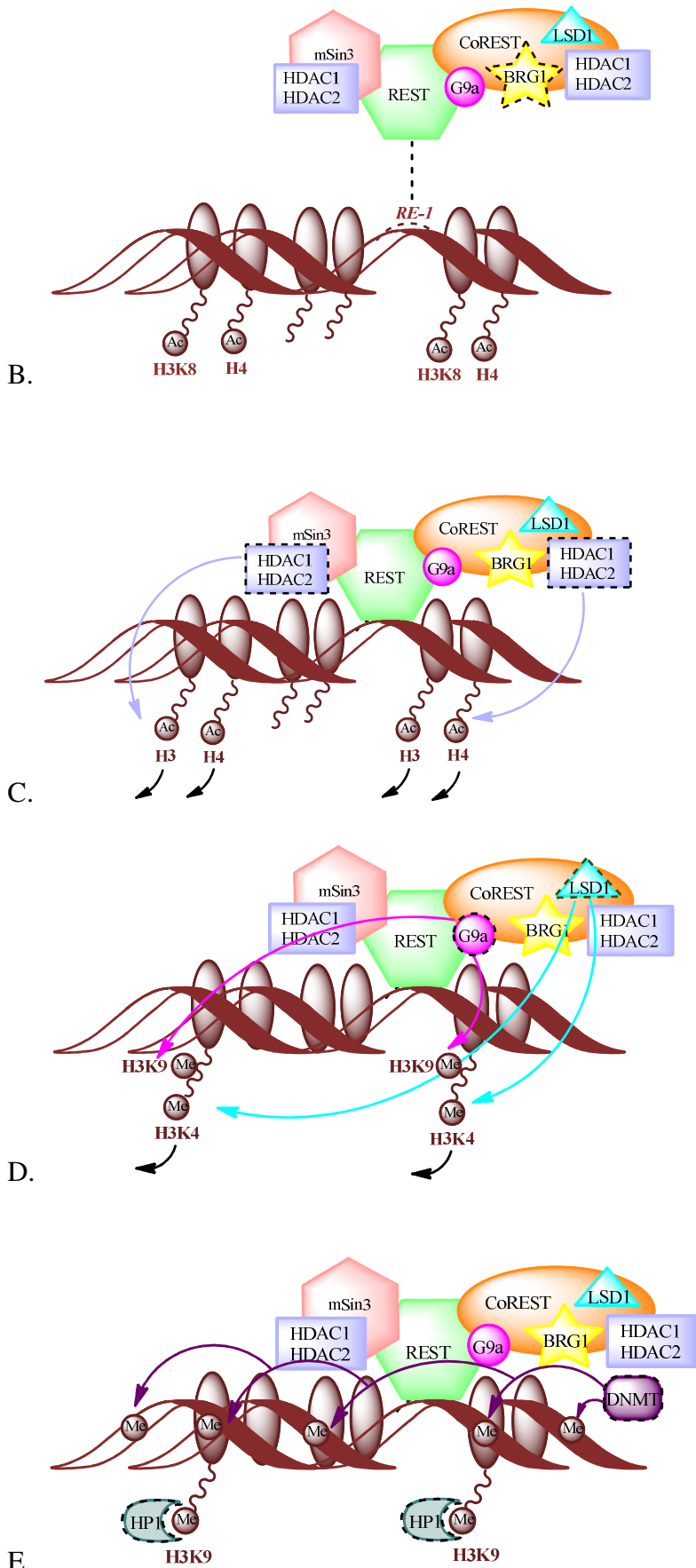
Figure 1: Structure of REST. REST is a zinc finger protein that consists of 9 zinc fingers, 8 of which comprise the DBD. There are two repression domains located on N- and C- termini, which can interact with two mSin3 and coREST complexes respectively. REST also contains lysine and proline rich domain. One of the NLS is present in the zinc finger 5, while the other is located in the lysine rich region. The two degron sequences and the last zinc finger are located on the C-terminus.

Mechanism of REST mediated repression

REST epigenetically modulates its target gene expression by interacting with the mSin3 and coREST complexes on the N- and C-termini respectively (Fig. 1, 2A) (58). These are

chromatin remodeling complexes composed of histone deacetylases (HDACs), histone methyltransferases (HMTs), and histone demethylases (HDMTs) along with other chromatin remodeling molecules that function together to epigenetically silence REST target gene expression (58). DBD of REST recognizes and binds to the *RE-1* site on REST target genes (Fig. 2B) (58). Brg1, an ATP-dependent chromatin remodeling enzyme that is usually part of the SWI-SNF complex, stabilizes the interaction by recognizing acetylated H4K8 (58). Increased H4K8 acetylation leads to increased recruitment of REST at the *RE-1* site (58). Brg1 complex repositions the nucleosomes in order to further stabilize the interaction of REST with *RE-1* site (58). HDAC1 and HDAC2, found in both co-repressor complexes, then deacetylate lysine residues on H3 and H4 (Fig. 2C) (58). Deacetylation of H3K9 stimulates LSD1 activity, a HDMT that removes mono- and dimethyl groups from H3K4 (Fig. 1D) (58). Deacetylation of H3K9 also leads to activation of HMT G9a, which then methylates H3K9 (Fig. 2D) (58). It is not clear whether G9a is recruited as part of the coREST complex or independently (58). Dimethylation of H3K9 signals the recruitment of heterochromatin protein-1 (HP1), which functions to promote chromatin condensation reminiscent of heterochromatin (Fig. 2E) (58). DNA methylation by DNMTs as well as binding of MeCP2 to the methylated DNA leads to permanent silencing of the target gene (Fig. 2F) (58). The mechanism behind initial recruitment of DNMTs remains to be determined (58). The overall effect of the REST complex on its target gene is generation of a heterochromatic conformation, with repressive marks such as H3K9 methylation, DNA methylation, and recruitment of methyl CpG binding protein (MeCP2) to methylated DNA (Fig. 2G).





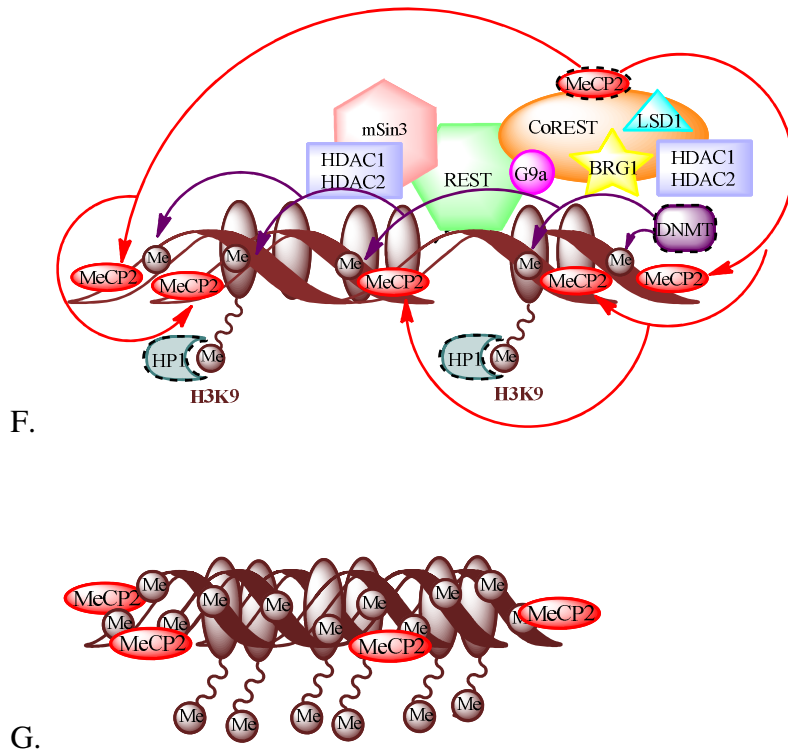


Figure 2: REST repression complex. Assembly of the REST repression complex is shown on REST target genes. A. REST complex consists of two chromatin re-modeling complexes, mSin3 and CoREST, associated with N-terminus and C-terminus of REST respectively. HDAC1 and HDAC2 are part of both complexes, while G9a, LSD1, Brg1 specifically interact with the coREST complex. REST target genes contain *RE-1* element to which REST DBD can bind. B. REST binds *RE-1* element on target gene via its DBD, and the interaction is stabilized by acetylation of H3K9 which is recognized by BRG1. C. HDAC1 and HDAC2 from both complexes deacetylate H3 and H4. D. Deacetylation of H3K9 leads to removal of mono- and di-methyl groups from H3K9 by LSD1, and addition of methyl groups to H3K9 by G9a. E. Dimethylation of H3K9 recruits HP1. F. DNA methylation by DNMTs occurs, followed by MeCP2 binding to methylated DNA. G. Overall effect of REST repression is stable silencing of its target gene expression via epigenetic modulation. Adapted from Oii and Wood, *Nature Reviews*, 2007.

Target genes and function

As previously stated, REST canonically functions as a master transcriptional repressor of neuronal genes, thereby maintaining ESCs and NPCs in an undifferentiated state in various rat, mouse, and human cell types (49, 52). Several screens using non-neural cells were performed in search of genes containing *RE-1* sites and REST occupancy at these sites to identify potential REST target genes (64-66). Interestingly, several variations of the canonical

RE-1 binding site exist in the regulatory elements of target genes, and REST has been shown to bind these non-canonical sites (64-66). As expected, many neuronal genes (some of which were previously known, while others were novel) involved in various neural-specific functions such as synaptic transmission, ion transport, nervous system development, ion channel activity were identified by the screens (64-66). Further experiments examining the repression profiles of these genes revealed two classes of REST target neuronal genes (53, 64, 67). Class I genes are occupied and repressed by REST and its complex, and their expression is up-regulated as REST levels decline (67). At the promoter of Class II genes (exemplified by Calbindin and BDNF) REST is present at the *RE-1* site along with its co-repressor complex (67). However, the coREST co-repressor complex, comprised of coREST, mSin3, MeCP2, and HDAC1, is additionally occupies the methylated CpG (mCpG) of these genes independent of REST in ESCs and NPCs (67). As REST levels decline, REST and its repression complexes no longer occupy the *RE-1* site, but the coREST repressor complex remains bound at mCpGs in cortical neurons (67). It is in response to additional stimuli (such as membrane depolarization) that most components (except coREST) are lifted from the mCpGs, thus allowing de-repression of these Class II genes (67). REST has been shown to regulate calcium channel genes in PC12 cells, thus affecting the calcium influx and responsiveness (68). Calcium is one of the most common second messengers, and calcium signaling is critical in neuronal cells, especially for membrane depolarization. The ability of REST to regulate such an important signaling mechanism allows it to regulate many further downstream processes (68).

Interestingly, only 40% of all potential REST targets identified in the screen are neuronal genes, while other potential REST targets comprise of non-neural genes, such as protocadherin- α (*Pcdh- α*), B-cell lymphoma-2 (*Bcl-2*), telomeric repeat-binding factor 2 (*TRF2*) that are involved in critical cellular functions such as adhesion, apoptosis, and genomic stability (49, 50, 64-66, 69). REST was also shown to directly and indirectly regulate cell cycle proteins (*MAD2*), proliferation, apoptosis, extracellular matrix components (ECM), self-renewal (27, 59, 64, 70-73). Furthermore, targeting miRNAs allows REST to potentially regulate pathways in the absence of *RE-1* sites (71, 72). Although, REST has also been implicated in self-renewal and fate-determination, but its role is heavily debated (73, 74). Some groups have reported a decrease in self-renewal genes, such as *Oct4*, *Sox2*, *Nanog*, in *REST*^{+/+} mice and ESCs treated with siREST, and report that this occurs through the negative regulation of miR-21 (73). Other groups have challenged these findings with conflicting data

from similar experiments (74). *In vivo* models of REST disruption have shown that although REST does not switch the fate of a presumptive non-neural cell, it does repress the neuronal genes in other cell types (53). Others groups reported a conversion of myoblasts into neurons upon interference with REST using an activating mutant of REST called REST-VP16 which contains the activation domains of the VP-16 virus rather than the repression domains of REST (75).

In addition to the transcriptional repression of its target genes, REST has also been shown to function as an activator of target genes (76). This has been attributed to splice variants of REST, mainly REST4/5 in neural cells (76-78). REST4/5 is a C-terminus truncation mutant that contains zinc finger 1-5, and a neural specific exon leading to its neural-specific expression (77-79). It is responsible for induction of glucocorticoid response that full-length and C-terminus REST repress (76). The latter suggests a domain and context specific role of REST at promoters of various target genes. Together, these findings suggest that depending on the target gene itself as well as the cellular context, REST regulates its target differently, thus establishing REST as an important regulator of many critical cellular processes as they highlight the immense complexity of REST regulatory network within and across various cell types and across different stages of development (64, 66).

Expression

During development, REST is ubiquitously expressed until E11.5. At E13.5 specific expression of REST has been observed only in areas of proliferating cells such as the mesodermal structures along the neural tube, germinal layer of the hindbrain, cranial glia, and in the inner proliferative layer of the forebrain (53). REST protein is not detected in differentiated neurons of the hindbrain or the outer layer of the forebrain (49). As previously indicated, homozygous deletion of *REST* is embryonic lethal at E11.5, with gross changes in morphology and apoptosis beginning at E9.5 (53).

Consistent with its expression profile in development, REST levels are highest in ESCs, and as these cells differentiate into NPCs, a decrease in REST protein is noted, while the transcript remains high (67). The decline in REST levels along with the transition of ESCs to cortical progenitors is blocked upon MG132 treatment, thereby implying the involvement of the proteasome in this process (67). Transcriptional down-regulation of *REST* is observed as NPCs transition into fully differentiated neurons (67). In non-neuronal cells, REST levels are

maintained, and are regulated via proteasomal degradation of REST in a cell-cycle dependent manner (59, 60, 67), as well as through changes in sub-cellular localization of REST for REST is degraded in the cytoplasm (80, 81).

Regulation

Emerging evidence suggests that REST is regulated differentially by both transcriptional and post-transcriptional mechanisms. As stated previously, REST is highly expressed in ESCs. As these cells acquire lineage specificity, REST protein levels decline, while *REST* transcription is maintained. Depending on the neuronal subtype under consideration, *REST* expression can be regulated by multiple pathways (67, 82-85). In cortical neurons, *REST* transcription is repressed by the presence of unliganded retinoic acid receptor (RAR) and its co-repressor complex on the retinoic acid response element (*RARE*) that is located on the *REST* promoter (67). This represents one mechanism by which *REST* is down-regulated in neural cells. In the developing cerebellum and mice teratoma cells (P19), NeuroD2, a component of the neuroD family which plays a role in neurogenesis as well as maintenance of neurons, has been shown to indirectly modulate *REST* by *Zfhx1a* (84). β -catenin, a transcription factor involved in WNT signaling, has been shown to directly bind to exon1a of *REST* and up-regulate *REST* transcription, in the developing chick spinal cord (83). REST itself promotes β -catenin activity by negative regulation of tuberous sclerosis complex 2 protein (TSC2, a component of the mTOR pathway that promotes turnover of β -catenin) in both rat (PC12) and human (NT2/D1) models of neural cells (85). This positive modulation of β -catenin in turn leads to an increase of β -catenin target genes, including *REST*, thereby implying the presence of a feed-forward loop (85). Interestingly, a ChIP seq genome wide screen performed in lysates from non-neural Jurkat cells revealed that REST binds a *RE-1* site in its own intragenic region (0.5 kb downstream from transcription start (TS)), thus presenting a mechanism for another potential auto-regulatory loop (65). In non-neural HeLa cells, the Notch signaling effector, Hairy enhancer of split-1 (HES1), has also been shown to bind to the *REST* promoter and repress its expression (82).

As stated above, REST is regulated by proteasomal degradation in NPC and non-neural cells (59, 60, 67). REST contains two phospho-degron sequences at the C-terminus to which the E3 ligase β -Transducing Repeat-Containing Protein (β -TRCP) can bind, thereby targeting REST for proteasomal degradation (59, 60). Mutating the degron sequence stabilizes REST

and knockdown of β -TRCP both block the differentiation of NPCs into neurons, thus establishing the importance of proteasomal degradation of REST in the neurogenic program (60). In non-neural cells, REST degradation occurs in a cell cycle dependent manner, where REST accumulates during G1-S and is degraded during the G2 phase (59). REST in turn regulates the spindle assembly checkpoint, by transcriptional repression of MAD2, a critical component of this checkpoint. In fact, ectopic expression of a mutant non-degradable REST in these cells, leads to untimely repression of MAD2 and cell cycle defects characteristic of mis-regulation of the spindle assembly checkpoint (59).

Regulation of REST through changes in sub-cellular localization of REST has also been noted, and is controlled via an interaction between REST and RILP (80, 81). RILP interacts directly with REST and dynactin p150^{Glued}, and dynactin p150^{Glued} also interacts directly with huntingtin (80, 81). Huntingtin-associated protein (HAP) is expressed predominantly in neural cells, and its overexpression in HeLa leads to the breakdown of the (RILP)- dynactin p150^{Glued}- huntingtin complex followed by only cytoplasmic localization of REST and an up-regulation of REST target gene reporters (80). Analogously, HAP knockdown in neural cells in NT2 cells led to mis-localization of REST into the nucleus (80).

Finally, REST can also be regulated by differential splicing in various cell types. REST-4/5, a neural-specific splice variant, contains a neuron-specific exon that is skipped in all non-neural cells, and introduces a stop codon in the beginning of exon 4, thereby lacking four zinc fingers and C-terminal repression domain (77, 78, 80). REST-4/5 can hetero-oligomerize with full-length REST to prevent full-length REST from binding to the *RE-1* site, thus promoting activation of REST target genes (61, 76-78). Cell specific expression of REST-4/5 is achieved by strictly restricting expression of nSR100, the splicing factor responsible for this splicing event, to neural cells (86, 87). Furthermore, full length REST represses nSR100 expression in non-neural cells, again indicating the existence of a feedback loop (86, 87). Regulation of REST protein and mRNA involves careful coordination of several factors that are involved in this intricate process depending on the type of cell and the stage of development.

REST in neural tumors

REST protein has been shown to be overexpressed in medulloblastoma cell lines and patient samples (28). Furthermore, a recent study from our lab indicated that high levels of

REST protein in medulloblastoma patient samples correlate with poor patient overall and event free survival (28). Introduction of REST-VP16, an activating mutant of REST constructed by replacing both of the repression domains with the activation domains of the herpes simplex VP16 virus (HSV-VP16), led to up-regulation of differentiation markers, such as β -tubulinIII, Synapsin, glutamate receptor, as well as apoptosis in medulloblastoma cell lines (25, 26). *In vivo*, this construct abrogated the tumor forming potential of medulloblastoma cell lines DAOY and D283 (25, 26). Although REST is known to contribute to other pre-neoplastic events such as uncontrolled cell proliferation, expression of REST alone in NSCs appeared to be insufficient for tumor formation *in vivo* (27). In human tumors elevated REST expression is frequently associated with high N-Myc or c-Myc expression (27). The constitutive expression of REST and c-Myc in NSCs promoted tumor formation in mouse orthotopic models, suggesting that REST and Myc co-operate in tumorigenesis. Furthermore, this tumorigenesis was countered by infecting REST-VP16 into the tumor promoting myc-immortalized NSCs overexpressing REST, thus implicating the importance of REST activity in medulloblastomagenesis (27). However, the specific contribution of REST to tumor formation is not fully understood.

The role of REST remains largely unexplored in neuroblastoma. Although neuroblastoma cell lines have been used to study the contribution of REST to neurosecretion, neurite outgrowth, and epilepsy, studies regarding its role in neuroblastoma pathology have not been conducted (88, 89). REST-4 has been shown to be the major form of REST present in neuroblastoma cell lines, NEI115 and NS20Y, as compared with non-neural NIH3T3 cells, and an activator role for the variant has been suggested (62). Retinoic acid is a differentiation agent, and a mainstay of neuroblastoma treatment.

REST in non-neural tumors

REST has been shown to have a tumor suppressor role in epithelial tumors of colon, breast, ovarian, prostate, and lung among others (60, 90-92). These non-neural tissues normally express REST to silence neuronal genes, however decreased *REST* transcription has been noted in these cancers, along with expression of neuronal genes. Indeed, REST is deleted in one-third of colorectal tumors, and a frame-shift deletion mutants, hREST-N62 and REST-FS, which can potentially interfere with full-length REST function, have been observed in small cell lung cancer (SCLC) and colorectal cancer respectively (59, 60, 90-92). REST aberration is

associated with a more aggressive phenotype in prostate cancer cells. An RNAi screen also identified REST as a validated candidate tumor suppressor in mammary epithelial cells (TLM-HMECS) (60). Overexpression of REST E3 ligase, SCF ^{β -TRCP}, in TLM-HMECS led to increased proliferation and a transformation phenotype, which was countered by full-length REST and stabilized degron-mutant REST, thereby implicating a tumor suppressor role for REST (60). However, the latter finding was challenged by another study which showed that the effects of chromosomal instability upon introduction of REST-FS were indistinguishable from introduction of a non-degradable form of REST (REST E1009A/S1013A), which suggests that REST functions as an oncogene in these tumors (59). REST clearly appears to be important in non-neural tumors, although further studies are needed to delineate its exact role. These studies reinforce the tissue and tumor specific roles of REST. It may potentially be targeted as a therapeutic target if it indeed has a tumor suppressor function in non-neural cells.

Aim of the Study

REST is critical for neuronal differentiation, and down-regulation of *REST* transcription is required for the differentiation of NPCs into neurons (49, 51, 52). REST is overexpressed in medulloblastoma, where current evidence suggests that it has an oncogenic function (25-28).

In medulloblastoma, which arise from NPCs of the EGL of the cerebellum and hindbrain, REST maintenance is associated with a blockade of neuronal differentiation and in increase in proliferative potential of medulloblastoma cell lines (3, 4, 11, 27). Ectopic expression of REST is known to promote tumor formation *in vivo*, which is abrogated upon interference with REST activity (27). Mechanisms underlying the elevated levels of REST in medulloblastoma are not understood. Since REST has been shown to be transcriptionally regulated in NPCs, the cells of origin of medulloblastoma, **we hypothesize that *REST* is transcriptionally mis-regulated in medulloblastoma. Based on previous studies and bio-informatic evidence, we speculate that:**

- 1. Transcription factor HES1 regulates *REST* expression,**
- 2. REST regulates its own expression in an auto-regulatory feedback loop, and**
- 3. HES1 and REST co-regulate *REST* expression.**

In a separate study, we investigated the regulation of REST in neuroblastoma, where its role remains unexplored. Neuroblastoma occurs in the sympathetic tissues, and NSCs from the developing neural crest are considered to be the cells of origin. Retinoic acid is a differentiating agent, and is a mainstay for neuroblastoma treatment, but the mechanism by which retinoic acid mediates the differentiation of neuroblastoma cells remains unknown. Given the critical role of REST in neural differentiation as well as negative regulation of *REST* in cortical progenitors by retinoic acid, **we hypothesize that retinoic acid promotes differentiation of neuroblastoma tumors through transcriptional regulation of *REST*.**

Chapter 2: *REST* is transcriptionally mis-regulated in medulloblastoma patient samples

Rationale

Medulloblastoma is characterized by the bypass of normal differentiation and hyperproliferation of the NPCs of the EGL of the cerebellum, which contribute to the aberrant maintenance of the EGL in patient samples and well-characterized SHH mouse models of medulloblastoma (13, 31). REST is an important regulator of neuronal differentiation, and it maintains proliferation of NPCs while repressing the expression of neuronal differentiation genes (49-53). REST protein has been previously shown to be elevated in medulloblastoma patient samples and cell lines, and high REST levels correlate with poor patient overall survival and event-free survival (25-28, 92) (28). Interfering with REST function in medulloblastoma cell lines leads to up-regulation of its target genes, many of which are neuronal differentiation markers, such as β -tubulinIII, SynapsinI, Synaptophysin, as well as apoptosis *in vitro* (25-27). REST activity has been shown to contribute to tumorigenesis in xenograft models *in vivo* (27, 93). Although previous studies implicate a role for REST in medulloblastoma pathology, the mechanism by which REST is maintained in medulloblastoma tumors and cell lines remains unknown. Because medulloblastoma arises from progenitor populations of the cerebellum and hindbrain, and REST has been previously shown to be regulated transcriptionally in cortical progenitors, we want to determine whether or not *REST* is transcriptionally mis-regulated in medulloblastoma (25-28, 67, 92). **We hypothesize that *REST* is transcriptionally mis-regulated in medulloblastoma patient samples.**

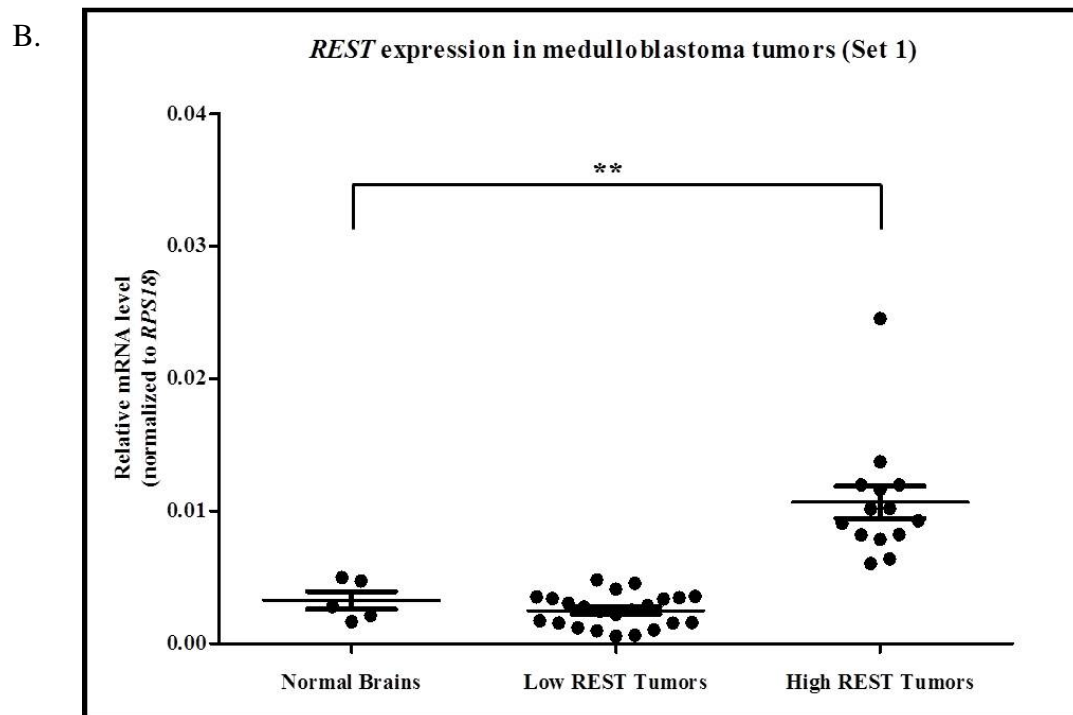
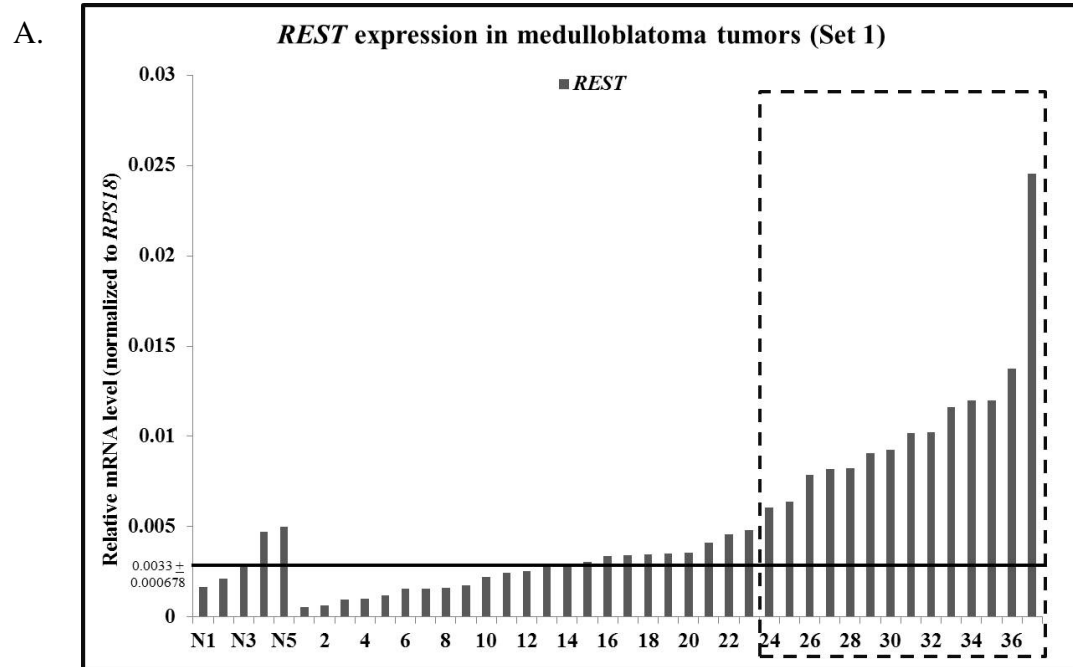
Results

***REST* is transcriptionally mis-regulated in medulloblastoma patient samples**

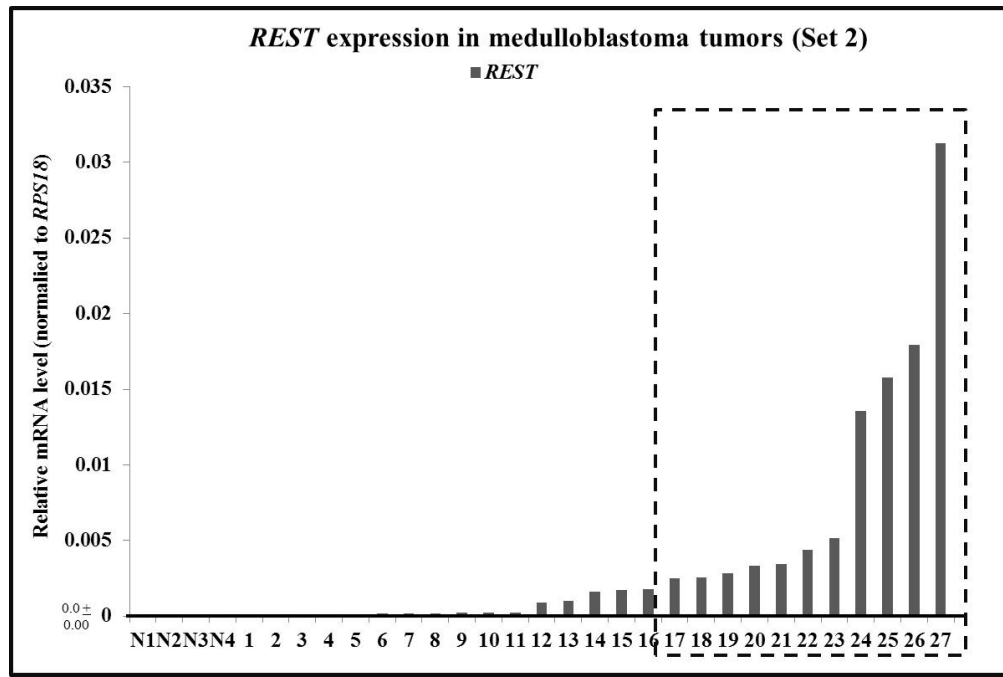
To determine the status of *REST* transcript in medulloblastoma patient samples, we analyzed two independent sets of medulloblastomas tumor samples for *REST* expression. The first set consisted of RNA from 37 snap-frozen medulloblastoma samples and 5 non-tumor brain samples (kindly provided by Dr. Charles Eberhart, Johns Hopkins University School of Medicine). RNA from these samples was analyzed via quantitative reverse transcriptase polymerase chain reaction (qRT-PCR) for *REST* expression. Samples were normalized to *RPS18* mRNA (internal control). *REST* transcript was elevated in 38% (13/37) of the samples as compared to the non-tumor samples, while it was comparable to normal cerebellar control in 62% (24/17) of the samples (Fig. 3A). To determine whether or not *REST* expression was significantly different from normal brain tissue in high *REST* expressing tumors, we divided the tumor samples into high and low *REST* expressing groups, and statistical analysis was performed by applying the T-Test (non-parametric) followed by Mann-Whitney post-hoc analysis using the program GraphPad Prism (Fig. 3B). Indeed *REST* expression in the 14/37 high *REST* expressing tumors is significantly higher as compared to the normal brain tissue ($p=0.0014$), whereas *REST* transcript in the rest of the tumors are not significantly different from the normal brain tissue (Fig. 3B).

These findings were validated by analysis of *REST* expression in an independent second set of 27 paraffin embedded medulloblastoma tumors and 4 non-tumor normal brain samples (kindly provided Dr. Martin Hasselblatt, University Children's Hospital, Munster, Germany). RNA was extracted from these samples, and analyzed by qRT-PCR and normalized to *RPS18* as previously described. *REST* expression is higher as compared to normal brains in 62% (17/27) of the samples (Fig. 3C). As with the previous set, we divided the tumor samples into high and low *REST* expressing groups to determine whether *REST* expression was significantly different from normal brain tissue in high *REST* expressing tumors (Fig. 3D). A comparison of 17/27 high *REST* expressing tumors to normal brain yielded that *REST* is significantly elevated ($p=0.003$), whereas *REST* transcript in the low *REST* expressing group is not significantly different from the normal brain samples (Fig. 3D). Overall, our analysis of two independent

patient samples suggests that *REST* is transcriptionally aberrant in a subset medulloblastoma tumors.



C.



D.

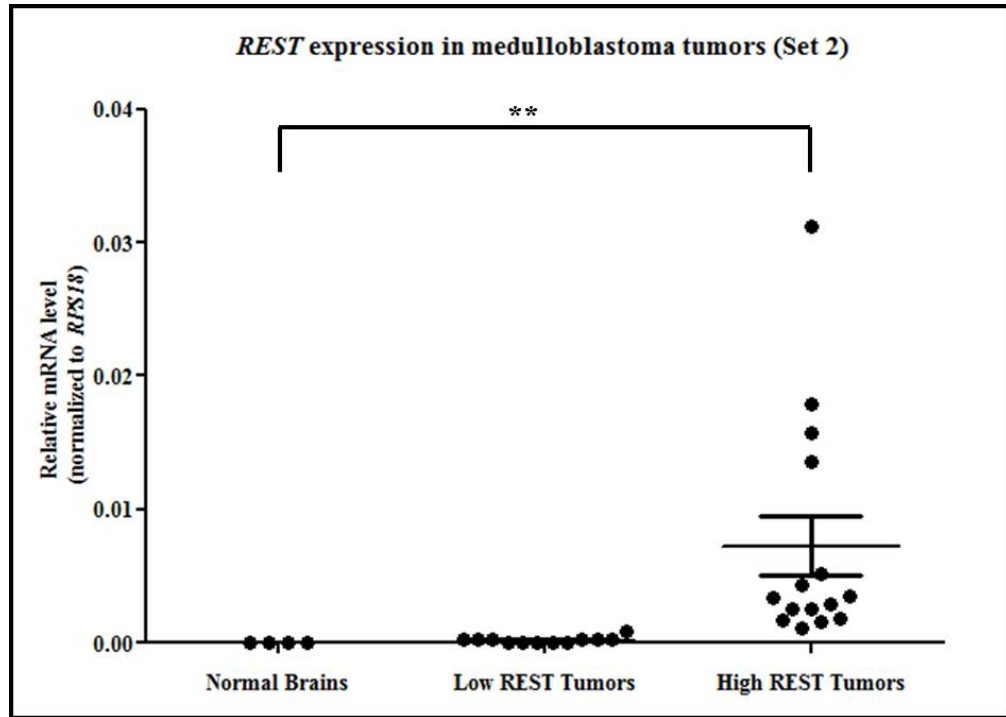


Figure 3: *REST* expression is aberrant in medulloblastoma patient samples. A. RNA was prepared from 37 snap-frozen tumor samples and 5 normal brain samples, analyzed by qRT-PCR for *REST* expression, and normalized to *RPS18*. B. Data from A represented as a scatter plot of high and low *REST* expressing groups and compared with normal brain controls C. RNA was prepared from 27 snap-frozen tumor samples and 4 normal brain samples, analyzed by qRT-PCR for *REST* expression, and normalized to *RPS18*. D. Data from A represented as a scatter plot of high and low *REST* expressing groups and compared with normal brain controls. T-Test (non-parametric) followed by Mann-Whitney post-hoc analysis using GraphPad Prism was conducted to determine statistical significance (* $p \leq 0.05$, ** $p \leq 0.01$, *** $p \leq 0.001$).

Summary

Consistent with previous results that REST protein is over-expressed in medulloblastoma patient samples, our data from two independent sets of medulloblastoma patient samples suggests that *REST* transcript is also elevated in a subset of the tumors as compared to non-tumor normal brain samples (25-27). Our findings indicate that *REST* is transcriptionally mis-regulated in a subset of medulloblastoma patient samples. Further analysis to determine if elevated *REST* transcription corresponds to a particular subtype of medulloblastoma and if *REST* mRNA could serve as a prognostic indicator would be interesting.

Chapter 3: HES1 regulates *REST* expression

Rationale

Current evidence suggests that both REST and Hairy Enhancer of Split-1 (HES1) are critical for normal brain development and neurogenesis (53, 94-96). Both proteins are required for the maintenance of NSCs as they function to promote NSC proliferation while inhibiting their differentiation into neurons (53, 94-96). HES1 and REST have overlapping time frames of expression during development, and homozygous deletion of these genes leads to embryonic lethality at E10.5 and E13.5 respectively (53, 94, 96).

Several studies have shown that HES1 is over-expressed in medulloblastoma patient samples and some SHH mouse models (31, 32, 97, 98). Canonically downstream of Notch signaling, other developmental pathways that have been implicated in medulloblastoma etiology, such as a SHH and WNT, have also been shown to regulate and interact with HES1 (35, 99-101). The latter suggests that perhaps HES1 serves as a convergence point for several developmental pathways in medulloblastoma pathology. Although these studies have implicated HES1 in medulloblastoma pathology, its exact role remains to be delineated (31, 32, 97, 98). HES1 has been previously shown to bind to *N-boxes* on the *REST* 5' upstream region and regulate *REST* expression in non-neural HeLa cells (82). However, the biology of REST is different between neural and non-neural cells, and the role of HES1 in *REST* regulation has not been studied in a neural context.

Since HES1 and REST are both implicated in normal brain development and medulloblastoma pathology, and HES1 has been previously shown to regulate *REST* in non-neural HeLa cells, we wanted to determine whether this regulatory pathway is operational in medulloblastoma. HES1 is a transcription factor that binds to *N-boxes*, so we manually searched the -7 kb of 5' upstream region of *REST* for *N-boxes*, and discovered five, three of which have been previously described (Fig. 4). Presence of *N-boxes* on the *REST* 5' upstream region represents potential for HES1 to regulate *REST* expression. **We hypothesize that HES1 represses *REST* in medulloblastoma cell lines.**

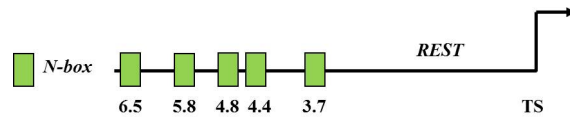


Figure 4: Location of *N*-boxes on the 5' upstream region of *REST*. Previous studies and manual analysis revealed the presence of 5 *N*-boxes on the *REST* 5' upstream region. Three of these *N*-boxes, located -3.7 kb, -4.4 kb, and -6.5 kb from TS, have been previously described.

HES1

HES1 is one of the seven genes that comprise the HES family of proteins (HES1-7) (95). Originally discovered as the mammalian homolog of *Drosophila Hairy (h)* and *Enhancer of Split (E(spl))*, which were previously known to inhibit neurogenesis in *Drosophila*, HES1 shares the greatest homology (81%) of any HES proteins with the *Drosophila h* protein, and significant portions of the protein correspond to the HLH domain of the *Drosophila E(spl)* protein as well (102-108). HES1 is a basic helix loop helix (bHLH) protein that functions canonically as a transcriptional repressor (95). Although HES1, 3, and 5 are important in brain development and neurogenesis, we have focused on HES1 because of its role in medulloblastoma pathology (95).

Structure

HES1 is comprised of bHLH, orange, proline, and WRPW domains (Fig. 5) (95, 102). The basic (b) portion of bHLH domain is important for DNA binding, while the helix-loop-helix (HLH) part is important for homo- and heterodimerization (95, 102). The orange domain functions in protein-protein interaction. It, along with bHLH domain, has been specifically shown interact with PARP which is associated with an activation function for HES1 (109, 110). The proline domain has been shown to interact with the chromatin modifying mSin3 complex which includes HDACs. The WRPW domain, comprised of tryptophan-arginine-proline-tryptophan residues, is located on the C-terminus, and is critical for recruitment and binding of co-repressor complex (53, 111, 112).



Figure 5: Structure of HES1. HES1 is comprised of basic, HLH, orange, proline, and WRPW domains. Basic and HLH domains are important for DNA binding and dimerization. Orange domain is important for protein-protein interaction. Proline and WRPW domains bind mSin3 and Transducin-like enhancer protein 1 (TLE-1) complexes respectively.

Mode of repression

HES1 is a downstream effector of canonical Notch signaling that functions largely to transcriptionally silence its target genes, which are pro-neural differentiation genes, thereby

promoting proliferation of NPCs (94, 95). It can function through two types of consensus DNA sequences, *N-boxes* and *E-boxes*, located on the regulatory regions of its target genes. Depending on which of these sequences is present at the regulatory region, either an active or a passive mode of repression can be employed (94, 95, 113). If an *N-box* is present, then HES1 represses via an active mode, where it homo- or heterodimerizes with another HES molecule, and binds to the bHLH region, leading to the recruitment of a co-repressor complex at the WRPW domain of the protein (94, 95, 113). This results in silencing of target gene expression (94, 95, 113). HES1 binding activity is critical to its function as a transcriptional repressor, and it is inhibited by phosphorylation of two adjacent serine residues in the basic domain by protein kinase C (PKC). PKC is activated in response to neurogenic signals such as nerve growth factor (NGF). Mutation of these serine residues leads to constitutively active HES1 (114). The presence of an *E-box* on the regulatory elements mandates a passive mode of repression, where HES1 forms a non-functional dimer with an activator type bHLH molecule, such as E47 (95, 113). Activator type bHLH molecules (Mash1, Math1, Neurogenin) normally dimerize with each other to turn on neuronal gene expression (94, 113). Thus, the HES-E47 non-functional dimer acts in a dominant negative fashion by sequestering the activator molecules, thereby repressing target gene expression (95, 113). HES proteins can potentially bind *E-boxes*, but they have a much greater affinity for *N-boxes*, which is atypical of other bHLH factors (95). A conserved proline residue in the basic domain may be responsible for its preferential binding to an *N-box* versus an *E-box* (94).

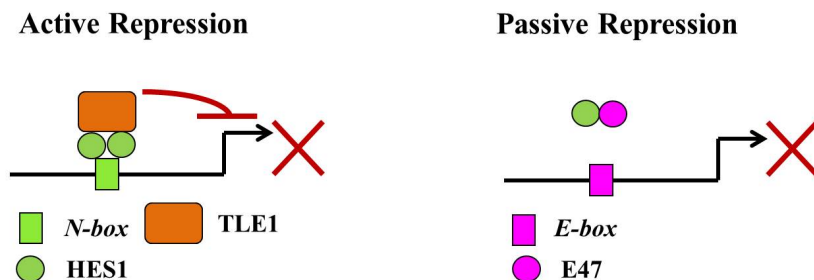


Figure 6: Two modes by which HES1 represses its target gene expression. A. If an *N-box* is present in the regulatory region of the target gene, then HES1 represses by an active mode, where it homo- or heterodimerizes with another HES molecule, and binds to the bHLH region, leading to the recruitment of a co-repressor complex at the WRPW domain of the protein. B. The presence of an *E-box* on the regulatory elements of HES1 target gene mandates a passive mode of repression, where HES1 forms a non-functional dimer with an activator type bHLH molecule, such as E47, thus preventing the activator type bHLH molecule from dimerizing with another activator type bHLH molecule to turn on target gene expression.

Function in the Brain

HES1 is expressed in most precursor cells during development, and its over-expression leads to an inhibition of differentiation in many tissues (94). HES1 deficient mice show precocious differentiation of several tissues, including pancreas, eyes, and brain (94). The most pronounced phenotype is observed in the brain, where HES1 functions to maintain NSC population and cellular diversity, and is critical in controlling the timing of neuronal differentiation during development (94, 96). Because of premature neuronal differentiation, 70% of HES1 deficient mice have defects in neurulation (96). Neurulation is the process of closing the neural tube, which a structure that is composed largely of NPCs. This leads to exencephaly, anencephaly, and embryonic lethality at E10.5 (96). The remaining 30% that do not display morphological defects still do not survive after birth (96). As seen with most other critical developmental molecules, some degree of functional redundancy is apparent between the HES proteins. For example, although mice lacking HES1, HES3, or HES5 show a partial phenotype of precocious differentiation and decreased glial cells and NPCs, simultaneous knockout of all three *HES* genes is required for excessive neuronal differentiation of radial glia at the cost of glial differentiation (95). An exceptionally early differentiation of neuroepithelial cells at E8.5 in the triple knockout mice (95). However, the striking phenotype of HES1 deficient mice (as well as other single knockouts) while other HES proteins are intact attests that each HES protein still maintains its unique function (95).

Cross-talk between HES1 and other pathways

Although HES1 is canonically downstream of Notch signaling, its expression can be regulated by other developmental pathways as well. In the neuroepithelial stage of development, Notch signaling is not active, yet *HES1* is expressed (95). In the latter instance, LIF may be responsible for *HES1* expression in the absence of Notch signaling (95). SHH signaling has also been shown to up-regulate *HES1* transcription independent of Notch signaling in mouse multipotent mesodermal C3H10T1/2 cells as well as multipotent rat neural MNS70 cells (99). Cyclopamine, an SHH pathway antagonist, inhibited SHH-mediated increase of *HES1* mRNA (99). Disruptions in the SHH pathway in mouse models have been shown to contribute to HES1 mis-regulation as well, although alterations in other Notch

proteins are also observed (35). HES1 in turn can modulate other developmental pathways. For example, HES1 has is shown to directly bind and regulate the expression of SHH downstream effector, *Gli1*, in glioma cells (100). The latter appears to be a Notch signaling dependent function of HES1, since treatment with γ -secretase inhibitor, MRK-003, leads to decreased HES1 mRNA and protein levels along with the de-repression of *Gli1* (100). Some evidence suggests that ectopic expression of HES1 in NPCs from the mouse sub-ventricular zone (SVZ) leads to increased protein levels of WNT signaling molecules, β -catenin and GSK-3 β (101). Indirect regulation of *HES1* by β -catenin through direct interaction with Notch intracellular domain (NICD) and modulation of Notch signaling has been reported in HEK293 and MEF cells (115). Such intricate cross-talk between HES1 and other pathways in development as well as multiple disease processes suggests that perhaps HES1 serves as a convergence point of multiple developmental pathways.

HES1 and medulloblastoma

HES1 has been implicated in medulloblastoma but its exact role remains unclear. In patient samples, *HES1* mRNA is up-regulated in 46% of patient samples, and high HES1 protein is associated with poor patient survival (31, 97). Decrease in colony formation potential of the medulloblastoma cell line, DAOY, upon knockdown of HES1 via siRNA has been reported (97). Similar results were seen upon treatment of DAOY with the notch inhibitor, γ -secretase inhibitor-18 (GSI-18), which also leads to an 80% decrease in HES1 mRNA and protein (116). The latter effect on *in vitro* and *in vivo* tumorigenic potential was rescued by ectopic expression of NICD2, which is important for EGL maintenance during cerebellar development (116, 117). However, interpretation of these findings have been complicated by the fact the presence of an auto-regulatory loop that leads to oscillation of HES1 mRNA and protein in synchronized cell lines *in vitro* and in post-mitotic somites *in vivo* (118, 119). This auto-regulation involves transcriptional repression as HES1 binds to its own promoter, as well as a post-translational mechanism via temporal regulation of proteasomal degradation of HES1 (118, 119). Additionally, the involvement of other unknown HES1 binding partners in the regulation of HES1 transcription and protein stability has been speculated because the system does not fall into equilibrium as would be expected if it was only regulated by HES1 (119). The existence of this auto-regulatory loop of HES1 cautions against concluding that *HES1* mRNA expression necessarily correlates with its protein levels, thus

necessitating independent measurements of both in order to ensure an accurate interpretation of results of HES1 modulation experiments. In the light of these observations, additional experiments may be needed to more accurately interpret findings of studies wherein HES1 transcript has been knocked down. The latter also cautions against making conclusive statements regarding the role of HES1 in medulloblastoma pathology from the measurement of *HES1* transcript alone in patient samples.

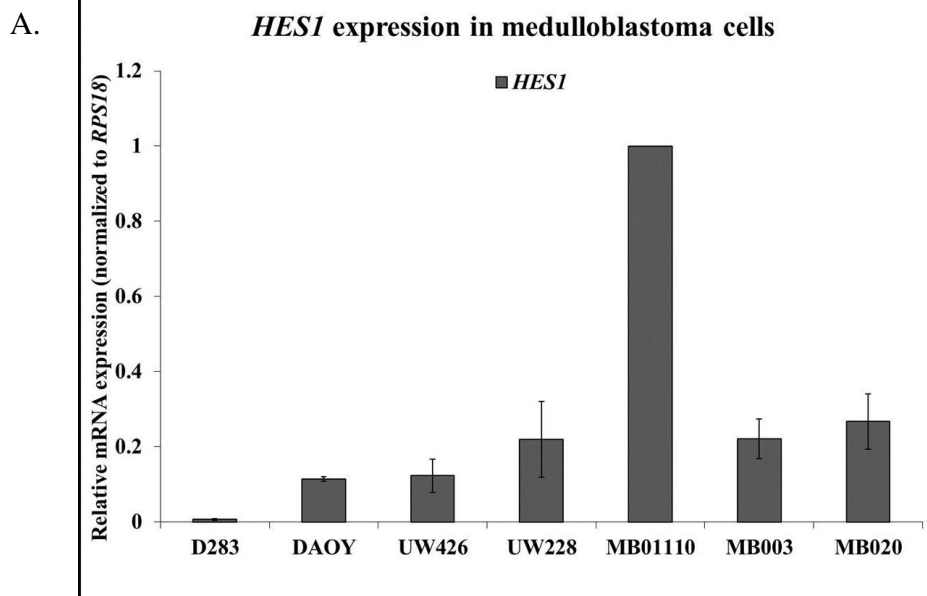
In mouse models of medulloblastoma, *Ptc*^{+/-} mice with overactive SHH signaling, display increased transcription of WNT and Notch signaling components, including *HES1* (35). However, the latter finding is not recapitulated in *ND2-SMOA1* model of medulloblastoma which also has overactive SHH signaling, but no significant alteration of HES1 was observed (31). *In vivo* modulation by Notch inhibitors as well as deletion of the Notch component *RbpJ*, a convergent point of most canonical Notch signaling, showed that Notch signaling itself may not be necessary for medulloblastoma tumor formation because no change in tumor growth, size, and presentation is observed upon these treatments (120). However, *HES1* transcription continued to be maintained in the absence for Notch signaling, thereby suggesting that it continues to be a key player in medulloblastoma biology independent of Notch pathway potentially through its regulation by other pathways (120).

In the light of the background presented above, the rationale for exploring the role of HES1 in regulation of *REST* is re-emphasized. HES1 and REST are both implicated in normal brain development and medulloblastoma pathology (53, 82, 94-96). REST is transcriptionally mis-regulated in medulloblastoma, and the 5' upstream region of *REST* contains *N-boxes*, some of which HES1 has been shown to occupy in non-neural HeLa cells (Fig. 4) (82). However, the biology of REST is different in neural and non-neural cells, and we want to determine whether HES1 contributes to aberrant maintenance of *REST* in medulloblastoma by regulating its transcription. **We hypothesize that HES1 represses *REST* in medulloblastoma cell lines.**

Results

HES1 levels in MB tumor samples and cell lines

We first determined the levels of HES1 mRNA and protein in a panel of medulloblastoma cells. We used established medulloblastoma cells lines (DAOY and D283) and primary cultures derived from patient samples (UW426, UW228, MB0110, MB020, and MB003). Normal cerebellum served as the negative control. Whole cell RNA and protein lysates were prepared and subjected to qRT-PCR and Western blot analysis for detection of HES1 mRNA and protein respectively. HES1 mRNA and protein levels show a reciprocal trend, which suggests that the HES1 auto-regulatory feedback loop is intact in all the medulloblastoma cells tested (Fig. 7). Low HES1 mRNA and high HES1 protein levels were observed in most medulloblastoma cells relative to normal cerebellum. Interestingly, MB0110 did not follow the same trend as the other medulloblastoma cells, and had the highest HES1 transcript expression but no detectable 37 kDa form of HES1 protein (Fig. 7). Since we are concerned with the transcriptional activity of HES1 protein on *REST* 5' upstream region, we decided to use DAOY and D283 (high HES1 protein) for our loss of function analyses, and MB0110 (no detectable HES1 protein) for gain of function assays.



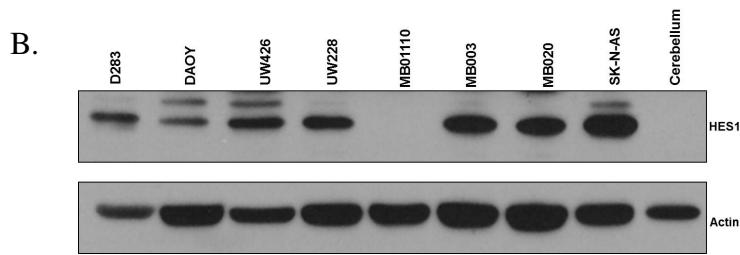
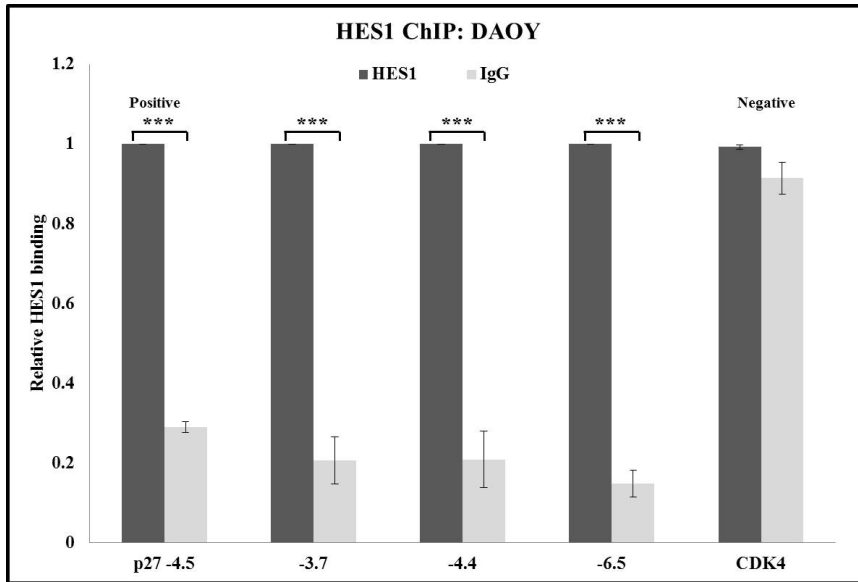


Figure 7: HES1 mRNA and protein levels in medulloblastoma cells compared to normal cerebellum. Whole cell lysates prepared from medulloblastomas cell lines and normal cerebellar lysate were subjected to A. qRT-PCR analysis for *HES1*. Samples are normalized to the internal control *RPS18*, and scaled relative to the highest value. Experiments were done in triplicate. B. Western blot analysis to determine HES1 protein level. Actin was used as a loading control. Experiment was done in duplicate, and the image above is a representative of the duplicate.

HES1 binds to *REST* 5' upstream region

HES1 is a transcription factor that primarily regulates the expression of its target genes by binding to *N-boxes* located on the regulatory regions of those genes, so we wanted to determine whether HES1 directly occupied the *N-boxes* located on *REST* 5' upstream region. Nuclear lysates were prepared from HES1 protein expressing DAOY and D283 cells, and subjected to chromatin immunoprecipitation (ChIP) assay using rabbit anti-HES1 antibody or control serum immunoglobulins (IgG) (Fig. 8). Immunoprecipitated DNA was analyzed via qPCR using primers specific to *N-boxes* located -3.7 kb, -4.4 kb, and -6.5 kb from the TS (previously validated sites for HES1 binding in HeLa cells (82)). Relative HES1 binding to the region of interest was determined by comparing the non-specific control values (IgG) with the specific sample values (HES1). The *p27 N-box* was previously reported to be positive for HES1 occupancy and was used as a positive control in both cell lines, while *CDK4* and *p63* served as negative controls in DAOY and D283 respectively (121). A statistically significant difference in relative HES1 binding with the specific antibody pull-down as compared to IgG is seen, suggesting that HES1 associates with *REST* 5' upstream region in both DAOY and D283 cells (Fig. 8).

A.



B.

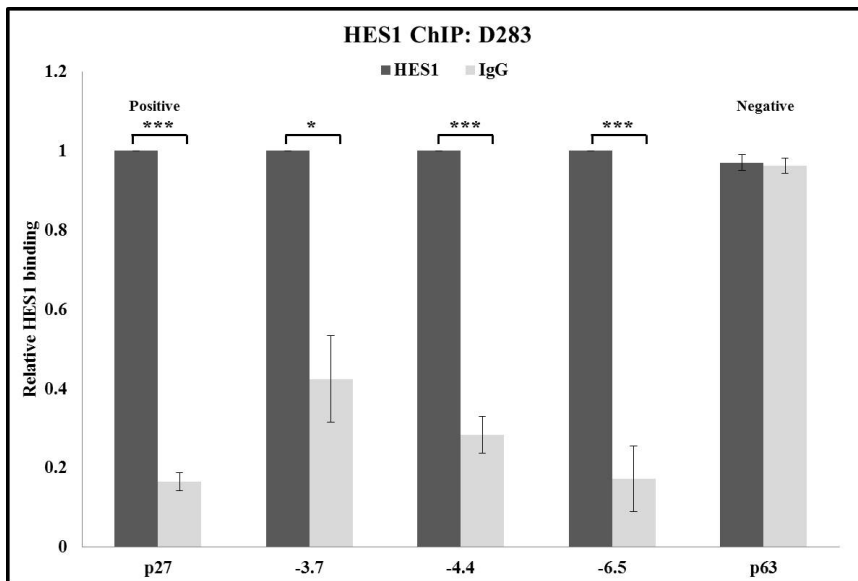


Figure 8: HES1 binds to 5' upstream region of *REST* in medulloblastomas cells. A. DAOY and B. D283 cells were subjected to ChIP assay by immunoprecipitation with rabbit anti-HES1 antibody or control IgG, followed by qPCR analysis using primers specific to *N-boxes* located -3.7 kb, -4.4 kb, and -6.5 kb from the TS. Experiments were done in triplicate. One-way ANOVA followed by Fisher least significant difference (LSD) post-hoc analysis using Statistica 6.0 was conducted to determine statistical significance (* $p \leq 0.05$, ** $p \leq 0.01$, *** $p \leq 0.001$).

HES1 represses *REST* expression in medulloblastoma cells

In order to determine whether HES1 regulates *REST* expression in medulloblastoma cell lines, we interfered with endogenous HES1 activity and measured changes in *REST* transcript. Full length HES1 construct (MigR1-HES1-GFP), or two mutants of HES1 (MigR1- Δ BHLH-

OR-GFP and MigR1- Δ WRPW-GFP) kindly provided by Dr. Zweidler-McKay were employed for these assays (Fig. 9) (109). All constructs contain the retroviral backbone of the murine stem cell virus (MigR1) vector, with the viral long term repeat (LTR) driving the expression of the transgene and green fluorescent protein (GFP) sequence (122). The transgene and GFP sequences are separated by an internal ribosomal entry site (IRES) (122). MigR1-HES1-GFP contains full length flag-tagged HES1 transgene. MigR1- Δ bHLH-OR-GFP is a 154 aa C-term deletion mutant of HES1 in which the proline and WRPW domains have been deleted. Both of the tryptophan residues (W) were mutated to glycine residues (G) to make MigR1- Δ WRPW-GFP. Both mutants are designed to abrogate the recruitment of the co-repressor complex to HES1, and have been shown to interfere with endogenous HES1 activity in a dominant negative capacity.

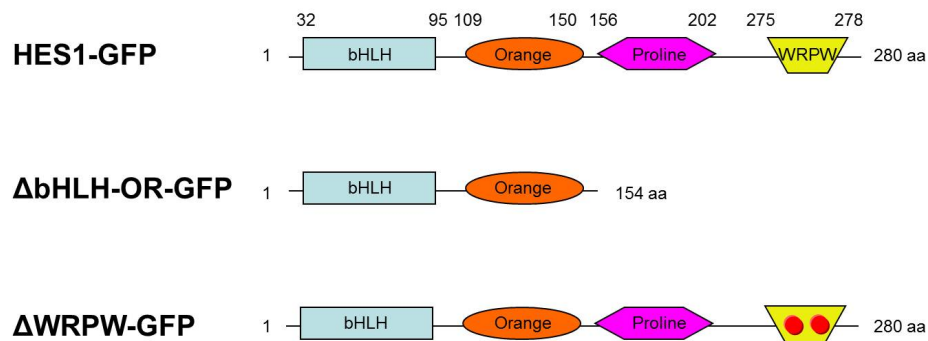
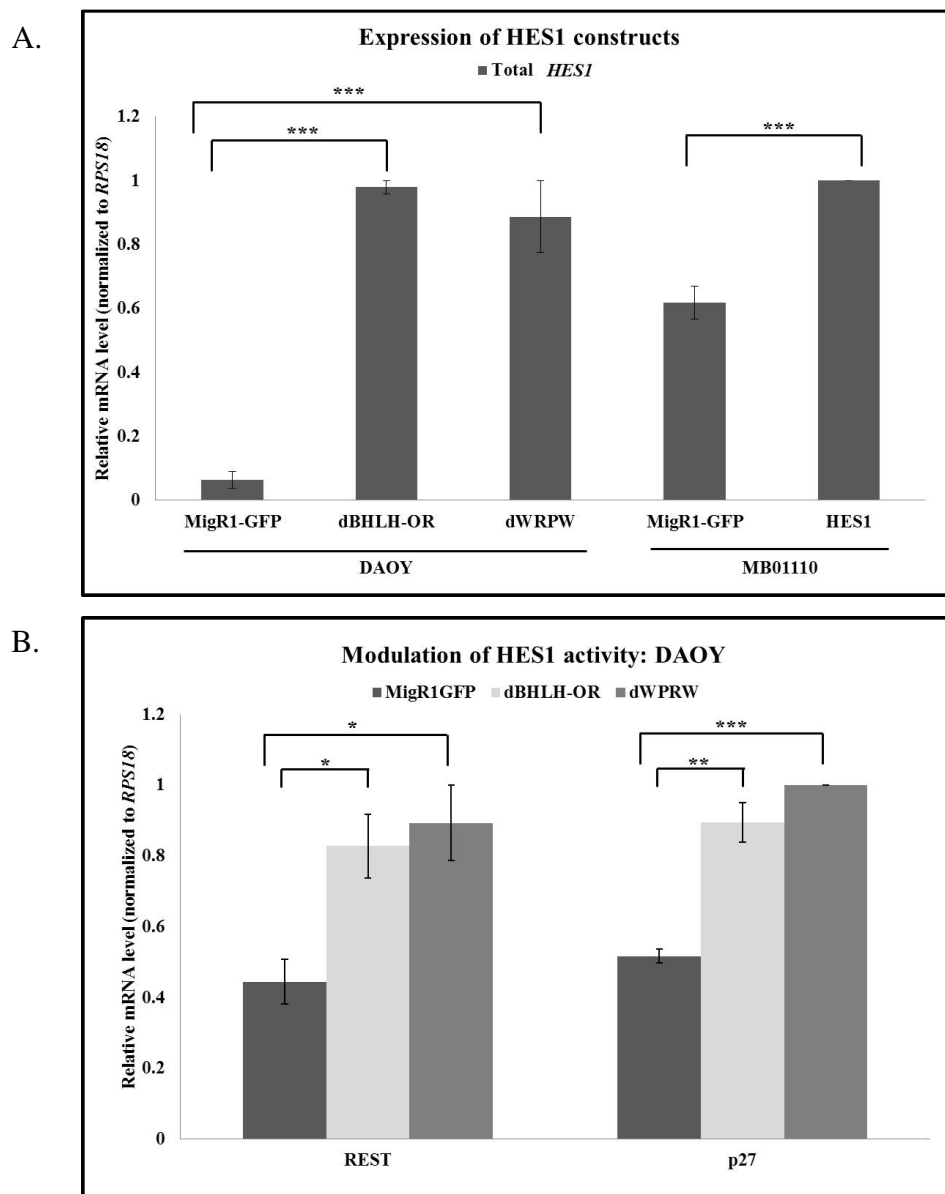


Figure 9: Structure of HES1 constructs. HES1-GFP contains full length HES1. MigR1- Δ bHLH-OR-GFP is a 154 aa C-term deletion mutant of HES1 that lacks proline and WRPW domains. MigR1- Δ WRPW-GFP contains two tryptophan to glycine point mutations in the WRPW domain. All are retroviral constructs with a MigR1 backbone.

In HES1 expressing cell line, DAOY, we interfered with HES1 activity by infecting the cells with retrovirus containing either the HES1 mutants or control MigR1-GFP vector. Conversely, HES1 was ectopically expressed using infection with MigR1-HES1-GFP in MB01110, where HES1 protein was not detected (as depicted in Fig. 7). GFP expression as detected by fluorescence activated cell sorting (FACS) was used as an indicator of transgene expression. GFP positive cells were collected at 72 hour post-infection, and further processed to prepare total RNA and whole cell protein extract.

RNA was analyzed by qRT-PCR using primers specific for human *HES1*, *REST*, *p27*, and *RPS18* transcripts. HES1 has been previously shown to repress *p27*, which is used as a

positive control in all cases (121). Relative *HES1*, *REST*, and *p27* mRNA expression was determined, and *RPS18* was used as the internal control for each sample. We first wanted to ensure that HES1 constructs were indeed expressed upon infection in the two cell lines. We designed primers specific to the bHLH region of the HES1 mRNA which is common to all the HES1 constructs. As expected, an increase in total *HES1* (endogenous and exogenous) was observed in samples infected with HES1 constructs as compared to control infected samples (Fig. 10A). Interfering with endogenous HES1 activity in DAOY cells increased *REST* expression as compared to vector control, whereas ectopic expression of HES1 in MB01110 led to decreased *REST* transcription (Fig. 10B, C). Together, these results suggest that HES1 functions as a repressor of *REST* transcription in medulloblastoma cells.



C.

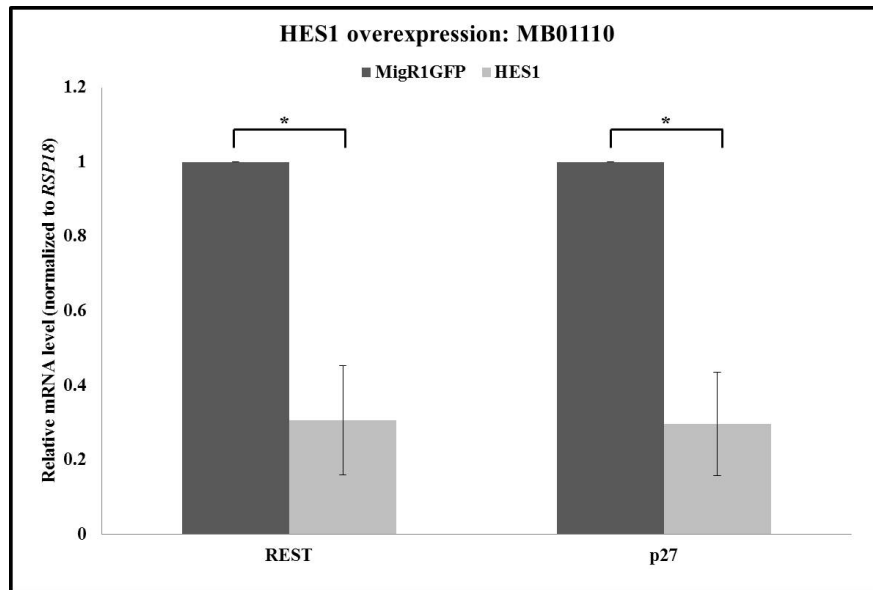
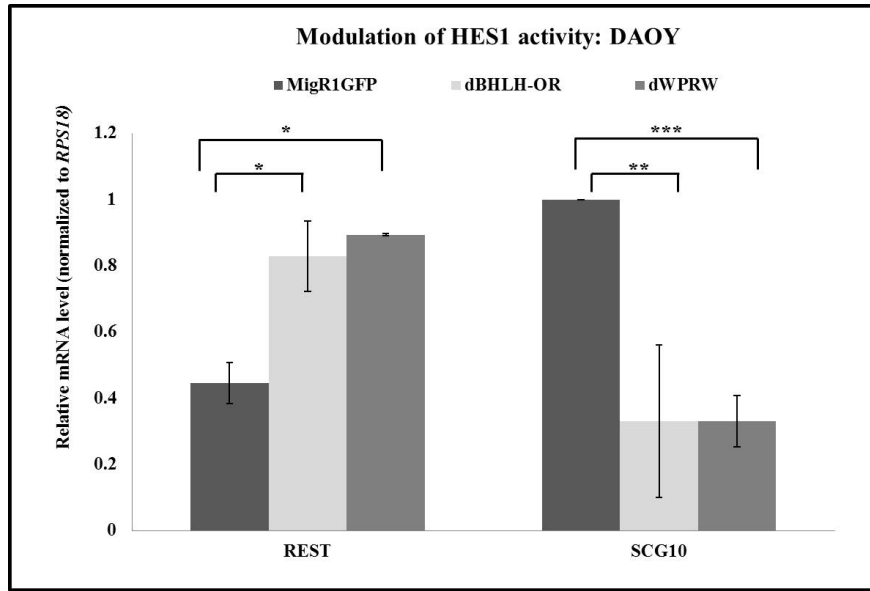


Figure 10: Modulation of HES1 affects *REST* transcription in medulloblastoma cells. A. Total *HES1* expression in DAOY cells infected with MigR1-GFP empty vector, MigR1- Δ BHLH-OR-GFP, or MigR1- Δ WRPW-GFP, and in MB01110 cells infected with MigR1 empty vector or MigR1-HES1-GFP. B. *REST* and *p27* expression in B. DAOY cells C. MB01110 cells infected with above mentioned constructs. Total RNA was extracted and subjected to qRT-PCR analysis to measure *HES1*, *REST*, and *p27*. Samples are normalized to the internal control *RPS18*, and scaled relative to the highest value. Experiments were done in triplicate. One-way ANOVA followed by Fisher LSD post-hoc analysis using Statistica 6.0 was conducted to determine statistical significance (* $p \leq 0.05$, ** $p \leq 0.01$, *** $p \leq 0.001$).

HES1-dependent modulation of *REST* transcription alters *REST* target gene expression.

We next determined whether HES1 mediated changes in *REST* transcription altered the expression of canonical *REST*-target neuronal differentiation genes. RNA prepared from DAOY cells infected with either control virus or virus expressing HES1 mutants, as well as MB01110 cells infected with control virus or HES1 expressing virus, was analyzed via qRT-PCR to measure *Synapsin (SYN1)* and *Superior cervical ganglion-10 (SCG10)* mRNA using *RPS18* as the internal control. Both *SYN1* and *SCG10* are previously validated *REST* targets (50, 57, 123). An inverse correlation is observed between *REST* transcript and its target gene expression in both cell lines (Fig. 11).

A.



B.

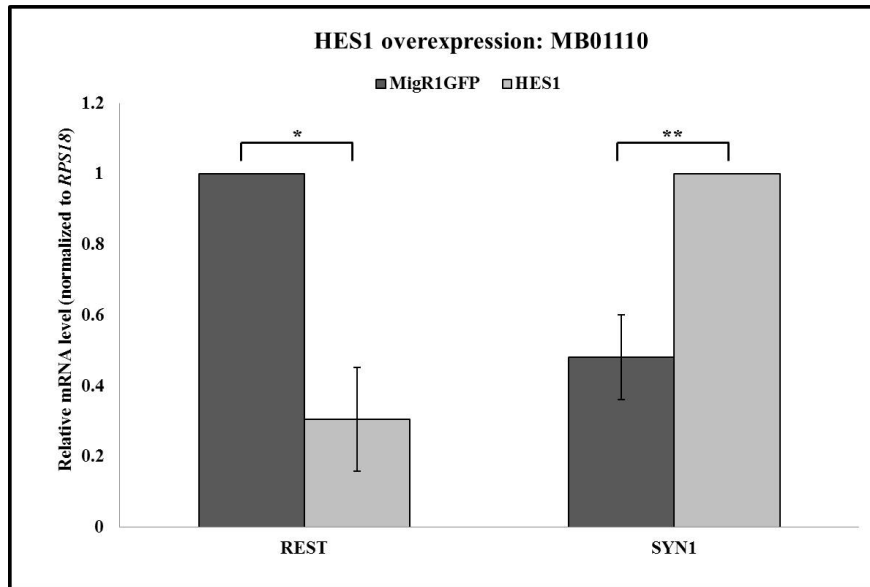


Figure 11: Modulation of *REST* via HES1 affects expression of differentiation genes in medulloblastomas cells. A. DAOY cells infected with either MigR1-GFP empty vector, MigR1- Δ BHLH-OR-GFP, or MigR1- Δ WRPW-GFP. B. MB01110 cells infected with MigR1-GFP empty vector or MigR1-HES1-GFP. Total RNA was extracted and subjected to qRT-PCR analysis to measure *SYN1* and *SCG10*. Samples are normalized to the internal control *RPS18*, and scaled relative to the highest value. Experiments were done in triplicate. One-way ANOVA followed by Fisher LSD post-hoc analysis using Statistica 6.0 was conducted to determine statistical significance (* $p \leq 0.05$, ** $p \leq 0.01$, *** $p \leq 0.001$).

An increase in REST protein was observed upon interference with HES1 activity in DAOY cells at some but not all time points across the time course (48-96 hours). Furthermore,

the change (increase or decrease) in protein was transient and inconsistent when same time points were compared across triplicates. For example, in one of the triplicates REST protein was elevated relative to control infected cells at 48 hours, but decreased at 72 hours, while in another set REST protein levels were lower compared to control at 48 hours, followed by an increase at 72 hours, and a decline at 96 hours. Because of inconsistency in REST protein across triplicates, a representative image is not available. The pattern of transient elevation of REST protein followed by a decline relative to control infected cells suggests either a compensatory mechanism by the cell lines, or differential regulation of REST on a transcriptional and post-transcriptional level so that *REST* transcript does not necessarily correlate with REST protein. In cortical progenitor cells previous studies have shown that REST protein is down-regulated while *REST* transcription remains high, thus providing evidence for differential transcriptional and post-translational regulation of REST in neural cells (52). A separate study investigating the role of REST in retinoic acid mediated differentiation of neuroblastoma cells from our laboratory also reported independent transcriptional and post-translational regulation of REST transcription and protein levels. While *REST* transcription increases in response to retinoic acid treatment in both retinoic acid sensitive and insensitive cells, REST protein levels declined in retinoic acid sensitive cells but were maintained in the insensitive cells (Fig. 34, 35) (124). This disparity in the two cell lines was because of up-regulation of SCF ^{β -TRCP} transcript and protein, the E3 ligase that ubiquitinates REST thereby promoting its proteasomal degradation, in the sensitive cells, while SCF ^{β -TRCP} mRNA and protein were down-regulated in the insensitive cells (Fig. 37) (124).

Interference with HES1 activity provides a survival advantage to DAOY cells

Since we observed a change in the expression of differentiation genes upon HES1 modulation in medulloblastoma cells, we wanted to determine if HES1 modulation also affected survival of these cells. We did a competitive proliferation assay with DAOY cells. We infected DAOY cells with either control MigR1-GFP vector, or HES1 mutants as well as full-length HES1. Cells were analyzed for GFP expression via flow cytometry at either day 3 or 4 post-infection, and analyzed again at day 8, 12, 16, and 23. Percentage of GFP positive cells were calculated for each construct at each time point, and normalized to the first day of flow cytometric analysis (day 4) to provide the change in percentage of GFP positive cells for each construct over time relative to day 4 post-infection. An increase in GFP positive cells over time is considered a survival advantage, while a decrease in GFP positive cells over time

is considered a survival disadvantage. A steady decline in control infected GFP positive cells was observed over time culminating in a 10% decrease at day 23 post-infection (Fig. 12). The latter reflects the effect of the treatment and/or GFP expression itself, and suggests that GFP may be toxic to DAOY cells. Cells infected with Δ BHLH-OR-GFP displayed an positive change in percentage of GFP positive cells at all the time points as compared to control infected cells, thereby suggesting a proliferative advantage over the control infected group (Fig. 12). However, a steady increase in proliferation over time was not observed as indicated by a lack of significant change in GFP positive Δ BHLH-OR-GFP cells at day 4 as compared to other subsequent days. It appears that slight increases in GFP positive cells for the Δ BHLH-OR-GFP group (observed at day 8 and day 16) are quickly adjusted back to the value measured on first day of flow cytometric analysis (day 4), so that overall GFP positive Δ BHLH-OR-GFP cells are maintained at similar percentages across various time points (Fig. 12). The trend noted above may be either because of GFP toxicity to the cells, so that the cells can only maintain GFP positivity for a finite amount of time, or because of up-regulation of compensatory changes by the cells to the modulation of HES1 activity and increase in REST protein. Interestingly, change in the percentage of GFP positive cells from cells from cells infected with Δ WRPW-GFP group appear are maintained at a percentage close to the percentage measured on first day of flow cytometric analysis (day 4) with slight decrease and increase observed at various time points (Fig. 12). No significant difference was observed in the percentage of GFP positive cells over time were between the control infected cells and the cells infected with the Δ WRPW mutant. Since the Δ BHLH-OR mutant lacks the proline and the WRPW domains, while Δ WRPW mutant is a point mutant, the pro-survival effect of the former construct as compared to the latter construct may represent a domain specific contribution of HES1 activity to survival of medulloblastoma cells.

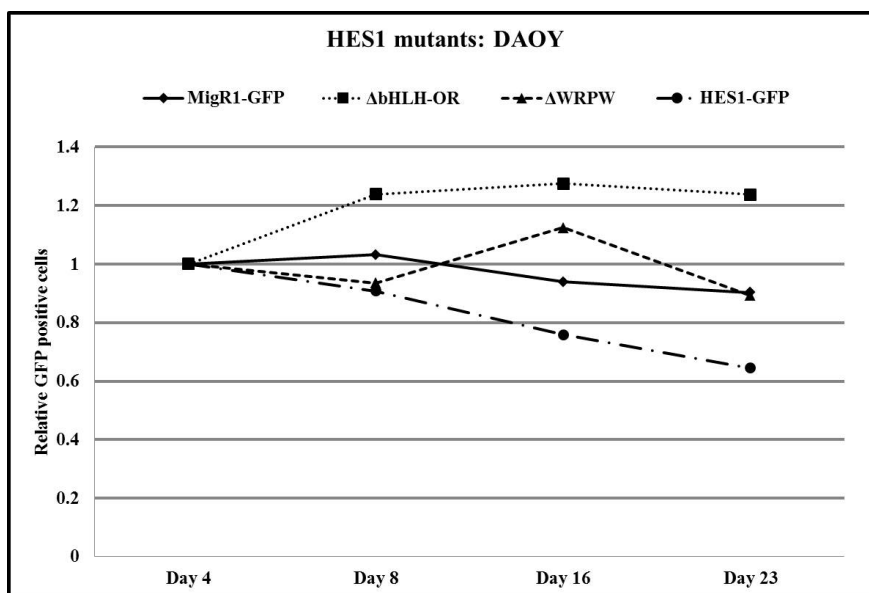


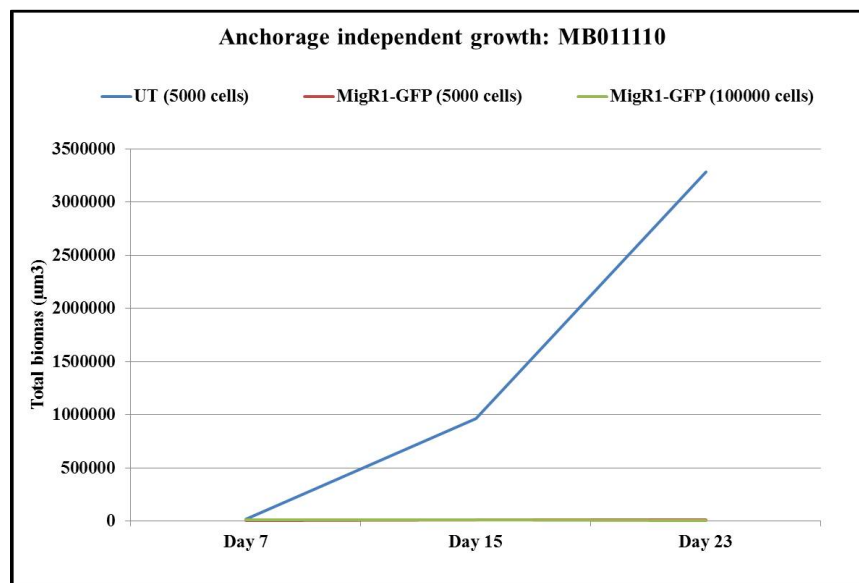
Figure 12: HES1 interference provides a survival advantage, while HES1 overexpression is disadvantageous to cell survival. DAOY cells were infected with either MigR1- ΔbHLH-OR-GFP, MigR1-ΔWRPW-GFP, MigR1-HES1-GFP, or MigR1-GFP vector control. Change in the number of GFP expressing cells was determined over time as compared to vector control, and scaled relative to the number of GFP positive cells observed on the first day of measurement.

Anchorage independent growth assay

Since a change in the survival of medulloblastoma cells was observed upon HES1 modulation of *REST* expression, we next investigated the effect of altering *REST* expression by interfering with HES1 activity on the ability of medulloblastoma cells to grow in an anchorage independent manner. Potential for anchorage independent growth is a hallmark of transformed cells. We used the cell line MB01110 for anchorage independent growth assays, because it is a recently derived cell line from a primary tumor, and therefore may more faithfully recapitulate patient tumor behavior as compared to an established cell line. Data regarding the potential of these cells to display anchorage independent growth is unavailable, so we first determined whether untreated MB01110 were capable of anchorage independent growth. To this end, we plated 5×10^2 , 1×10^3 , 5×10^3 , 1×10^4 , 2.5×10^4 , and 1×10^5 cells in 0.4% agar (top) in 24-well plate, and placed the cells at 37°C with 5% CO₂. Significant colony growth was observed at ~10-12 days after plating in wells with 5×10^3 - 2.5×10^4 cells, with 5×10^3 cells yielding ~250-300 colonies (Fig. 13). We plated 5×10^3 cells in each of the 24 wells for all subsequent experiments. MB01110 cells appear to be sensitive to the process of infection as well as the subsequent increase in PSF concentration (from 1% to 4%) necessary after sorting to avoid

contamination. Treatment with control plasmids and reagents caused increased cell death, morphological changes, and a decreased cell growth rate. We wanted to know if these changes would affect the capacity for anchorage independent growth of these cells, so we compared the untreated with control MigR1-GFP infected and sorted cells after increased PSF treatment. While only 5×10^3 cells of untreated MB01110 were plated, MigR1-GFP infected cells were plated at varying densities of 5×10^3 , 1×10^4 , 2.5×10^4 , and 1×10^5 cells (Fig. 13). Cells were plated, and scanned starting at day 7 at indicated time points. Total colony number ($>80 \mu\text{m}$) and approximate colony volume (total biomass in μm^3) were determined using Gel Count software. The data shown below is for 5×10^3 and 1×10^5 MigR1-GFP infected cells. Indeed our results show a stark decrease in capacity for anchorage independent growth in MigR1-GFP infected PSF-treated cells (700-820 versus 8-20 at day 23) (Fig 13). As of now, because of the sensitivity of this cell line, meaningful analysis across various treatment groups is not feasible. The assay was attempted with sorted cells that were not treated with PSF, but were terminated because of contamination issues. A feasible alternative may be to altering *REST* expression by interfering with HES1 activity in DAOY cells, and measuring the change in the potential for anchorage independent growth between cells infected with mutants and control infected cells.

A.



B.

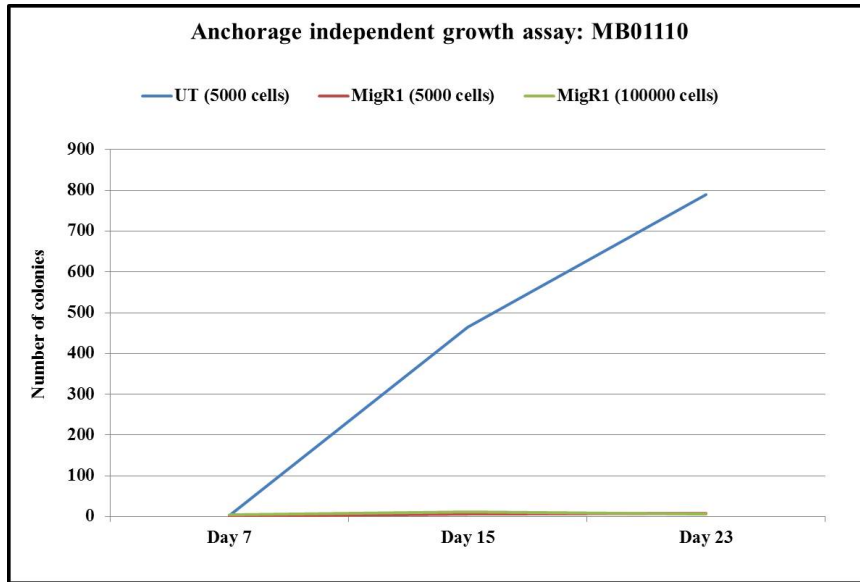


Figure 13: Treatment with reagents lead to a decrease in anchorage independent growth potential of MB01110 cells. Infection of MB01110 cells with vector alone followed by increased PSF exposure leads to a drastic decrease in soft agar growth potential of these cells as compared to untreated cells as measured by A. Total biomass and B. Number of colonies.

Summary

We have shown that HES1 binds to the *REST* 5' upstream region in both DAOY and D283 cell lines. Interference of HES1 activity using mutagenic HES1 constructs in DAOY cells, which express HES1 protein, led to an increase in *REST* and *p27* transcription, whereas overexpressing HES1 in MB01110, a cell line with no detectable HES1 protein, led to a decrease in *REST* and *p27* expression. These findings are consistent with the function of HES1 as a repressor of its target genes, as well as its previously published role in regulation of *REST* expression in non-neural cells (82). Furthermore, HES1-mediated modulation of *REST* also leads to changes in the expression of REST target genes, *SCG10* and *SYN1*. Transcriptional repression of *REST* by HES1 perhaps serves to counterbalance REST overexpression observed in a subset of medulloblastoma tumors. Given the previously published oncogenic role of REST in medulloblastoma as well as the increase in HES1 protein in some medulloblastoma samples, down-regulation of *REST* transcription by HES1 may partially counter the oncogenic capacity of REST, thereby providing an anti-tumorigenic role for this mechanism (25-27). The latter interpretation is supported by the results from our survival analysis of DAOY cells which reveal that interfering with HES1 activity using a C-terminus deletion mutant of HES1 (MigR1- Δ bHLH-OR-GFP) provides a survival advantage over time to DAOY cells as measured by a competitive proliferation assay, while a decrease in proliferation is observed upon overexpression of HES1.

Chapter 4: REST regulates its own transcription by an auto-regulatory loop

Rationale

To evaluate if factors other than HES1 contribute to the transcriptional regulation of *REST* in medulloblastoma, we analyzed *REST* 5' upstream region for potential binding sites of various transcription factors using transcription factor search tool, <http://mbs.cbrc.jp/research/db/TFSEARCH.html>. We validated the search results with our own detailed analysis of specific sequences based on an extensive literature search. These analyses identified binding sites to additional transcription factors, of which some were novel, while others were previously known to regulate *REST* expression. Since medulloblastoma is a developmental tumor, and *REST* regulates lineage specificity during development, we focused on the molecules that were relevant to these processes.

Interestingly, the *REST* 5' upstream region contains three *RE-1* sequences located 0.8 kb downstream of TS, and -6.2 kb and -6.8 kb upstream of TS (Fig. 14). A ChIP screen for *REST* binding in the non-neural Jurkat cells identified the *RE-1* site located 0.8 kb downstream of TS, thereby providing potential for self-regulation (65). The latter provided more confidence to our analysis, which revealed three potential binding sites.

A recent study demonstrated a feedback loop involving *REST*, beta-catenin, and tuberous sclerosis-2 (TSC-2) in the regulation of *REST* transcription in both rat (PC12) and human (NT2/D1) neural cells (83). However, to our knowledge, direct regulation of *REST* transcription by *REST* has not been explored and is the focus of this section. **We hypothesized that *REST* can bind to *RE-1* sites located in its own 5' upstream region, and regulate its own expression in an auto-regulatory loop.**

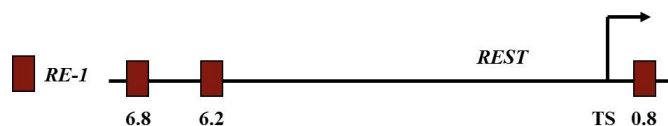


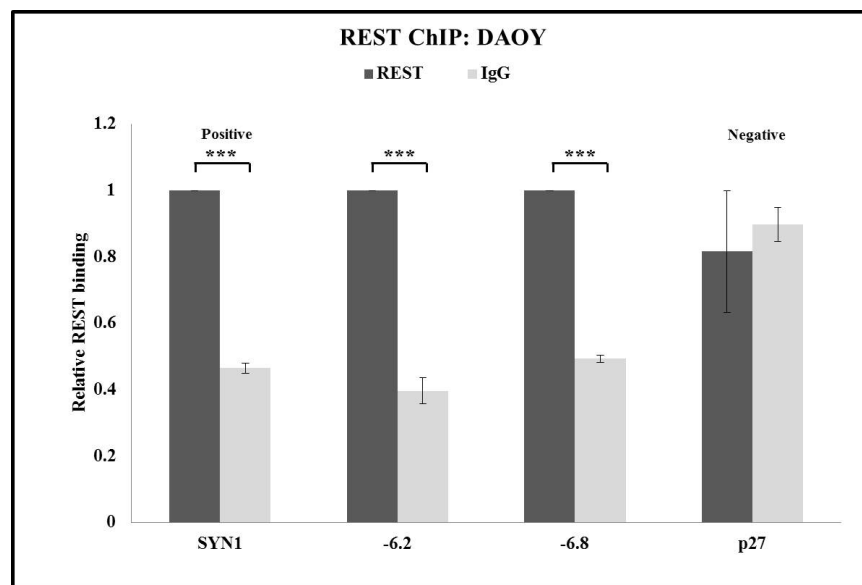
Figure 14: *RE-1* sites on the 5' upstream region of *REST*. Shown here is the -7 kb region of *REST* 5' upstream region containing the three *RE-1* sites. The consensus site located +0.8 kb from TS was previously identified in a ChIP-seq screen.

Results

REST binds to the *RE-1* sites on *REST* 5' upstream region

We first determined whether REST binds to the *RE-1* sites discovered on its 5' upstream region in medulloblastoma cell lines. DAOY and D283 cells, which have been previously shown to have high levels of REST protein, were used for this experiment (25). Nuclear lysates from the two cell lines were subjected to ChIP using with rabbit anti-REST antibody or control serum IgG, and immunoprecipitated DNA fragments were analyzed by qPCR using primers specific to *RE-1* sites located -6.2 kb and -6.8 kb from TS (Fig. 15). High GC content of the region surrounding the *RE-1* site located +0.8 kb from TS precluded its analysis by qPCR despite multiple attempts. Relative REST binding to the region of interest was determined by comparing the non-specific control values (IgG) with the specific sample values (REST). REST occupancy at *RE-1* located at *SYN1* promoter was used as a positive control as before. Regions within *p27* and *p63* 5' upstream regions that lack *RE-1* sites were used as the negative controls for DAOY and D283 cells respectively. A statistically significant difference in relative REST binding with the specific antibody pull-down as compared to IgG was seen, suggesting that REST associates with *REST* 5' upstream region in both DAOY and D283 cells.

A.



B.

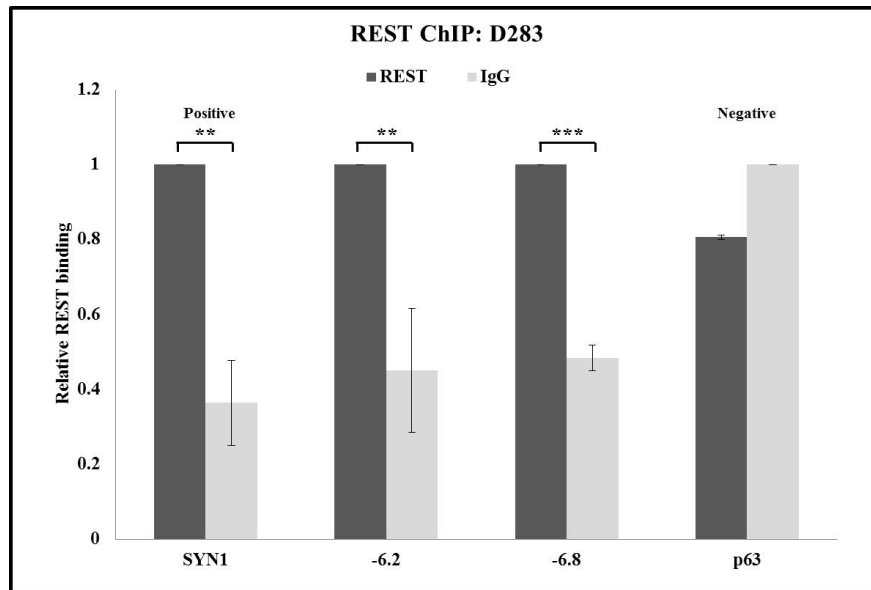


Figure 15: REST binds to 5' upstream region of *REST* in medulloblastomas cell lines. ChIP was performed in A. DAOY and B. D283 with rabbit anti-REST antibody or control IgG, followed by qPCR analysis using primers specific to *N-boxes* located -3.7 kb, -4.4 kb, and -6.5 kb from the TS. Experiments were done in triplicate. Experiments were done in triplicate. One-way ANOVA followed by Fisher LSD post-hoc analysis using Statistica 6.0 was conducted to determine statistical significance (* $p \leq 0.05$, ** $p \leq 0.01$, *** $p \leq 0.001$).

REST directly represses its own expression via an auto-regulatory feedback loop

To determine if REST regulated its own expression by an auto-regulatory feedback loop, we interfered with endogenous REST activity by using a mutant of REST (MigR1-DBD-GFP). This mutant contains only the DBD of REST (73-542 aa), but not the two repression domains, thereby allowing REST to bind to its target site, but abrogating its repressive function (Fig. 16). MigR1-DBD-GFP was a modified from pcDNA3.1-DBD, by moving the DBD region from pcDNA3.1 to MigR1-DBD. As with the HES1 constructs, it contains the retroviral backbone of the MigR1-GFP.

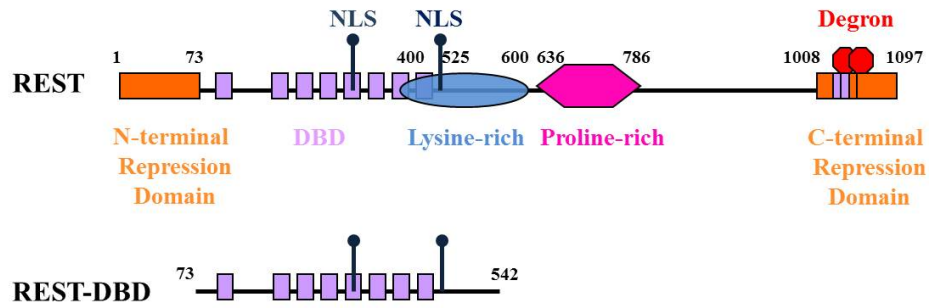


Figure 16: Structure of full-length REST and REST-DBD. Top diagram shows the structure of full length REST, while the bottom shows the structure of MigR1-DBD-GFP. Lacking both repression domains, MigR1-DBD-GFP contains 73-542 aa. It is a retroviral construct with a MigR1-GFP backbone.

DAOY cells were infected with either retrovirus expressing empty vector or REST-DBD. GFP expression was used as an indicator of transgene expression, and the GFP positive cells were sorted by FACS at 72 hours post-infection, and further processed for extracting total RNA. RNA was analyzed via qRT-PCR using primers specific for human *REST*, *SYN1*, *SCG10*, and *RPS18* transcripts. *SYN1*, a known REST target gene, is used as a positive control in all cases as before. Relative *REST*, *SYN1*, and *SCG10* mRNA expression was determined, and *RPS18* was used as the internal control for each sample. Interfering with endogenous REST activity in DAOY cells increased *REST* expression as compared to vector control, thereby suggesting that REST regulates its own transcription via a feedback loop (Fig. 17).

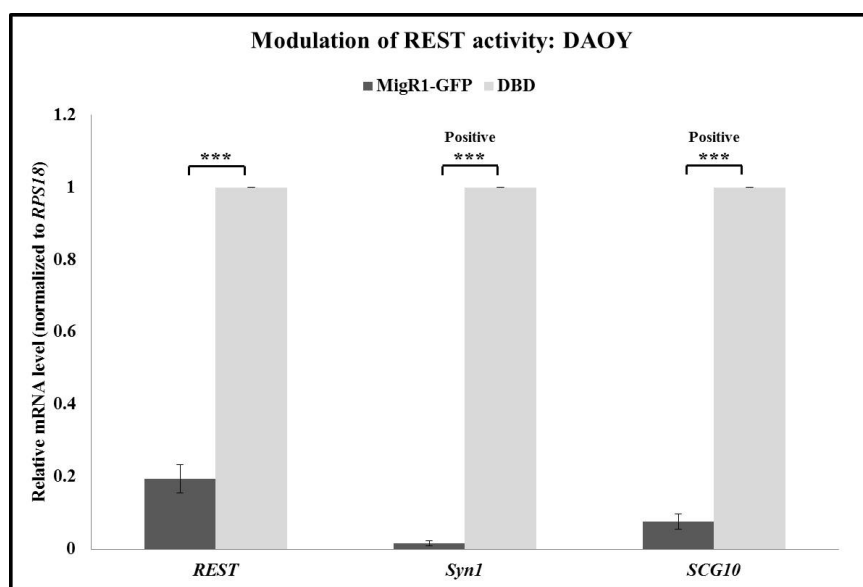


Figure 17: Countering REST activity represses *REST* transcription in medulloblastoma cells. Endogenous *REST*, *SYN1*, and *SCG10* expression in DAOY cells infected with above mentioned constructs. Total RNA was extracted and subjected to qRT-PCR analysis to measure total *REST*, endogenous *REST*, *SYN1*, and *SCG10*. Samples are normalized to the internal control *RPS18*, and scaled relative to the highest value. Experiments were done in triplicate. One-way ANOVA followed by Fisher LSD post-hoc analysis using Statistica 6.0 was conducted to determine statistical significance (* $p \leq 0.05$, ** $p \leq 0.01$, *** $p \leq 0.001$).

To test whether the effect of REST regulation of its own expression was directly modulated by REST binding to the *RE-1* sites, we performed a luciferase assay with either wildtype *RE-1* sites or mutagenized *RE-1* sites. We used pGL4.15 which contains a mammalian selection marker (hygromycin), so that stable lines containing the luciferase construct could be generated. Because we were unable to clone the entire *REST* 5' upstream region, we decided to clone only the -6.2 kb to -6.8 kb piece with the *RE-1* sites. However, pGL4.15 does not have a minimal promoter, which is necessary since the entire REST promoter could not be used. We therefore introduced an sv40 minimal promoter from pGL3 promoter vector upstream of the *luciferase* gene to yield pGL4.15-sv40. Genomic DNA extracted from DAOY cells was used as the template to PCR the 5' upstream region from -7 kb to -6 kb using specific primers flanked with unique restriction sites, and further cloning was done to ensure the validity of the piece. The insert was then ligated into pGL4.15-sv40 immediately upstream of the sv40 promoter to yield pGL4.15--7to-6-sv40 (hereby called pGL-sv40-WT) (Fig. 18). Since the consensus sequence for *RE-1* is not very well conserved, careful

consideration was taken to ensure that the mutated sequence did not match any *RE-1* of the potential *RE-1* sequences. Below are the *RE-1* sequences for each of the *RE-1* sites on the REST 5' upstream region as well as the mutagenized sequence (Table 1). The luciferase construct with mutagenized *RE-1* sites was generated using specific primers (hereby called pGL-sv40-*RE-1*mut) (Fig. 18).

Table1: Sequence of *RE-1* sites and mutated *RE-1*

<i>RE-1</i> site	Wild-type	Mutated
-6.8 kb from TS	5'- TTAGCTGGGCGTGGTGGTGTG -3'	5'- CAGTTAA <u>AA</u> ACCGCGGTTAATT - 3'
-6.2 kb from TS	5'- CCAGCTACTCGGGATGCTGAA -3'	5'- CAGTTAA <u>AA</u> ACCGCGGTTAATT - 3'

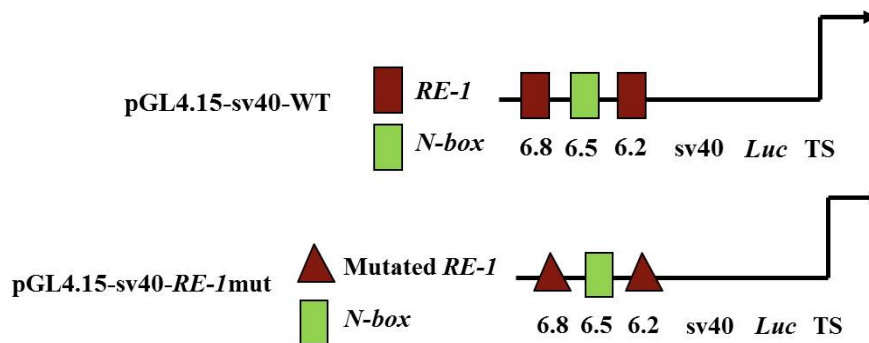


Figure 18: Structure of REST luciferase constructs: pGL4.15-sv40-WT and pGL4.15-sv40-*RE-1*mut used in our analyses.

Both pGL4.15-sv40 and pGL4.15-6.8to-6.2-sv40 were transfected into DAOY cells and selected with hygromycinB (0.3µg/mL) to generate stable expression of the luciferase construct. Cells were lysed, and luciferase activity of cells infected with both wildtype and mutagenized construct was measured using a luminometer (Fig. 19). Luciferase activity increases upon mutagenizing the *RE-1* site as compared to the wildtype construct, thus suggesting that REST directly represses its own expression in an autoregulatory feedback loop (Fig. 19).

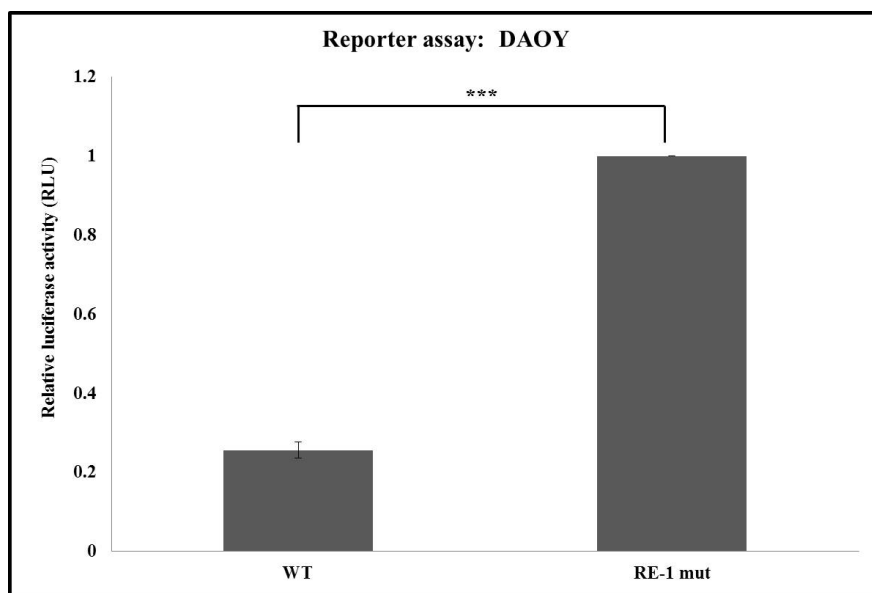


Figure 19: Mutating *RE-1* sites leads to increased luciferase activity. Luciferase constructs with either wildtype *RE-1* sites or mutated *RE-1* sites were stably expressed in DAOY cells and luciferase expression was measured, and scaled from 0 to 1. Experiments were done in triplicate. One-way ANOVA followed by Fisher LSD post-hoc analysis using Statistica 6.0 was conducted to determine statistical significance (* $p \leq 0.05$, ** $p \leq 0.01$, *** $p \leq 0.001$).

Interference with REST activity does not provide a survival advantage to DAOY cells

Since REST has been shown to have a tumorigenic effect in medulloblastoma cells, we to know if disrupting the auto-regulatory mechanism contributing to *REST* regulation would alter survival potential of these cells. We infected DAOY cells with either control MigR1-GFP vector or MigR1-REST-DBD and performed a competitive proliferation assay as previously described. Flow cytometric analysis to determine percentage of GFP positive cells was done at the times indicated. As described previously, a steady decline in control infected GFP positive cells was observed over time culminating in a 10% decrease at day 23 post-infection (Fig. 20). The latter reflects the effect of the treatment and/or GFP expression itself, and suggests that expression of GFP may be toxic to these cells. Overall, no change in percentage of GFP positive cells was detected between control and vector treated cells (Fig. 20). This is consistent with what we expected since REST appears to be auto-regulating its transcription. These results corroborate our mRNA findings upon REST modulation (Fig. 20).

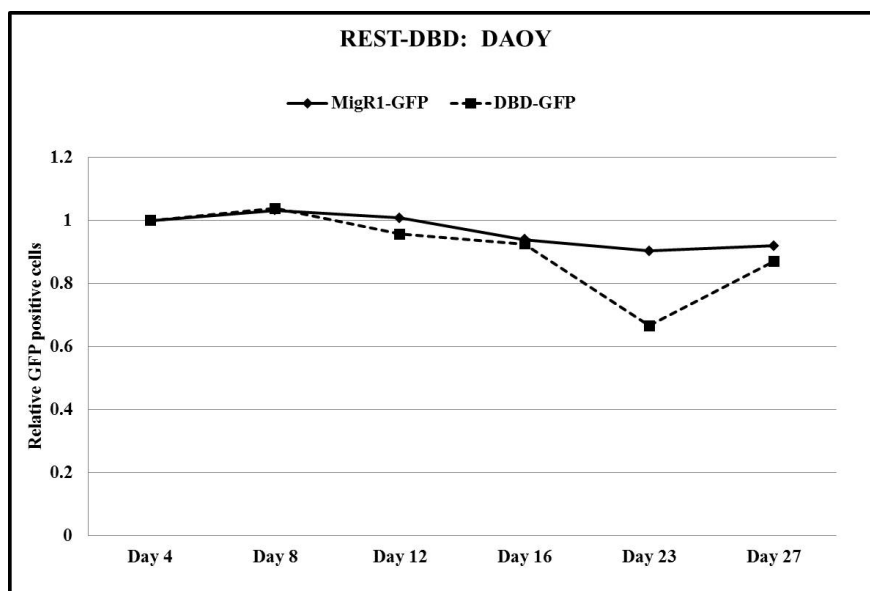


Figure 20: No change in cell survival is observed upon REST interference. DAOY cells were infected with either control MigR1-GFP vector or MigR1-DBD-GFP. Change in the number of GFP expressing cells was determined over time as compared to vector control, and scaled relative to the number of GFP positive cells observed on the first day of measurement.

Summary

In this section we have shown that REST binds to the *RE-1* sites located -6.2 kb and -6.8 kb upstream of TS on the 5' upstream region of REST. Interference with REST activity using a mutant of REST (REST-DBD) leads to an increase in *REST* transcription and a reciprocal up-regulation of other REST target genes, thus suggesting that REST represses its own transcription through an auto-regulatory loop. The repressive function of REST on its own transcription is consistent with the canonical role of REST as a repressor of its target genes. Our findings are further supported by the increase in the luciferase expression of the cells containing the luciferase construct with mutagenized RE-1 sites as compared to those with the wildtype luciferase construct, which indicated that the effect of REST on its expression was directly mediated by its binding to the *RE-1* sites. No change in survival was observed upon in the cells expressing mutant REST construct as compared to the control construct. Since expression of REST-DBD leads to an increase in *REST* expression, the presence of increased REST protein can potentially compete with REST-DBD for binding to the *RE-1* site, thereby restoring the REST levels back to baseline, so that no significant change would be observed in survival between REST-DBD and control vector expressing cells. It would be interesting to determine whether increased REST transcription correlates with decreased REST protein in patient samples.

Chapter 5: HES1 and REST co-regulate of *REST* transcription

Rationale

Interestingly, we noticed that the previously validated *N-box* for HES1 binding located -6.5 kb upstream of TS was in close proximity to the two *RE-1* sites (-6.2 and -6.8 kb upstream of TS) (Fig. 21). Both HES1 and REST interact with mSin3 and HDAC 1 and HDAC2, which are important in their co-repressor function, and as mentioned before, HES1 and REST are both implicated in medulloblastoma and normal brain development. Since we have shown both proteins independently bind to the *REST* 5' upstream region, and repress *REST* expression, we wanted to determine whether the HES1 and REST could potentially function together to co-regulate *REST* transcription. **We hypothesized that REST and HES1 co-regulate *REST* expression.**

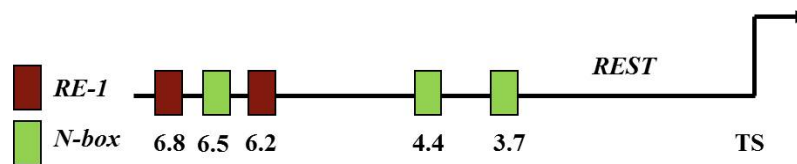


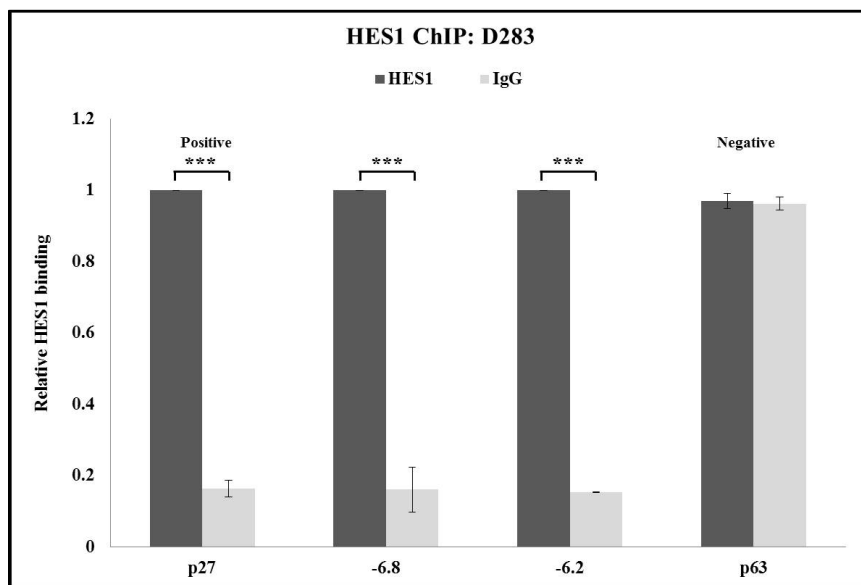
Figure 21: *RE-1* sites and *N-boxes* on the 5' upstream region of *REST*. Shown here is the -7 kb region of *REST* 5' upstream region containing the two *RE-1* sites and three *N-boxes*. The *RE-1* sites located -6.8 kb and -6.2 kb from TS are in close proximity to the *N-box* located -6.5 kb from TS.

Results

HES1 and REST bind to *RE-1* sites in *REST* 5' upstream region.

To study whether HES1 and REST could potentially co-regulate *REST* expression, we first determined whether HES1 occupied the two *RE-1* sites located at -6.2 kb and -6.8 kb in close proximity to the *N-box* located at -6.5 kb from TS (previously validated for REST binding as show in Fig.15), as well as the status of REST occupancy at *N-boxes* located -3.7 kb, -4.5 kb, and -6.5 kb from TS (previously validated for HES1 binding as shown in Fig. 8). We subjected immunoprecipitated DNA from HES1 and REST ChIP assays performed in D283 and DAOY cells to qPCR with primers specific to the *RE-1* sites and *N-boxes* respectively (Fig. 22). A statistically significant difference in relative HES1 binding with the specific antibody pull-down as compared to control serum IgG was seen, thus suggesting that HES1 binds to the *RE-1* sites in D283 cells (Fig. 22A). No occupancy of REST is observed at any of the *N-boxes* in either cell line (Fig. 22B, C). The latter suggests that perhaps HES1 and REST may potentially co-occupy the two *RE-1* sites, and that HES1, in conjunction with REST, may modulate *REST* expression at these sites.

A.



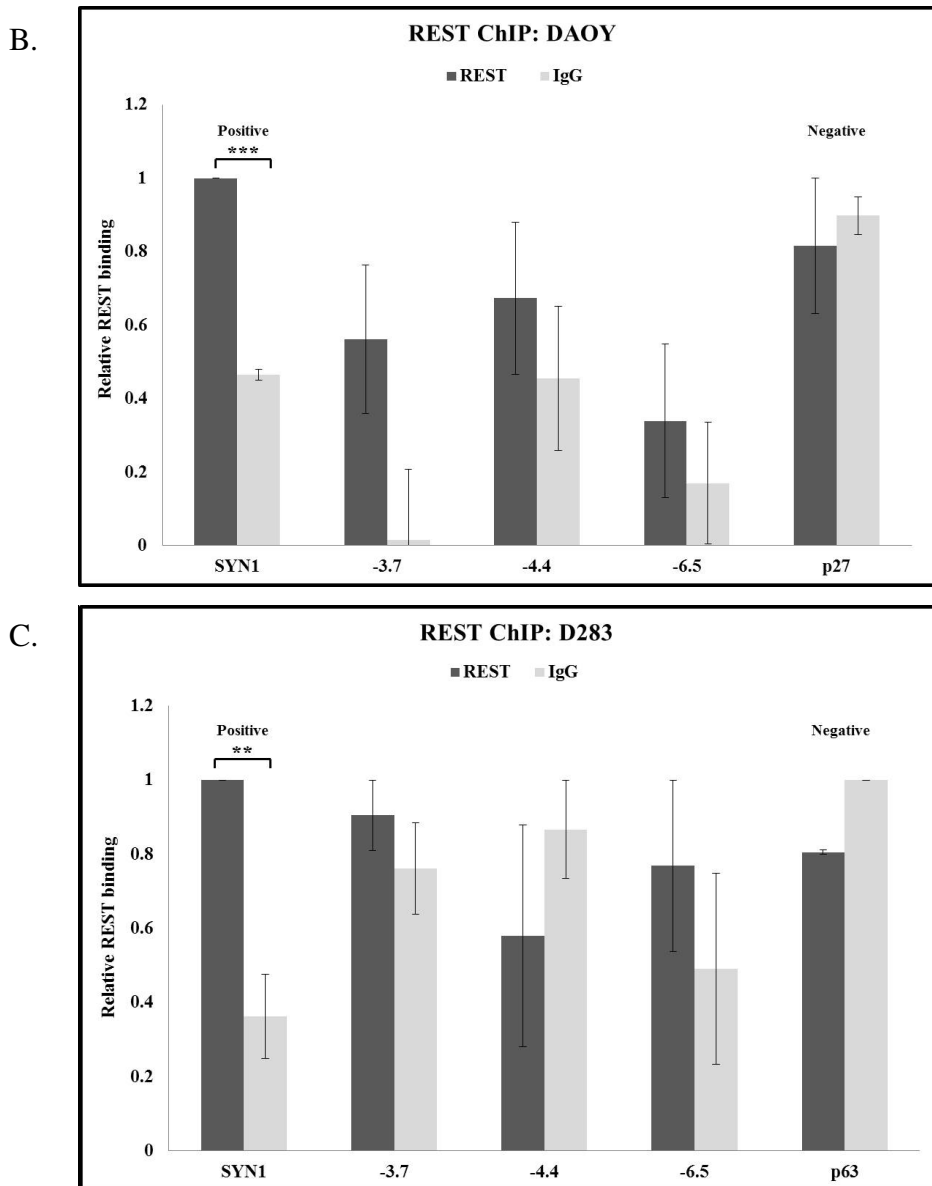


Figure 22: HES1 binds to the *RE-1* sites in 5' upstream region of *REST* in medulloblastomas cells. HES1 ChIP samples from A. D283 were analyzed by qPCR using primers specific to N-boxes located *RE-1* site located -6.2 kb and -6.8 kb from TS. REST ChIP samples from B. DAOY and C. D283 cells were analyzed by qPCR using primers specific to -3.7 kb, -4.4 kb, and -6.5 kb from the TS. Experiments were done in triplicate. One-way ANOVA followed by Fisher LSD post-hoc analysis using Statistica 6.0 was conducted to determine statistical significance (* $p \leq 0.05$, ** $p \leq 0.01$, *** $p \leq 0.001$).

HDAC1 and HDAC2 are part of REST as well as HES1 repressor complexes (HDAC1 is associated more consistently with HES1 as compared to HDAC2), so we determined whether HDAC1 and HDAC2 occupied our sites of interest as indicators of REST and HES1 occupancy and repressive function. ChIP assays was done by immunoprecipitating with mouse anti-

64

HDAC1 and anti-HDAC2 antibodies or control sera IgG followed by incubation with rabbit anti-mouse linker incubated beads. Immunoprecipitated DNA was analyzed by qPCR using primers specific to -3.7 kb, -4.4 kb, -6.5 kb, and -6.2 kb and -6.8 kb from the TS (Fig. 23). Based on the statistically significant difference in relative HDAC1 and HDAC2 binding with the specific antibody pull-downs as compared to control IgG, both HDAC1 and HDAC2 appear to be bound to the two *RE-1* sites, whereas neither is bound at the *N-box* located at -6.5 kb upstream of TS (Fig. 23). Only HDAC1 occupancy was detected to *N-boxes* located at -3.7 and -4.4 kb upstream of TS (Fig. 23). Differential HDAC1 and HDAC2 occupancy at the sites tested indicates unique regulation of these sites, with HES1 and REST perhaps co-regulating gene expression via the two *RE-1* sites. The absence of both HDACs, despite the presence of HES1, at -6.5 kb region suggests that either HES1 is bound but not functional at this site, or that HES1 is regulating gene expression but not by its canonical function as a repressor at this site. A luciferase with each site of interest mutagenized individually as well as in combination would be required to better understand the significance of presence and absence of these complexes at individual sites. Furthermore, HES1 or REST may be required for the other one to bind at these sites and ChIP experiments with deletions of each would be needed to evaluate this.

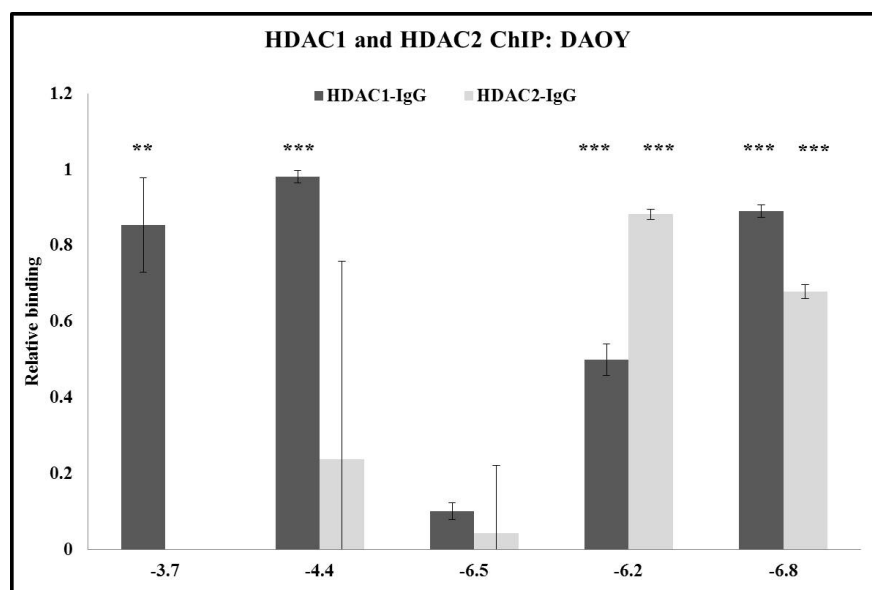


Figure 23: HDAC1 and HDAC2 bind to the *RE-1* sites in 5' upstream region of *REST* in medulloblastomas cells. CHIP was performed in DAOY with mouse anti-HDAC1 and anti-HDAC2 antibodies or control IgG, followed by qPCR analysis using primers specific to *RE-1* sites and *N-boxes* located -3.7 kb, -4.4 kb, -6.2 kb, -6.5 kb, and -6.8 kb from the TS. Experiments were done in triplicate. One-way ANOVA followed by Fisher LSD post-hoc analysis using Statistica 6.0 was conducted to determine statistical significance (* $p \leq 0.05$, ** $p \leq 0.01$, *** $p \leq 0.001$).

HES1 and REST co-occupy *RE-1* sites in *REST* 5' upstream region.

Thus far we have shown that HES1 and REST independently occupy the two *RE-1* sites, and HDAC1 and HDAC2 occupancy at these sites suggests the presence of REST and HES1 repression complexes. To determine whether HES1 and REST simultaneously co-occupy the *RE-1* sites, nuclear lysates prepared from DAOY cells were subjected to a sequential ChIP assay (SeqChIP) by immunoprecipitating first with the rabbit anti-HES1 antibody or control serum IgG, and then with rabbit anti-REST antibody or control serum IgG. The immunoprecipitated DNA was analyzed by qPCR using primers specific to the -6.2 kb and -6.8 kb (*RE-1* sites), and -3.7 kb, -4.4 kb, -6.5 kb (*N-boxes*) from TS. Relative HES1-REST binding to the region of interest was determined by comparing the control values (IgG/IgG) from the sample values (HES1/REST) (Fig. 24). A statistically significant difference using HES1 and REST co-occupancy using specific antibodies as compared to control sera IgG is seen at the *RE-1* sites located at -6.2 kb and -6.2 kb from TS, thus suggesting that HES1 and REST co-occupy the two *RE-1* sites. No co-occupancy was detected at the *N-boxes* located -3.7 kb, -4.4 kb, and -6.5 kb upstream of TS (Fig. 24). Co-occupancy of REST and HES1 suggests that HES1 could potentially cooperate with REST to regulate *REST* transcription at the *RE-1* sites.

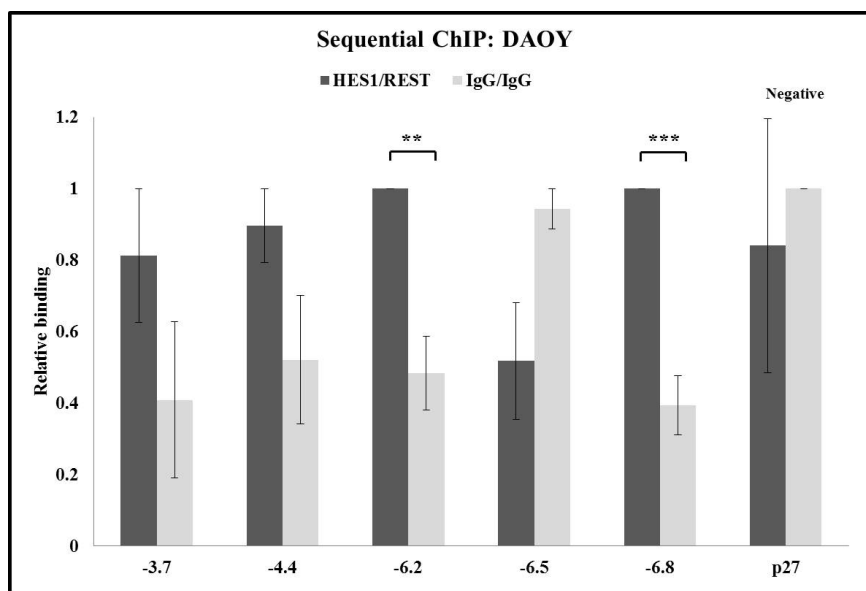


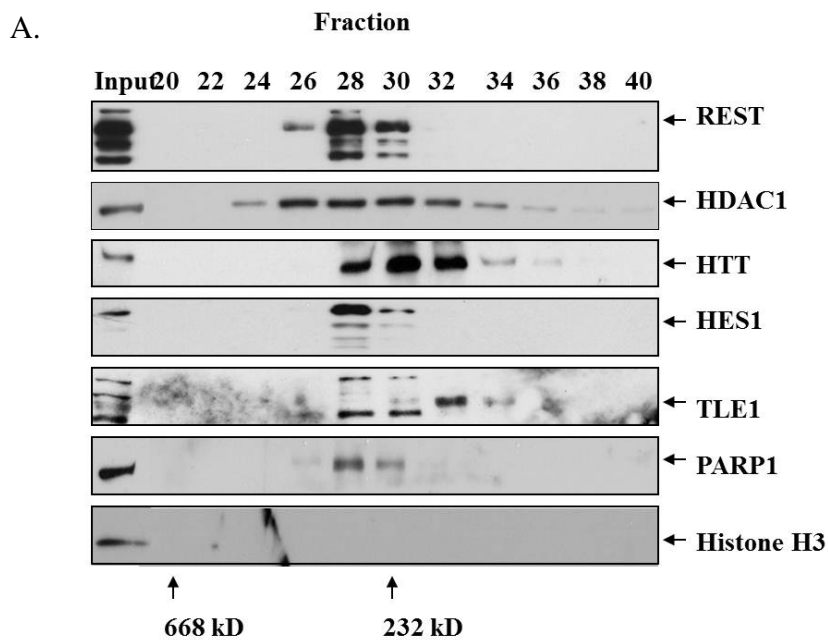
Figure 24: HES1 and REST co-occupy *RE-1* sites in DAOY cells. Sequential ChIP was performed in DAOY by immunoprecipitating first with rabbit anti-HES1 antibody or control IgG, and subjecting the eluents to a second immunoprecipitation with rabbit anti-REST antibody or control IgG. Samples were analyzed by qPCR analysis using primers specific to *RE-1* sites and *N-boxes* located -3.7 kb, -4.4 kb, -6.2 kb, -6.5 kb, and -6.8 kb from the TS. Experiments were done in triplicate. One-way ANOVA followed by Fisher LSD post-hoc analysis using Statistica 6.0 was conducted to determine statistical significance (* $p \leq 0.05$, ** $p \leq 0.01$, *** $p \leq 0.001$).

HES1 and REST interact in DAOY cells.

Since the SeqChIP data suggests that REST and HES1 co-occupy *RE-1* sites on the *REST* 5' upstream region in medulloblastoma cell lines, we wanted to determine whether REST and HES1 form a complex in these cells. We did a co-fractionation experiment in which whole cell lysate prepared from DAOY cells were subjected to a sephadex column, and separate fractions were collected every 5.5 minutes. Fractions were analyzed by Western blot analysis for REST, HDAC1, Huntingtin (HTT), HES1, TLE-1, Poly adenosine diphosphate (ADP) – ribose polymerase (PARP), and histone H3 (Fig. 25A). HTT has been shown to interact with REST, whereas TLE-1 and PARP have been shown to complex with HES1, and were used as positive controls for interaction with each protein (80, 81, 109, 110, 112). HDAC1 has been shown to interact with both REST and HES1. We consolidated two adjacent fractions into one to allow visualization of all fractions on one SDS-PAGE gel (in order to avoid variability from one gel to another). Detection of proteins in the same fraction suggests potential interaction between them. REST and HES1 were detected in the some of the same fractions, although both

proteins appear independently of one another in other fractions as well (Fig. 25A). The latter suggests that a portion of REST and HES1 proteins may interact together in DAOY cells. Positive controls for HES1 and REST also appear in the same fractions as each protein respectively, thereby validating our findings. Histone H3 was not observed in the fractions, which suggests that the potential HES1-REST interaction maybe independent of DNA binding of HES1 and REST, although further experiments are necessary to conclusively exclude the necessity of DNA to the HES1-REST interaction.

To verify the results of the co-fractionation experiments, we did a co-immunoprecipitation (co-IP) experiment using lysates prepared from DAOY transfected with either MigR1-FlagREST-GFP or MigR1-FlagHES1-GFP, and performed co-IP by immunoprecipitating with the anti-flag antibody, and subjecting the immunoprecipitated lysates to Western blot analysis for HES1 and REST (Fig. 25B). HES1 and REST were both detected in immunoprecipitates from DAOY cells overexpressing REST and HES1 respectively, thereby suggesting an interaction between that the two proteins in DAOY cells (Fig. 25B).



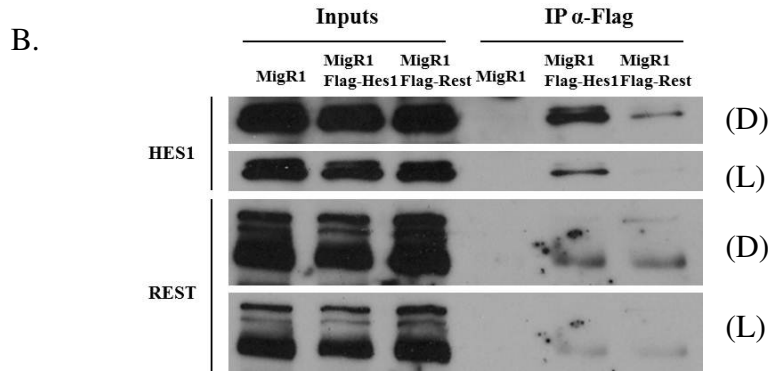


Figure 25: HES1 and REST interact in DAOY cells. A. Lysates from DAOY cells were subjected to a co-fractionation assay by passing through a Sephadex column followed by analysis of samples by Western blot analysis. B. Lysates prepared from DAOY cells transfected with either control MigR1-GFP vector, MigR1-HES1-GFP, or MigR1-REST-GFP were immunoprecipitated with anti-Flag antibody or control IgG, and analyzed by Western blot analysis. Both dark (D) and light (L) exposures are shown.

Interfering with REST activity in the absence of HES1 increases *REST* transcription

To study the effect of interference with REST activity in the absence of HES1 on REST transcription, we infected MB01110 (a cell line that does not have any detectable HES1 protein) with retrovirus expressing REST-DBD or control vector. GFP positive cells were sorted by FACS at 72 hours post-infection, and further processed for extracting total RNA. qRT-PCR was performing using primers specific for human *REST*, *SYN1*, *SCG10*, and *RPS18* transcripts. As mentioned above, REST has been previously shown to repress *SYN1* and *SCG10*, which were used as a positive control in all cases. Relative *REST*, *SYN1*, β -*TUBB3*, and *SCG10* mRNA expression was determined, and *RPS18* was used as the internal control for each sample. Interfering with endogenous REST activity in MB01110 cells increased *REST* expression as compared to vector control, which suggests that REST represses its own transcription in the absence of detectable HES1 protein (Fig. 26). Modulation of REST activity also increased *REST* transcription in DAOY cells where HES1 protein is present (Fig. 17B). However, a trend towards a greater increase in *REST* transcription is observed in MB01110 (~ 10 fold) as compared to DAOY (~ 5 fold). The latter trend may suggest the potential for co-repressor function for HES1 and REST. Luciferase experiments described below were used to validate this possibility.

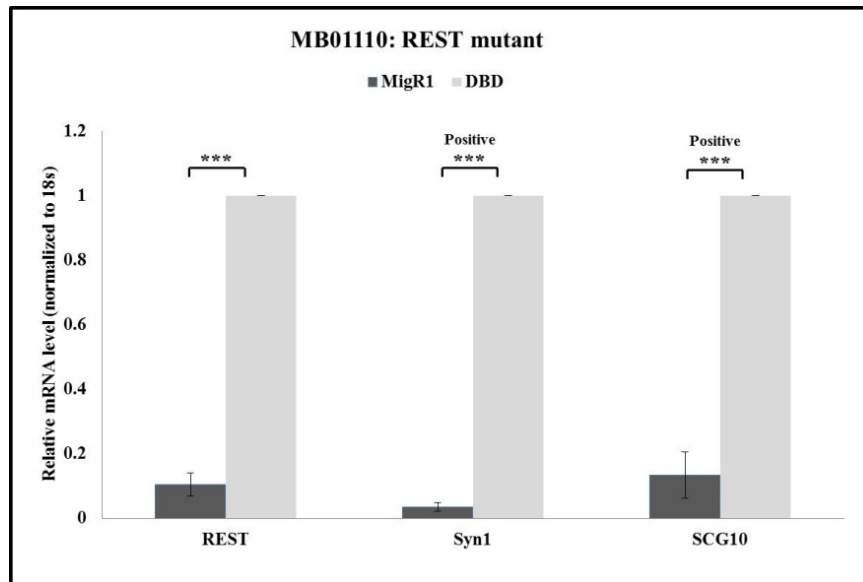
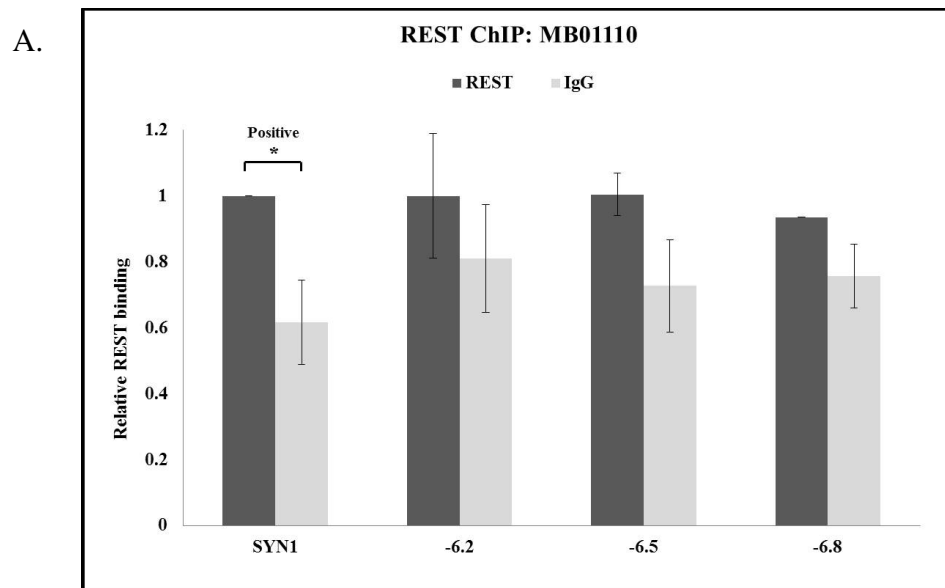


Figure 26: Countering REST activity represses *REST* transcription in the absence of HES1. A. Total *REST* expression in MB01110 cells infected with either MigR1-GFP empty vector or DBD-GFP. B. Endogenous *REST*, *SYN1*, and *SCG10* expression in MB01110 cells infected with above mentioned constructs. Total RNA was extracted and subjected to qRT-PCR analysis to measure total *REST*, endogenous *REST*, *SYN1*, and *SCG10*. Samples are normalized to the internal control *RPS18*, and scaled relative to the highest value. Experiments were done in triplicate. One-way ANOVA followed by Fisher LSD post-hoc analysis using Statistica 6.0 was conducted to determine statistical significance (* $p \leq 0.05$, ** $p \leq 0.01$, *** $p \leq 0.001$).

REST does not bind to *RE-1* sites in the *REST* 5' upstream region in the absence of HES1.

Thus far we have shown novel HES1-REST co-occupancy of the *RE-1* sites in DAOY cells, and that a greater increase in *REST* transcription is observed upon interfering with REST activity in MB01110 cells (a cell line in which no HES1 protein is detected) as compared to DAOY cells (high levels of both proteins). Next, we determined whether the latter effect of increased *REST* transcription upon REST modulation in MB01110 was because of altered REST binding to the *RE-1* sites in the absence of HES1. Nuclear lysates were prepared from MB01110 and subjected to ChIP assay by immunoprecipitating with rabbit anti-REST antibody or control serum IgG, and immunoprecipitated DNA was analyzed by qPCR using validated primers specific to *RE-1* sites located at -6.2 kb and -6.8 kb and *N-box* located -6.5 kb from TS. No REST occupancy at the *RE-1* sites or the *N-box* was detected in MB01110 cells, which suggests that perhaps HES1 is required for REST binding at these regions (Fig. 27A). This was unexpected, because modulation of REST activity leads to increase in *REST* transcription in these cells, thus leading us to speculate that perhaps the effect of REST interference by the

DBD on *REST* transcription is indirect, or perhaps that REST binds to and represses the *RE-1* site located +0.8 kb from TS (which could not be tested). ChIP assay to detect HES1 binding was also done as a negative control since HES1 protein was not detected in these cells (Fig. 27B). Surprisingly, the -6.2 kb and -6.8kb *RE-1* sites were positive for HES1 binding, but the binding was significantly lower compared to that observed in the HES1-expressing DAOY and D283 cells ($p < 0.02$ and $p < 0.004$ for each site as compared to D283 HES1 ChIPs). Indeed a possibility remains that very low amounts of HES1, undetectable by Western blot analysis, may be present and may bind to the *RE-1* sites, but the lack of HES1 occupancy at the regulatory region of Mash1 (used as the positive control for our experiments) in MB01110 precludes clear interpretation of HES1 occupancy at the *RE-1* site. It would be interesting to determine whether ectopic expression of HES1 in MB01110 would lead to increased REST occupancy at the *RE-1* sites as compared to vector control.



B.

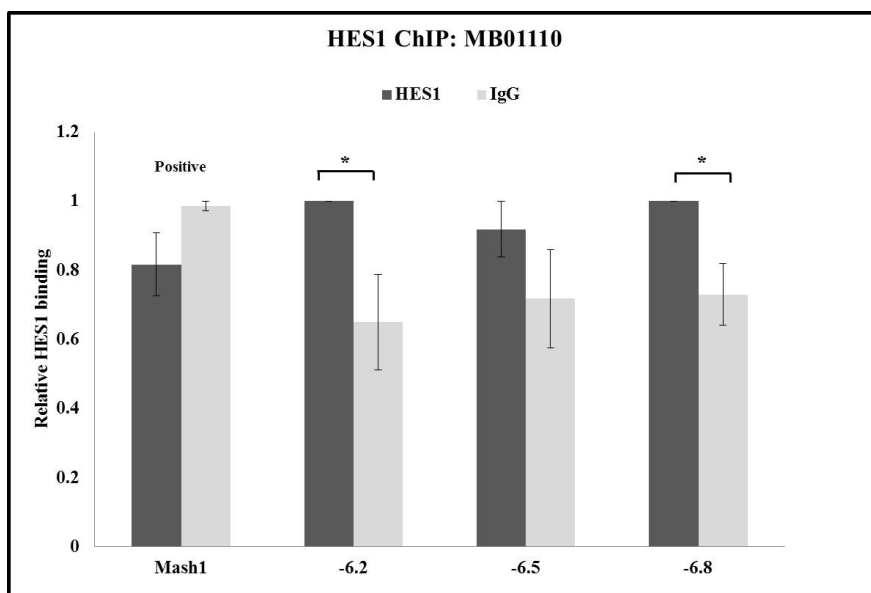


Figure 27: REST does not bind to 5' upstream region of *REST* in the absence of HES1. ChIP was performed in MB01110 with A. rabbit anti-REST antibody or control IgG, B. rabbit anti-HES1 followed by qPCR analysis using primers specific to *RE-1* sites and *N-boxes* located -6.2 kb, -6.5 kb, and -6.2 kb from the TS. Experiments were done in triplicate. One-way ANOVA followed by Fisher LSD post-hoc analysis using Statistica 6.0 was conducted to determine statistical significance (* $p \leq 0.05$, ** $p \leq 0.01$, *** $p \leq 0.001$).

HES1 and REST co-repress *REST* transcription

To gain further insight into the roles of REST and HES1 as potential co-repressors of *REST* transcription, we designed luciferase constructs with both of the *RE-1* sites located -6.8 and -6.2 as well as the *N-box* located at -6.5 kb upstream of TS mutagenized (Fig. 28). Mutating the *RE-1* sites and *N-box* abrogates the ability REST and HES1 to bind to these particular sites respectively, thus allowing us to study the unique and combined contribution of each of *RE-1* sites and *N-box* on *REST* transcription, as measured by luciferase activity. The following luciferase constructs were used: pGL4.15-sv40, pGL4.15-sv40-WT, pGL4.15-sv40-*RE-1*mut (both *RE-1* sites mutagenized), pGL4.15-sv40-*Nbox*mut (-6.5 *N-box* mutagenized), and pGL4.15-sv40-*RE-1*mut-*Nbox*mut (both *RE-1* sites and *N-box* mutagenized).

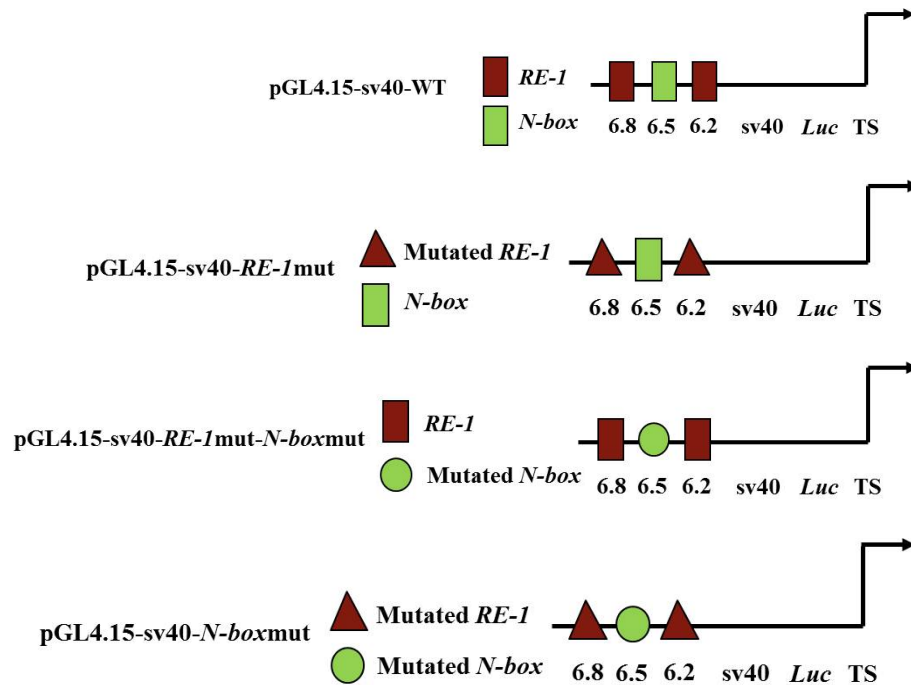


Figure 28: Structure of the *REST* luciferase constructs: pGL4.15-sv40-WT, pGL4.15-sv40-*RE-1*mut, pGL4.15-sv40-*N-box*mut, pGL4.15-sv40-*RE-1*mut-*N-box*mut.

Luciferase constructs were stably transfected into DAOY cells, followed by hygromycinB selection, and measurement of luciferase activity (Fig 29). The baseline luciferase activity was assessed by the control pGL-sv40-WT construct by measuring luminescence using a luminometer as described above. Consistent with the repressive function of both HES1 and REST, an increase in luciferase activity was observed upon mutagenizing the two *RE-1* sites (-6.2 kb and -6.8 kb from TS) and *N-box* (-6.5 kb from TS) independently relative to the luciferase activity of the control construct. Concurrent mutations of both *RE-1* sites and *N-box* led to a statistically significant increase in luciferase activity relative to mutations of either the *RE-1* sites or the *N-box* alone, thus suggesting that REST and HES1 function as co-repressors of *REST* transcription in medulloblastoma cells.

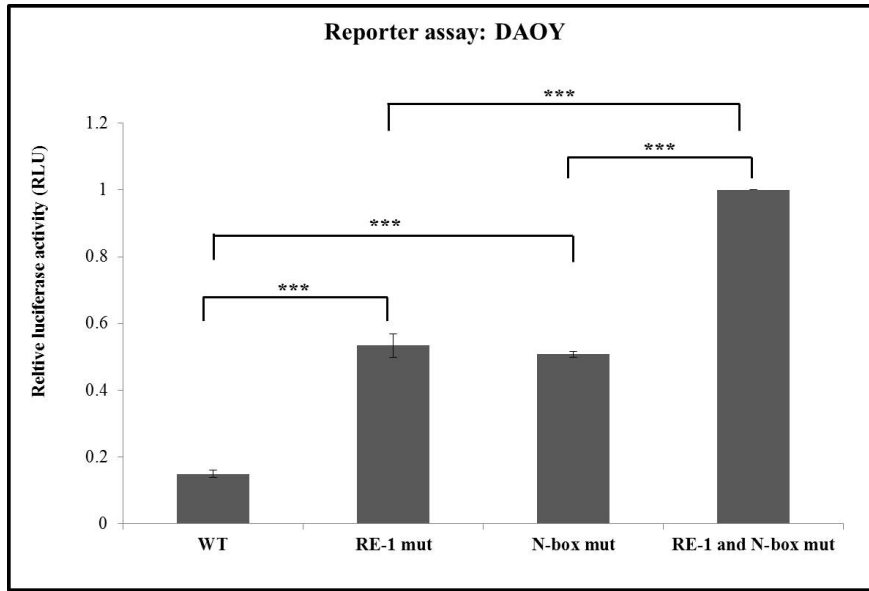


Figure 29: Mutating *N-box* and *RE-1* sites leads to increased luciferase activity as compared to either mutation alone. Luciferase constructs with either wildtype *RE-1* sites, mutated *RE-1* sites, mutated *N-box*, or mutated *RE-1* sites and *N-box* were stably expressed in DAOY cells and luciferase expression was measured, and scaled from 0 to 1. Experiments were done in triplicate. One-way ANOVA followed by Fisher LSD post-hoc analysis using Statistica 6.0 was conducted to determine statistical significance (* $p \leq 0.05$, ** $p \leq 0.01$, *** $p \leq 0.001$).

Summary

HES1 occupancy was detected at the *RE-1* sites previously validated for REST binding, but REST did not occupy the *N-boxes* tested. We further showed that HES1 and REST co-occupy the *RE-1* sites located at -6.2 kb and -6.8 kb from TS in the *REST* 5' upstream region, while no co-occupancy was not observed at the sites containing *N-boxes*. Both HES1 and REST are known to associate with HDACs, and the presence of HDAC1 and HDAC2 at both *RE-1* sites suggests that the presence of repressive complexes at these sites. The latter, along with our preliminary data indicating that the two proteins interact in DAOY cells, presents potential for co-regulation of *REST* transcription. We interfered with REST activity using REST-DBD in MB01110 cells, which do not have any detectable HES1 protein, and observed an increase in *REST* transcription. This result is consistent with DAOY cells, which have high levels of HES1. However, a greater increase in *REST* expression is noted in MB01110 cells as compared to DAOY upon interference with REST activity. The latter suggests the possibility that HES1 may cooperate with REST to further repress *REST* expression, and since HES1 is not detectable in MB01110, a greater de-repression of REST expression is observed upon interfering with REST activity. The lack of REST occupancy in the absence of HES1 as observed in MB01110 cells suggests that HES1 may be required for REST binding to *RE-1* sites. Change in REST transcription observed upon modulation of REST activity in the absence of REST binding suggests that perhaps the effect of REST-DBD on *REST* expression may be indirect, or it may be mediated by REST occupancy *RE-1* box located +0.8 kb of TS. To determine the contribution of the *RE-1* sites and *N-box* to *REST* transcription, luciferase assay was performed using constructs with either wildtype or mutated consensus sequences for *RE-1*, *N-box*, or both. Mutagenizing both *RE-1* sites and *N-box* concurrently results in a greater de-repression of luciferase activity as compared to mutating either *RE-1* sites or *N-box* alone, thus suggesting that REST and HES1 function as co-repressors of *REST* transcription in medulloblastoma cells.

Chapter 6: Retinoic acid regulates REST protein by modulation of SCF ^{β} -TRCP

Rationale

Retinoic acid, a differentiation agent, is a mainstay for neuroblastoma treatment, and leads to differentiation of a subset of tumors, while other tumors show resistance to the treatment. The mechanism behind retinoic acid mediated differentiation remains unknown. A better understanding of this mechanism may provide insight into the factors that contribute to the resistance and sensitivity of various neuroblastoma tumors and cell lines to retinoic acid treatment.

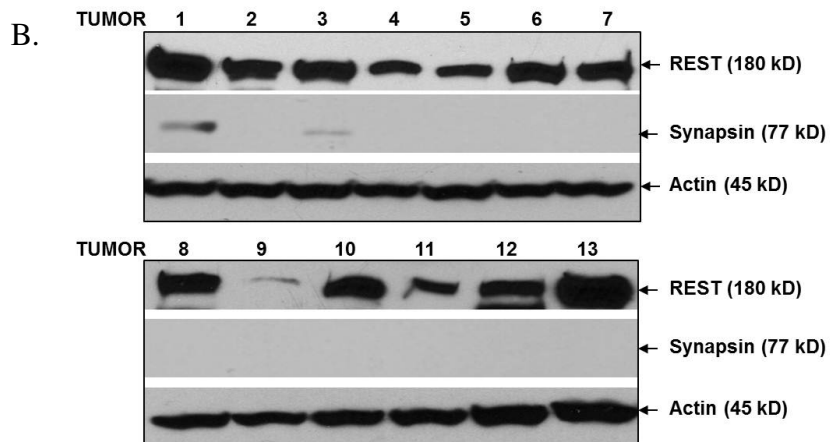
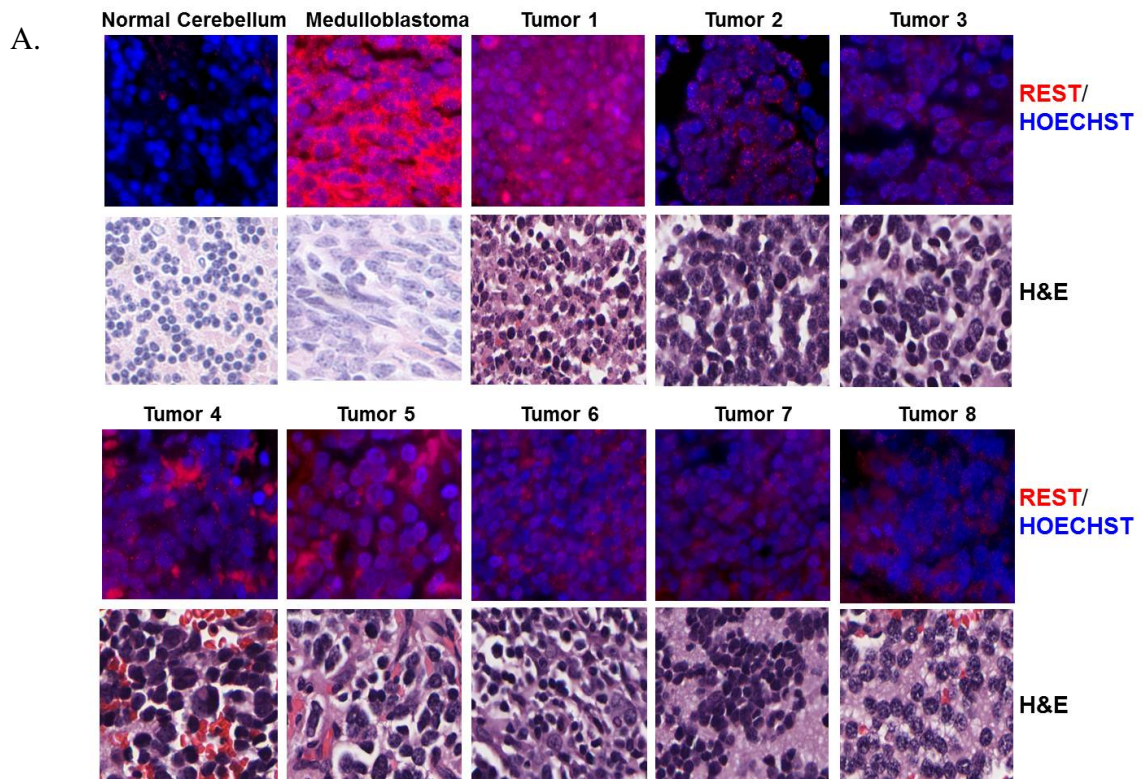
REST is a critical mediator of normal neurogenesis as it functions to repress neuronal differentiation genes, and it has been previously shown to be regulated by unliganded RAR- α . We wanted to determine whether REST plays a role in retinoic acid mediated differentiation of neuroblastoma cell lines. **We hypothesize that retinoic acid promotes differentiation of neuroblastoma tumors through transcriptional regulation of *REST*.**

Results

Maintenance of REST protein in neuroblastoma patient samples and cell lines.

Given that REST is overexpressed and has been associated with an oncogenic role in medulloblastoma, we first wanted to determine the status of REST protein in neuroblastoma tumors. We stained 41 paraffin embedded neuroblastoma patient samples for REST protein via immunofluorescence analysis (obtained from Children's Oncology Group and the Biopathology Center, Columbus, Ohio) (Fig. 30A). Indeed, REST protein was detected in 97.5% (40/41) of patient samples (Fig. 30A). Normal cerebellum, which is known to lack REST protein, served as the negative control, while medulloblastoma tumor served as the positive control (27). Similar results were recapitulated by Western blot analysis of REST protein in lysates prepared from additional 13 snap-frozen tumor samples (Fig. 30B) (125). REST protein was elevated in 92% (12/13) tumor samples analyzed. Protein levels of Synapsin1, a differentiation marker and a previously validated target of REST, were also examined (Fig. 30B). Low levels of synapsin1 correlated to maintenance REST protein in some but not all samples. Actin served as a loading control for Western blot analysis.

We next wanted to know if neuroblastoma cell lines showed a similar trend with respect to REST protein, so we examined lysates prepared from a panel of neuroblastoma IMR-32, SK-N-AS, SHEP, SK-N-SH, SK-N-SY5Y, NBL-S, and NGP for REST protein by Western blot analysis. REST was maintained in all neuroblastoma cell lines, albeit at various levels. Synapsin1 was either not detected or very faintly detected in these cell lines in accordance with maintenance of REST protein, and actin was used as a loading control (FIG. 30C).



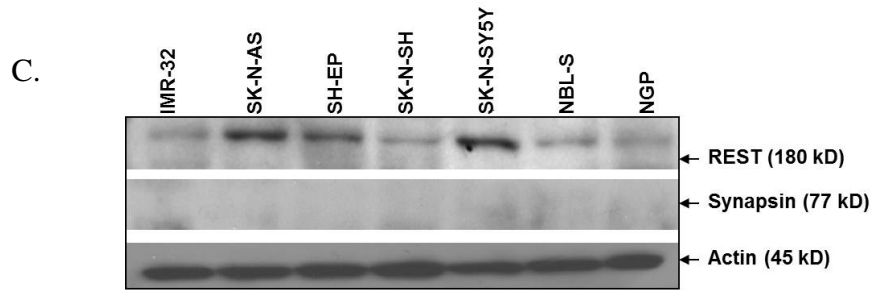
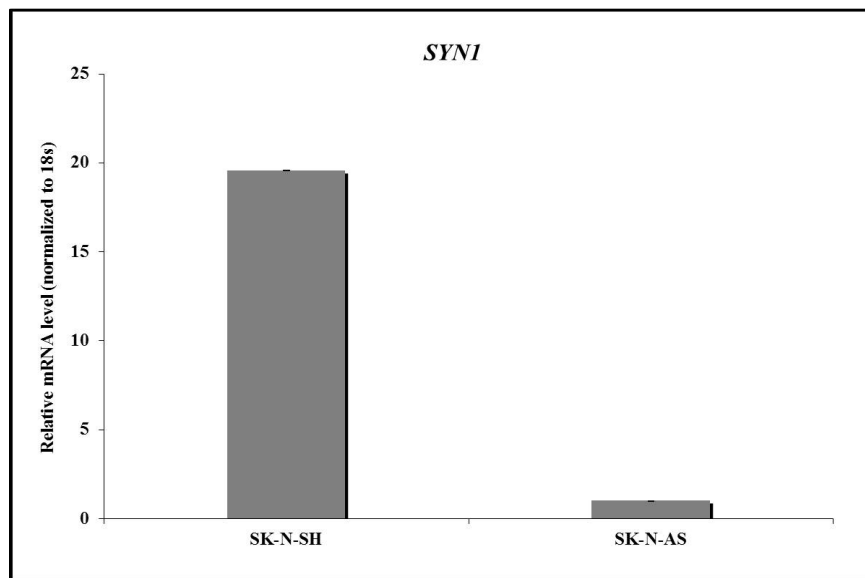
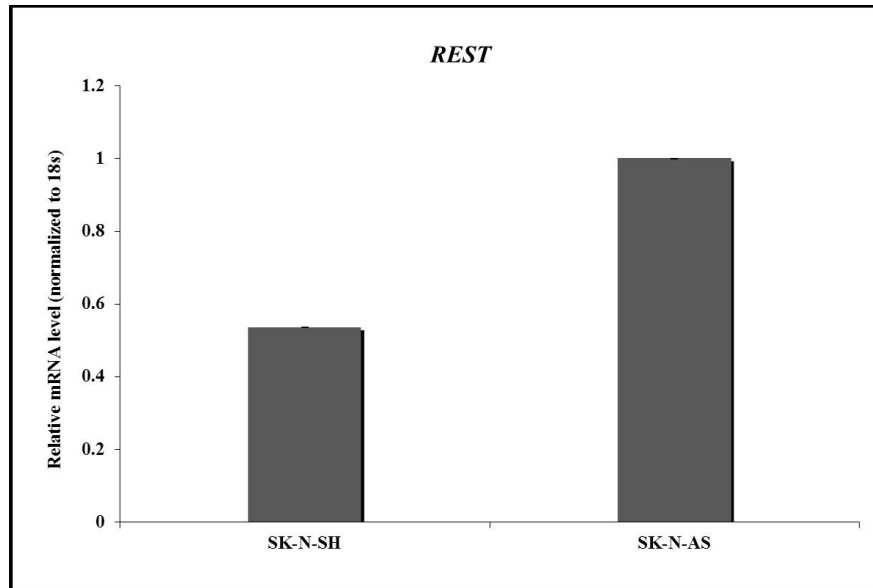


Figure 30: REST protein is overexpressed in neuroblastoma patient samples and cell lines. A. 41 neuroblastoma patient samples were evaluated for REST levels by immunofluorescence analysis. B. Protein lysates from an independent set of 13 tumor samples were subjected to Western blot analysis for REST and Synapsin1. C. Lysates were prepared from neuroblastoma cell lines and analyzed by Western blot analysis for REST protein levels. Actin was used as a loading control for Western blot analyses.

Differential expression of REST is observed in retinoic acid sensitive, SK-N-SH, versus retinoic acid insensitive, SK-N-AS, cells.

SK-N-SH and SK-N-AS cells have been previously characterized as retinoic acid sensitive and retinoic acid insensitive cells respectively (126, 127). From our initial analysis, it appears that although REST protein is detected in both cell lines, the levels are different between the two, with SK-N-SH cells showing significantly lower levels as compared to SK-N-AS cells. To further characterize the status of REST in these neuroblastoma cell lines, lysates were prepared from both cell lines for RNA and protein analysis. RNA was extracted, and subjected to qRT-PCR for *REST* and *SYN1* transcripts. *REST* transcript shows a similar trend as the protein displaying lower transcript levels in SK-N-SH as compared to SK-N-AS cells (Fig. 31A). Accordingly *SYN1* expression was higher in the SK-N-SH as compared to SK-N-AS. Immunofluorescence and Western blot analyses confirmed our initial findings regarding differential levels of REST in both cell lines, concurrent with lower levels of β -tubulinIII (immunofluorescence) and Synapsin1 (Western blot) observed in SK-N-AS cells as compared to SK-N-SH cells (Fig. 31B). Actin was used as the loading control for Western blot analysis, whereas the *RPS18* served as the internal control for qRT-PCR analysis. Overall, we have shown that retinoic acid sensitive SK-N-SH cells had lower levels of REST mRNA and protein with greater expression of differentiation markers, whereas the retinoic acid insensitive SK-N-AS cells displayed higher levels of REST mRNA and protein with poor expression of differentiation markers.

A.



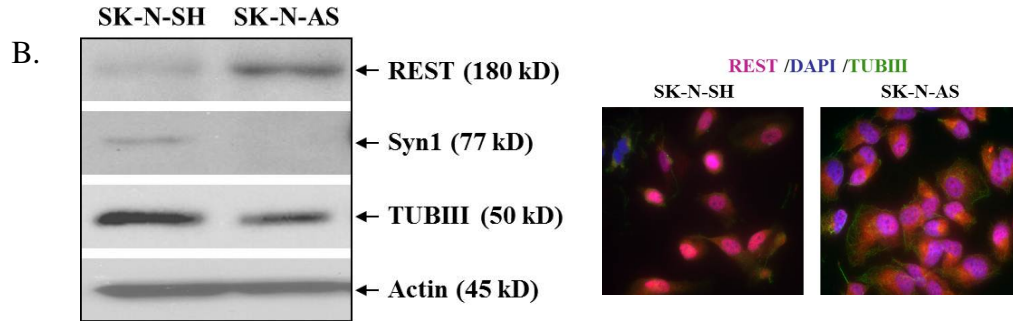


Figure 31: SK-N-SH cells have lower levels of REST mRNA and protein as compared to SK-N-AS cells. Lysates were prepared from SK-N-SH and SK-N-AS cells, and analyzed for A. mRNA expression of *REST* and *SYN1* expression RNA was converted to cDNA and analyzed via qRT-PCR, with *RPS18* serving as the internal control B. Protein levels of REST, Synapsin1, and β -tubulinIII were analyzed via Western blot and immunofluorescence analyses. Actin was the loading control.

Retinoic acid treatment leads to decreased REST protein levels in SK-N-SH, but not SK-N-AS cells

Because REST is critical in neuronal differentiation, and has been previously shown to be transcriptionally repressed via binding of unliganded RAR to the *RARE* element located upstream of REST TS, we wanted to determine if REST played a role in retinoic acid mediated differentiation of certain neuroblastoma cell lines, thereby contributing to their retinoic acid sensitivity or insensitivity (67). To this end we used previously published retinoic acid sensitive, SK-N-SH, and retinoic acid insensitive, SK-N-AS cells (124, 125).

SK-N-SH and SK-N-AS cells were treated with 10 μ M retinoic acid for 24 hours to 120 hours, and neurite like morphological changes, reminiscent of differentiation, were noted in SK-N-SH, but not SK-N-AS, cells (Fig. 32). Cell cycle analysis via flow cytometry was used to examine the changes in sub-G1 content, an increase in which would be indicative of cell cycle arrest and apoptosis. Percentage of cells in each phase of the cell cycle was calculated for both vehicle (DMSO) and retinoic acid treated cells. No significant changes in sub-G1 population were observed between DMSO treated and retinoic acid treated cells, thereby excluding the cell-cycle arrest and apoptosis as major mechanisms behind sensitivity to retinoic acid treatment of some cell lines and not others (Fig. 33).

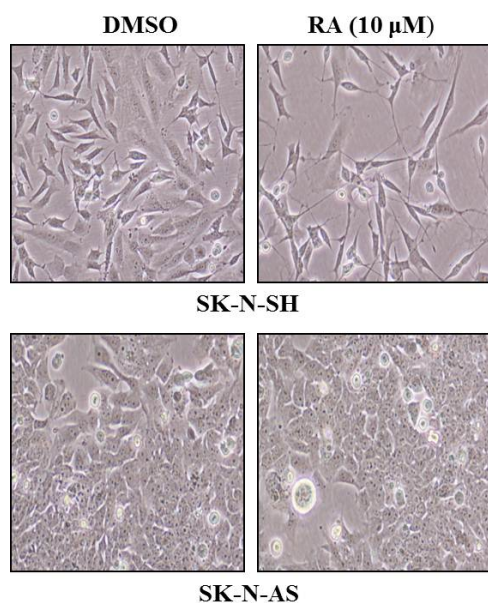
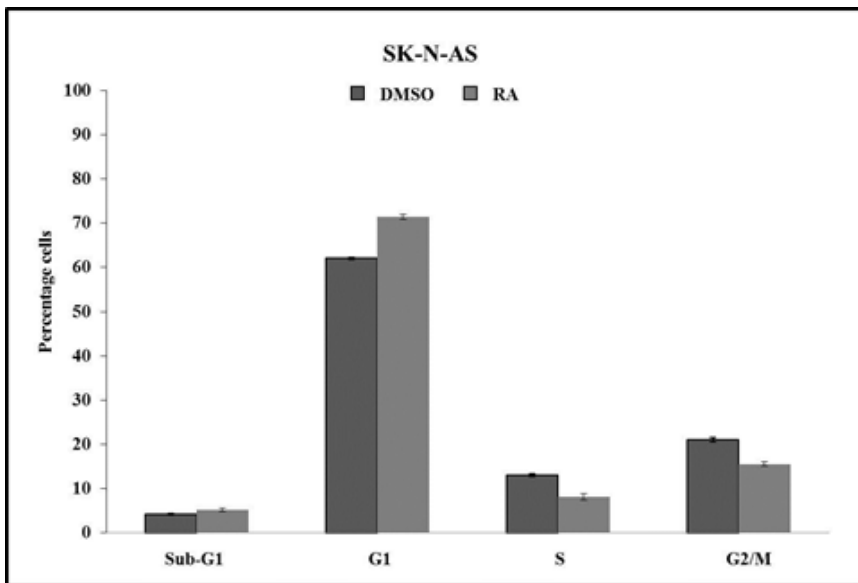
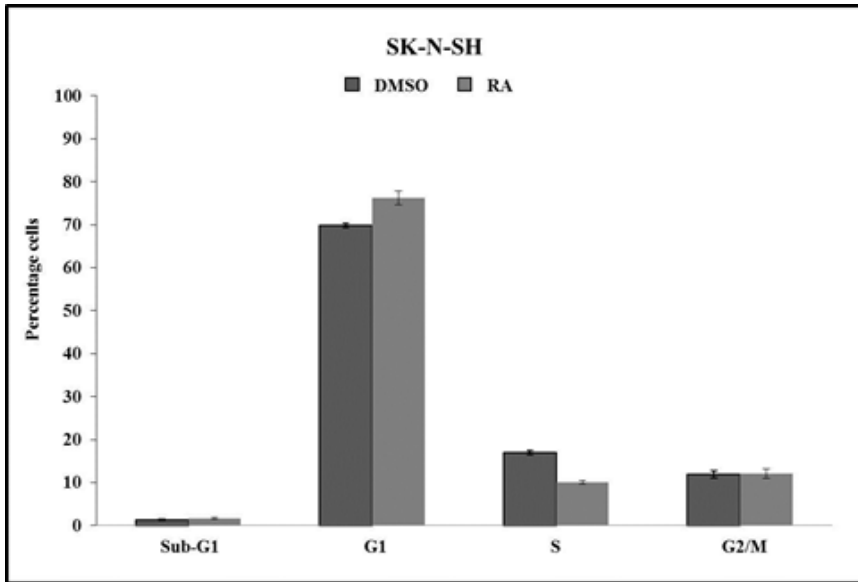


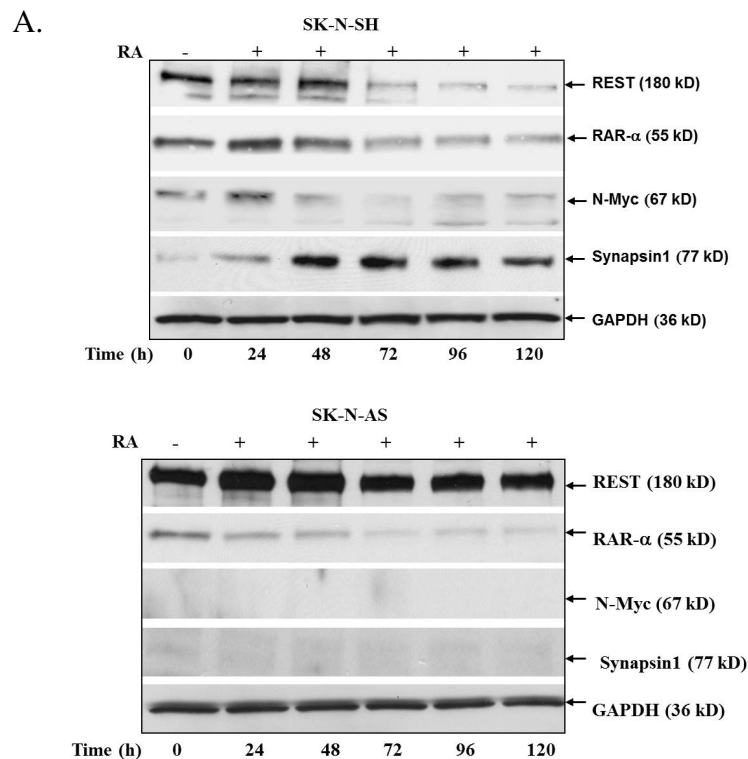
Figure 32: Differentiation like morphological changes observed in retinoic acid treated SK-N-SH but not SK-N-AS cells. SK-N-SH and SK-N-AS cells were treated with 10 μ M retinoic acid for 24 hours to 120 hours, morphological changes were detected via light microscopy. The image above is a representative image of three separate trials.



acid treated
 d with 10 μ M
 eriment was

DMSO and retinoic acid treated SK-N-AS and SK-N-SH cells were used for protein analysis, and levels for REST, RAR- α , N-MYC, SKP2, and Synapsin1 were determined via Western blot analysis and immunofluorescence. A decline in REST protein was observed upon retinoic acid treatment at 72 hours post-treatment and maintained through the remaining length of the treatment, while no such change was noted in SK-N-AS cells (Fig. 34A). In fact, REST protein appeared to increase slightly at 24 and 48 hours and declined back to baseline through

the remaining length of the treatment (Fig. 34A). RAR- α is known to decline upon retinoic acid treatment, and thus serving as a control for the treatment. As expected, RAR- α protein levels declined in both cell lines upon treatment as compared to vehicle treated cells. Similarly, retinoic acid treatment has also been previously correlated with decreased N-Myc levels. SK-N-SH cells express *MYCN*, and the observed decrease in N-Myc protein upon retinoic acid treatment is consistent with previously published data. SK-N-AS cells are not *MYCN* amplified, and accordingly no changes in the protein were noted. Consistent with a differentiation phenotype, increase in Synapsin1 protein was detected in retinoic acid treated SK-N-SH cell, but not in SK-N-AS cells (Fig. 34A). Furthermore, immunofluorescence analysis was conducted at 120 h after treatment, and corroborated the findings of the Western blot analysis, for an increase in β -tubulinIII levels, concomitant with a decline in REST protein, was observed in retinoic acid treated SK-N-SH, but not in SK-N-AS cells (Fig. 34B). In SK-N-SH cells showed REST translocation from the nucleus to the cytoplasm, where it is known to be degraded, while no such change was noted in SK-N-AS cells (Fig. 34B). These results suggest that retinoic acid treatment leads to a decrease in REST protein levels and an increase in REST targets (many of which are differentiation proteins) in SK-N-SH, but not SK-N-AS cells.



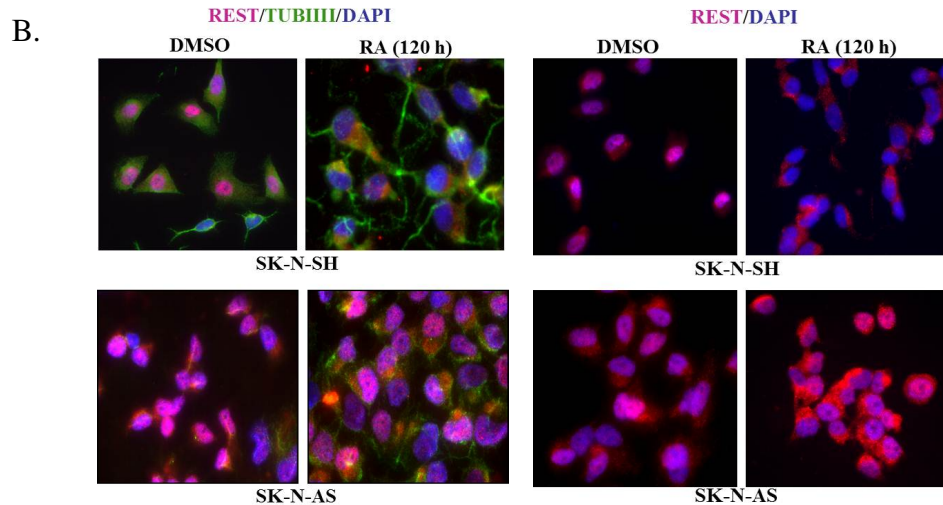
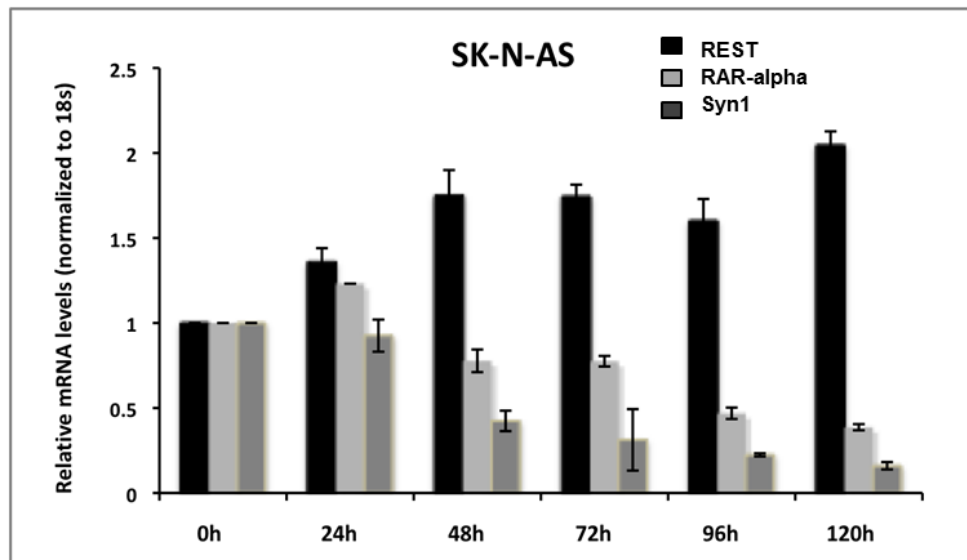
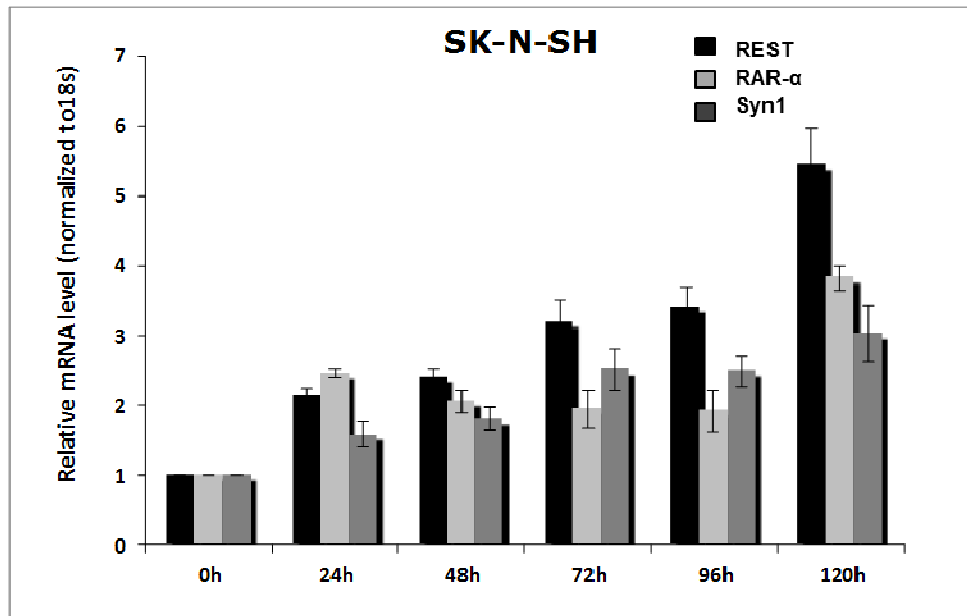


Figure 34: Retinoic acid treatment leads to decline in REST protein and increased differentiation in SK-N-SH, but not SK-N-AS cells. SK-N-SH and SK-N-AS cells were treated with 10 μ M retinoic acid for 24-120h. A. Protein lysates were analyzed for REST, RAR- α , N-MYC, SKP2, and Synapsin1 via Western blot analysis. GAPDH served as a loading control. B. Treated cells were subjected to immunofluorescence analysis for REST and β -tubulinIII levels. The images above are representative images of three separate experiments.

***REST* transcription increases upon retinoic acid treatment in both SK-N-SH and SK-N-AS cells.**

Since *REST* mRNA has been previously shown to be transcriptionally modulated by RAR- α , we wanted to determine if the decline in REST in response to retinoic acid treatment in neuroblastoma was due to transcriptional down-regulation of *REST* (67). Lysates were prepared from DMSO and retinoic acid treated SK-N-SH and SK-N-AS cells for 24-120 hours, and analyzed by qRT-PCR analysis for *REST*, *RAR- α* , and *SYN1*. *RPS18* was used as the internal control. Surprisingly, an increase in *REST* transcription was observed in both SK-N-SH and SK-N-AS cells upon retinoic acid treatment (Fig. 35). However, as noted in above, treated cells show differential effect on protein levels in SK-N-SH versus SK-N-AS cells, thus implicating a post-transcriptional contribution to the changes in REST protein observed in the two lines. Accordingly, *Syn1* transcription, which is negatively regulated by REST, increases in SK-N-SH and decreases in SK-N-AS cells, thereby mirroring the trend in REST protein rather than mRNA (Fig. 35).



transcription in
 treated with 10
 yzed via qRT-
 The

To better distinguish between the transcriptional and post-transcription modulation of REST in response to retinoic acid treatment, we treated SK-N-SH and SK-N-AS cells with cyclohexamide (10 μ g/ml), an agent that blocks translation of mRNA into protein, for 2 hours in the presence or absence of retinoic acid (data not shown). Protein extracts were then prepared and analyzed by Western blot analysis, and analyzed for REST and RAR- α with

87

GAPDH as the loading control. However, perhaps because of the short duration of treatment, our results were inconclusive (data not shown).

While increased transcription may partially explain the increase in REST protein observed up on retinoic acid treatment, mechanism leading to decrease in REST protein in SK-N-SH cells despite increased transcription remains unknown. REST regulation via the proteasome has been previously reported in cortical progenitors, where *REST* transcription remains high, while the protein is degraded (67). We wanted to determine the contribution of the proteasome to regulation of REST protein in response to retinoic acid treatment. To determine if the proteasome was involved, we treated the SK-N-SH and SK-N-AS with proteasomal inhibitor, MG132, in the presence or absence of retinoic acid as well as retinoic acid alone. Again, because of toxicity to MG132 (5 μ M), cells could only be treated with it for 4 hours, which may not be sufficient to detect the more striking changes in REST protein observed with 24-120 hours of retinoic acid treatment. Maintenance of higher levels of REST protein upon MG132 in the presence of retinoic acid as compared to retinoic acid treatment alone indicates that there is a proteasomal contribution to retinoic acid mediated decline in REST protein (Fig. 36).

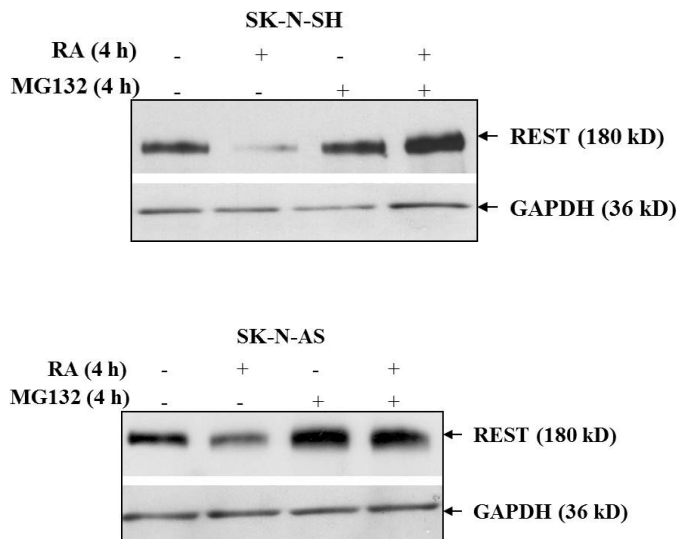
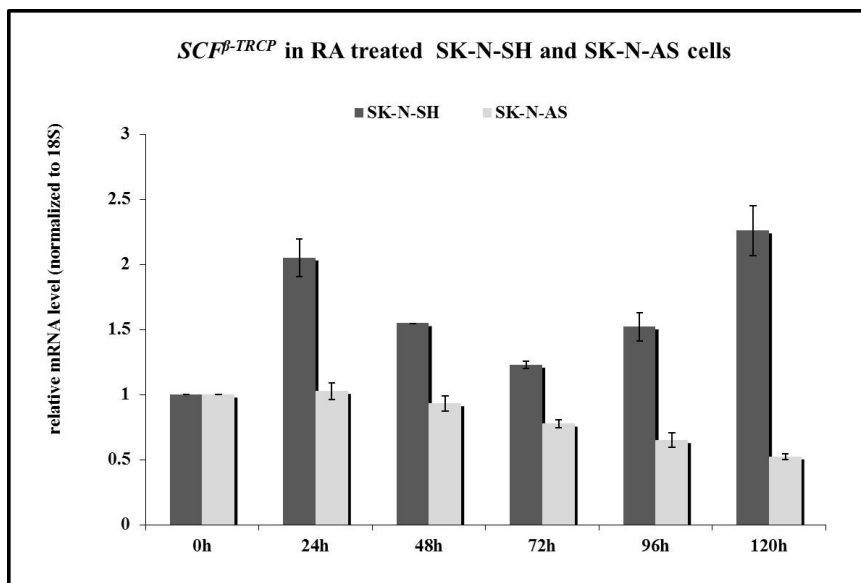


Figure 36: MG-132 treatment in the presence of retinoic acid leads to an accumulation of REST protein in SK-N-SH and SK-N-AS cells. SK-N-SH and SK-N-AS cells were treated with 10 μ M retinoic acid, MG-132 alone, or with both agents for 4 h. Protein lysates were prepared and analyzed via Western blot analysis for REST and RAR- α while GAPDH served as a loading control. Experiments were repeated in duplicate, and the image above is a representative image.

Retinoic acid treatment leads to an increase in $SCF^{\beta-TRCP}$ mRNA and protein in SK-N-SH cells, but not SK-N-AS cells.

$SCF^{\beta-TRCP}$ is the E3 ligase that has been shown to bind to REST and promote its degradation via the proteasome in several epithelial tumors as well as HMECs (59, 60). To explore the role of the proteasome further, we wanted to examine the status of $\beta-TRCP$ in response to retinoic acid treatment. To assess this, we examined $\beta-TRCP$ expression in the cDNA prepared from previously described retinoic acid treated SK-N-SH and SK-N-AS cells. It appears that $SCF^{\beta-TRCP}$ expression as well as protein increased in SK-N-SH cells at 24-96 hours followed by a decline back to vehicle treated controls in protein level at 120 hours (while higher $SCF^{\beta-TRCP}$ mRNA levels are maintained) (Fig. 37). A decline in both that $SCF^{\beta-TRCP}$ expression and protein was noted in SK-N-AS cells at 48-120 hours after a transient increase at 24 hours, in response to retinoic acid (Fig 37). Overall, our data suggests that while retinoic acid functions to increase $SCF^{\beta-TRCP}$ transcription which would subsequently translate into REST degradation in the retinoic acid sensitive SK-N-SH cells, the same treatment in the retinoic acid insensitive line leads to the opposite effect of decreasing $SCF^{\beta-TRCP}$ transcription, thereby functioning to promote the maintenance of REST.

A.



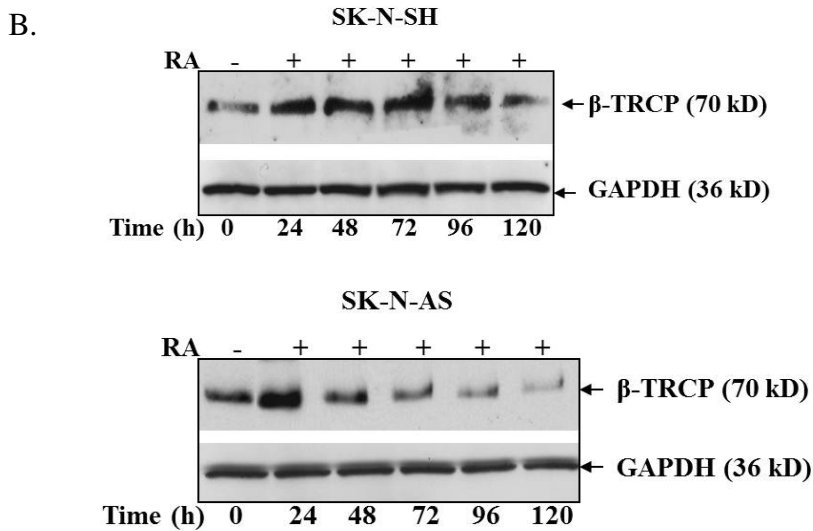
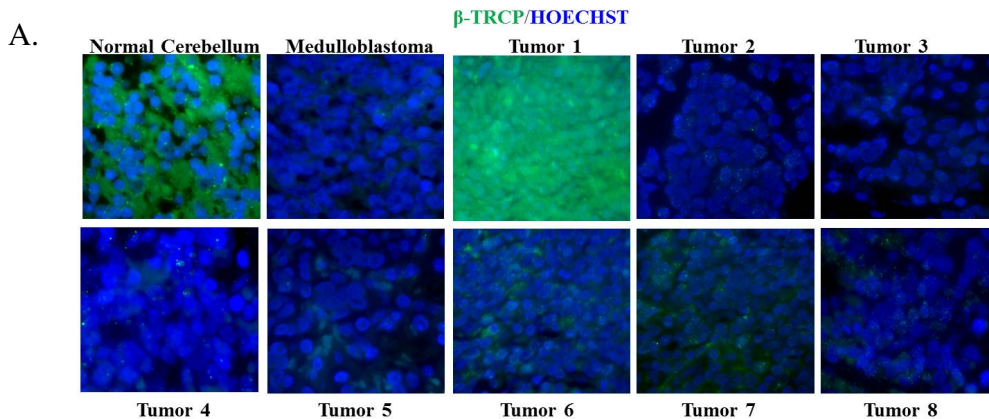


Figure 37: Retinoic acid treatment leads to increased SCF ^{β -TRCP} mRNA and protein in SK-N-SH, but not SK-N-AS cells. SK-N-SH and SK-N-AS cells were treated with 10 μ M retinoic acid for 24-120h. A. RNA was extracted, and analyzed via qRT-PCR for SCF ^{β -TRCP}. *RPS18* was used as the internal control. B. Protein lysates were prepared and subjected to Western blot analysis to detect SCF ^{β -TRCP} protein, and GAPDH was the loading control. The experiments were done in triplicate.

SCF ^{β -TRCP} protein in maintained in a subset of neuroblastoma patient samples.

We analyzed the levels of SCF ^{β -TRCP} in patient samples to ensure that our findings in neuroblastoma cell lines are relevant to the patient samples by subjecting the previously described patient samples to immunofluorescence and Western blot analysis. 54% of the patient samples (22/41) analyzed by immunofluorescence either had no or low levels of SCF ^{β -TRCP} (Fig. 38A). Furthermore, 73% of the samples with no or low SCF ^{β -TRCP} (16/22) also had high REST protein levels (Fig. 38B).



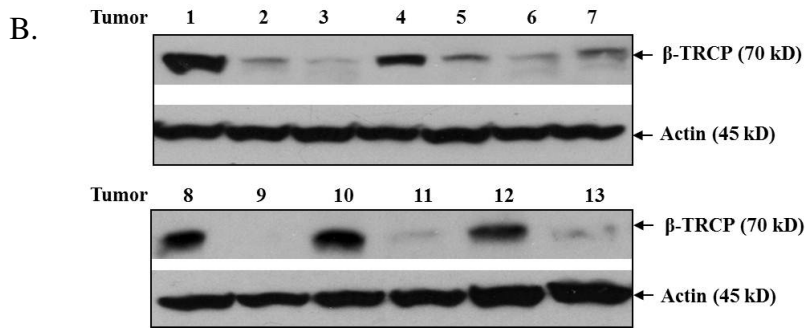


Figure 38: SCF^{β-TRCP} protein is overexpressed in a subset of neuroblastoma patient samples. A. 41 neuroblastoma patient samples were evaluated for SCF^{β-TRCP} levels by immunofluorescence analysis. B. Protein lysates from an independent set of 13 tumor samples were subjected to Western blot analysis for REST and Synapsin1.

Ectopic expression of SCF^{β-TRCP} in SK-N-AS cells leads to increased interaction with REST, REST ubiquitination, and decreased REST protein.

To determine whether down-regulation of SCF^{β-TRCP} indeed contributed for the maintenance of REST protein in addition to transcriptional up-regulation of *REST* in SK-N-AS cells, we transfected SK-N-AS cells with either the control plasmid, pQCXIP, or with a plasmid containing e-GFP-β-TRCP (kindly provided by Dr. Westbrook). To ensure that SCF^{β-TRCP} was ectopically expressed, transfected cells were collected 48h post transfection, and lysates were prepared for Western blot analysis. GFP tagged β-TRCP migrated at a slightly higher molecular weight as compared to the endogenous (Fig. 39). Accordingly, increased REST protein and decreased levels of Synapsin1 were observed, thereby indicating that increased expression of SCF^{β-TRCP} in SK-N-AS cells can lead to REST degradation. These results further validate our previous findings, and suggest that increase and decrease in SCF^{β-TRCP} levels noted in SK-N-SH and SK-N-AS cells respectively upon retinoic acid treatment, may indeed contribute to degradation or maintenance of REST (respectively) in response to retinoic acid treatment in both cell lines.

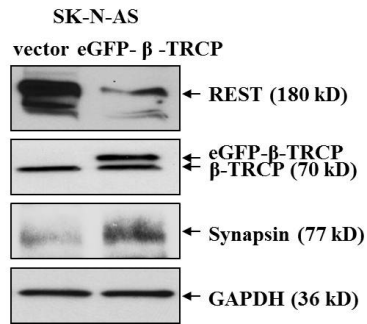


Figure 39: Ectopic expression of SCF^{β-TRCP} in SK-N-AS cells leads to decreased REST levels. SK-N-AS cells with either the vector control or with a plasmid containing e-GFP-β-TRCP. Protein lysates were prepared and analyzed via Western blot analysis for REST, SCF^{β-TRCP}, and Synapsin1 levels. GAPDH was the loading control. Experiment was done in triplicate, and the image above is a representative image.

Proteasomal degradation of a protein involves ubiquitination by an E3 ligase, thereby tagging the protein for degradation. Indeed SCF^{β-TRCP} has been shown to tag REST with ubiquitin leading to proteasomal degradation (60). To see if an increase in REST ubiquitination was observed upon overexpression of SCF^{β-TRCP} in SK-N-AS cells, lysates from vector or SCF^{β-TRCP} transfected cells, collected 24 hours post-transfection, were immunoprecipitated with anti-ubiquitin antibody and subjected to Western blot analysis with anti-REST antibody to determine the amount of ubiquitinated REST (Fig. 40). Indeed increased ubiquitinated REST is observed in SK-N-AS cells overexpressing SCF^{β-TRCP}. Accordingly, more SCF^{β-TRCP} was also detected in these immunoprecipitated lysates in SCF^{β-TRCP} transfected cells. These findings suggests that down-regulation of SCF^{β-TRCP}, in addition to transcriptional up-regulation of *REST*, contributes to maintenance of REST in retinoic acid treated SK-N-AS cells (Fig. 40).

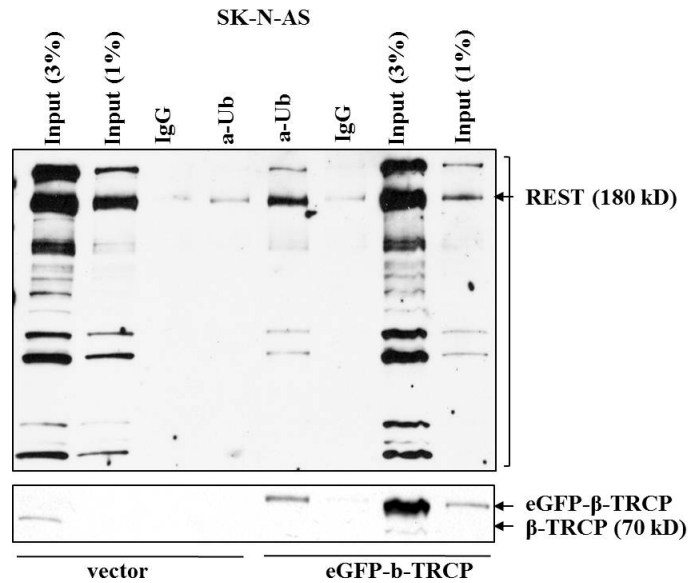


Figure 40: Ectopic expression of SCF^{β-TRCP} leads to increased ubiquitination of REST in SK-N-AS cells. SK-N-AS cells with either the vector control or with a plasmid containing e-GFP-β-TRCP. Lysates were immunoprecipitated with either anti-ubiquitin antibody or control IgG, and analyzed via Western blot analysis for REST and SCF^{β-TRCP} levels. Experiment was done in duplicate, and the image above is a representative image.

Next, we did co-immunoprecipitation experiments where we immunoprecipitated of the above mentioned lysates (24 hours) with SCF^{β-TRCP}, and probed for REST by Western blot analysis. Analysis of specific pull-down indicates that increased amount of REST protein immunoprecipitates with SCF^{β-TRCP} in lysates prepared from SK-N-AS cells overexpression SCF^{β-TRCP} (Fig. 41A). The converse experiment was also done in which the immunoprecipitation was done using anti-REST antibody or control IgG, and SCF^{β-TRCP} levels were analyzed by Western blot analysis. Again, increased SCF^{β-TRCP} interaction with REST is observed in lysates prepared from SK-N-AS cells overexpression SCF^{β-TRCP} (Fig. 41B). The latter confirms that regulation of REST by retinoic acid is at least in part mediated by changes in levels of SCF^{β-TRCP}, which then either lead to increased or decreased proteasomal degradation of REST.

Summary

Although a subset of neuroblastoma tumors and cell lines are sensitive to differentiation by retinoic acid treatment, the mechanism underlying retinoic acid mediated differentiation was unknown. REST is an important regulator of neuronal differentiation, and has been shown to play an oncogenic role in medulloblastoma. We have shown that REST is maintained in a subset of neuroblastoma tumors and cell lines. Lower REST protein and transcript are observed in retinoic acid sensitive SK-N-SH cells as compared to retinoic acid insensitive, SK-N-AS cells. Although both cell lines display an increase in *REST* expression in response to retinoic acid treatment, REST protein declines in SK-N-SH cells, while it is maintained in SK-N-AS cells after treatment with retinoic acid. This led us to speculate that perhaps retinoic acid regulated REST transcriptionally as well as post-transcriptionally. Maintenance of REST protein upon co-treatment with retinoic acid and MG132 in both cell lines suggested the contribution of the proteasome to maintenance of REST protein observed upon retinoic acid treatment. Analysis of $SCF^{\beta-TRCP}$ mRNA and protein in retinoic acid treated SK-N-SH and SK-N-AS cells revealed an increase $SCF^{\beta-TRCP}$ mRNA and protein in retinoic acid treated SK-N-SH cells, while a decrease was noted in SK-N-AS cells treated with retinoic acid. Ectopic expression of $SCF^{\beta-TRCP}$ in SK-N-AS cells led to increased $SCF^{\beta-TRCP}$ -REST interaction, increased REST ubiquitination, and a decline in REST protein concomitant with an increase in Synapsin1 as compared to vector control transfected cells. A subset of patient samples do indeed show an inverse correlation between REST and $SCF^{\beta-TRCP}$ levels, therefore further validating our findings as a potentially relevant mechanism in patient samples. Our results suggest that retinoic acid treatment functions to increase $SCF^{\beta-TRCP}$ transcription which then translates into REST degradation in the retinoic acid sensitive SK-N-SH cells, while the same treatment in the retinoic acid insensitive line leads to the opposite effect of decreasing $SCF^{\beta-TRCP}$ transcription, thus functioning to promote the maintenance of REST levels. Overall, retinoic acid regulates REST levels in neuroblastoma cell lines by both transcriptional (increase in *REST*) and post-transcriptional (regulation of $SCF^{\beta-TRCP}$) mechanisms.

Chapter7: Discussion, conclusions, and future directions

Discussion

REST is important for normal neurogenesis and medulloblastoma pathology.

REST is critical for normal brain development, and is an important regulator of NSC proliferation and differentiation into neurons as it promotes the proliferation of NSCs while repressing the expression of differentiation genes (49-53, 104). The requirement of REST during embryonic development is highlighted by the fact that *REST* knockout mice display premature neurogenesis and embryonic lethality by E13.5. Consistent with its role as a negative regulator of neurogenesis, its levels are highest in ESCs (67). As ESCs go through lineage specificity, REST is proteasomally degraded in cortical progenitors, while its transcription remains high (128). Down-regulation of *REST* transcription is required for NPCs to fully differentiate into neurons concomitant with expression of REST target neuronal genes (67).

REST is overexpressed in medulloblastoma tumors and cell lines, and countering REST activity in medulloblastoma cell lines leads to decreased proliferation and tumor forming potential in xenograft models (25-27). Although, REST alone is not sufficient for tumor formation, overexpression of REST with v-MYC (another oncogene commonly overexpressed in medulloblastoma) in NSCs, leads to tumor formation *in vivo* (27). Furthermore, the tumor forming potential of NSCs overexpressing REST and v-MYC was abrogated by countering REST activity, thus indicating that the tumor formation is a REST-dependent effect (27). A recent study from our lab has shown that high REST protein levels correlate with poor overall survival and event free survival in patients across all medulloblastoma subgroups (28). Although the REST plays a role in medulloblastoma pathology, mechanism underlying maintenance of REST levels unexplored.

REST is transcriptionally mis-regulated in medulloblastoma patient samples.

Since NPCs from the cerebellar EGL and dorsal brainstem are considered the cells of origin of medulloblastoma, and REST has been previously shown to be transcriptionally maintained NPCs of the cortex, we examined whether *REST* transcription was aberrant in medulloblastoma patient samples (67). Our analysis of two independent sets of patient samples showed that *REST* expression is higher as compared to normal brain tissue in a subset of medulloblastoma samples, thus suggesting that *REST* is transcriptionally mis-regulated in a

subset of medulloblastoma. To our knowledge, our study is the first to show maintenance *REST* transcript in medulloblastoma patient samples. Although a previous study analyzed snap-frozen medulloblastoma patient samples for *REST* expression, it was to correlate *REST* mRNA with *MYC* mRNA in the tumors, and the samples were not normalized to non-tumor normal brain tissue (27). Without the context of *REST* mRNA in normal brain, the status of *REST* transcript in these tumors remains unclear.

As exemplified by cortical progenitor cells, where *REST* transcription remains high, while the protein is degraded, *REST* is regulated differentially both by transcriptional and post-transcriptional mechanisms (67). We focused on the mechanisms contributing to transcriptional mis-regulation of *REST* because our analysis of medulloblastoma patient samples revealed increased *REST* transcription relative to normal brains in a subset of the tumors.

HES1 represses *REST* expression in medulloblastoma cells.

Although, several molecules have been implicated in regulation of *REST* transcription, such as RAR- α , NeuroD2, and β -catenin-TSC2 complex in neural cells, we focused our attention on HES1 because it is critical for normal brain development, serving a similar function as *REST* by maintaining NSCs population and cellular diversity, and is expressed during a similar developmental time frame as *REST* (67, 83-85, 95, 96, 113). HES1 has also been implicated in medulloblastoma pathology, although its exact role remains unclear. Given that HES1 is a transcription factor that generally functions to silence its target gene expression by binding to its consensus sequences (*N-boxes*) in the regulatory regions of the target genes, we analyzed -7 kb of the *REST* 5' upstream region which yielded the presence of five *N-boxes*, three of which have been previously validated for HES1 binding in non-neural HeLa cells (82). CHIP assays in DAOY and D283 cells, which have high levels of HES1 protein as compared to cerebellar lysate, revealed that HES occupies the *N-boxes* described above, thus providing a potential for regulation of *REST* in medulloblastoma.

We performed loss of function experiments by interfering with HES1 activity in DAOY cells, where HES1 protein is overexpressed, while gain of function experiments by ectopic expression of HES1 were done in MB01110 cells, where HES1 protein was not detected. This analyses revealed that HES1 represses *REST* expression in medulloblastoma cells, which is consistent with its role as a repressor of target gene expression. To our knowledge ours is the

first study to report regulation of *REST* expression by HES1 in the context of medulloblastoma. Our findings are supported by previous reports of HES1 binding to and repressing *REST* transcription in non-neural in HeLa cells (82).

Despite the changes in *REST* transcription observed upon HES1 modulation, changes in REST protein in response to modulation by HES1 were transient and inconsistent across triplicates at the same time points. This may occur either because of a compensatory mechanism by the medulloblastoma cells, or because differential regulation of REST on a transcriptional and post-transcriptional level so that *REST* transcript does not necessarily correlate with REST protein. Indeed, previous studies have shown that REST is regulated separately at both transcriptional and post-translational levels, which may account for our inconclusive protein data (67, 124). Cancer cells are known to up-regulate compensatory pathways as a survival mechanism in response to agents that modulate key cellular processes. It is possible that increase in *REST* transcription does not reliably translate into REST protein because of up-regulation of degradation machinery. A previous study from our lab showed that while retinoic acid treatment led to increased *REST* transcription in both retinoic acid insensitive and sensitive cell lines, a decrease in REST protein was noted in the sensitive cell line, while REST levels were maintained in the insensitive cell line (124). We discovered that the insensitive cell line down-regulated $SCF^{\beta-TRCP}$ mRNA and protein in response to retinoic acid treatment, which then translated into decreased REST protein and a lack differentiation of the cell line, despite the observed increase in *REST* transcription. This mechanism contributed to retinoic acid insensitive phenotype of the cells, for it was not seen in retinoic acid sensitive cell-line SK-N-SH, where an increase in the transcription of $SCF^{\beta-TRCP}$ is observed in response to retinoic acid treatment (124). Our findings are further corroborated by previously described down-regulation of REST protein by proteasomal degradation in cortical progenitor cells, while REST transcription is maintained (67). It would be interesting to see if increase in $SCF^{\beta-TRCP}$ mRNA and protein occurs in response to HES1 modulation in medulloblastoma cell lines. Increased apoptosis also remains a possibility as various cancer cells have been reported to increase apoptosis of certain cells in order to avoid undergoing differentiation. Regulation of HES1 mRNA and protein upon modulation of HES1 may also be occurring because of the existence of a HES1 feedback loop, thereby further complicating our interpretation of the results (118, 119).

HES1 modulation of *REST* led to reciprocal changes in REST target genes, many of which are neuronal differentiation genes, which is consistent with the function of REST as a repressor of its target genes. This was unexpected because conclusive protein data for REST upon HES1 modulation was unavailable. However, the changes in REST target genes may indeed be because of transient changes in REST protein, for western blot analyses did show an increase in REST protein at some time points in DAOY cells upon HES1 modulation (but as stated before, the changes were not reproducible across triplicates for the same time points). Alternatively, a possibility remains that the changes in differentiation genes are independent of REST, and may occur in response to HES1 modulation, since HES1 itself is a pro-proliferative anti-differentiation protein, and has been previously shown to repress pro-differentiation genes.

Interestingly, interference of HES1 activity using the C-terminus deletion mutant of HES1 (MigR1-Bhlh-OR-GFP) appeared to provide a survival advantage to DAOY cells over time as measured by the competitive proliferation assay. Accordingly, overexpression of HES1 into these cells led to decreased survival over time as much a fewer percentage of GFP positive cells remain as compared to control infected cells. These results were surprising because Fan et al., 2006 have previously reported a decrease in anchorage independent growth potential of DAOY cells upon HES1 knockdown. One reason for these seemingly disparate results may be because HES1 knockdown was measured by mRNA expression of HES1 in this study. Our data suggests that HES1 feedback loop is intact in medulloblastoma cells, so that a change in mRNA expression may not necessarily correlate with a similar change in HES1 protein, thus necessitating independent measures of both. Alternatively, the possibility remains that in a subset of medulloblastoma tumors, where HES1 represses *REST* expression, HES1 overexpression is disadvantageous to survival, while in another medulloblastoma subtype, where this mechanism is not functional, HES1 may serve a pro-proliferative function. Correlation of HES1 protein and *REST* transcript in medulloblastoma tumor samples with patient survival would be instrumental for determining whether the contribution of HES1 to survival is dictated by medulloblastoma subtype. Interestingly, the increase in survival of DAOY cells observed upon introduction of the C-terminus deletion mutant of HES1 (MigR1-Bhlh-OR-GFP) was not recapitulated upon infection of point mutant of HES1 (MigR1-WRPW-GFP). The deletion mutant of HES1 (MigR1-bHLH-OR-GFP) lacks the proline and WRPW domains, while the point mutant of HES1 (MigR1-WRPW-GFP) contains only two point mutations in the WRPW domain. The pro-survival effect of the deletion mutant as compared to

the point mutant may represent a domain specific contribution of HES1 activity to survival of medulloblastoma cells. Perhaps the lack of the proline domain of HES1, which has been shown to bind the mSin3 complex, promotes survival of medulloblastoma cells. Detailed analysis by mutagenizing various domains of HES1 would be required to determine the differential effect of each of the HES1 mutants observed on medulloblastoma cell survival.

We wanted to know whether the change in the survival of the medulloblastoma cells in response to HES1 modulation could potentially translate into a change in tumor forming potential *in vitro*. To explore this, we did an anchorage independent growth assay with MB01110 since it is a recently derived patient line, and therefore may more faithfully represent patient tumors. Although we successfully established that MB01110 cells do indeed display anchorage independent growth, technical difficulties because of sensitivity of the cells to our treatment, precluded conclusive analysis of the effect of HES1 overexpression on their anchorage independent growth capacity. Alternatively, we could modulate HES1 activity in DAOY cells using mutants of HES1, which would provide useful information regarding the effect of modulating HES1 activity on anchorage independent growth potential *in vitro*. DAOY cells have been previously shown used to study the effect of various treatments on the anchorage independent growth (116).

Thus far we have shown that HES1 binds to and regulates *REST* expression in medulloblastoma cell lines. Despite the fact that changes in REST protein are transient and inconsistent, modulation of HES1 leads to changes in the differentiation genes, many of which are REST target genes. We further showed that modulation of HES1 leads to a change in survival of medulloblastoma cells, and we are currently in the process of determining whether this change in the survival translates into to an altered tumor formation potential *in vitro*. To our knowledge, our study is the first to show that HES1 regulates *REST* expression in medulloblastoma cells, and that HES1 is disadvantageous to the survival of these cells.

REST represses its own transcription in an auto-regulatory loop

Interestingly, our search for potential transcription factor binding sites to the *REST* 5' upstream region yielded three *RE-1* sites, thereby suggesting the possibility for an auto-regulatory mechanism. Our findings were corroborated by the discovery of one of these *RE-1* sites discovered in the ChIP-seq screen for *REST* binding sites in non-neural Jurkat cells (65). We tested REST occupancy of the *RE-1* sites in medulloblastoma cell lines, DAOY and D283

cells, which have been previously shown to have high REST protein (25). Although we could not amplify the previously described *RE-1* site because of high GC content of the amplicon, REST was found bound to the other two sites, thereby providing a potential for auto-regulation.

Interfering with REST activity in DAOY cells by using a mutant of REST (MigR1-REST-DBD-GFP, which contained DNA binding domain of REST, while lacking the two repression domains), led to increased REST transcription, along with consistent changes observed in other previously validated *REST* target genes, such as *SYN1* and *SCG10*, thus suggesting that REST indeed regulates its own transcription. To ensure that REST repressed its expression by binding to the *RE-1* sites directly, rather than an indirect mechanism, was because of an indirect mechanism, we designed luciferase constructs with either wildtype or mutagenized *RE-1* sites. Stable expression of the constructs into DAOY cells, followed by measurement of the luciferase activity, indicated increased luciferase expression in cells with the mutagenic luciferase construct as compared to the cells with the wildtype construct, thus supporting our mRNA findings. These experiments led us to conclude that REST indeed regulates its own transcription in medulloblastoma cells in an auto-regulatory loop, and that this effect is specifically mediated through REST binding to the *RE-1* sites.

Consistent with the presence of a feedback loop, no global changes in survival potential upon interference with REST DBD were observed. Although, the increase in previously validated REST target differentiation genes upon interference with REST activity lends credence to our novel finding of REST regulating its own transcription, it once again demonstrates that changes in *REST* mRNA do not necessarily correlate with REST protein and activity. It remains to be determined if changes in *REST* transcription translate into REST protein, but the presence of REST-DBD may mask any effect that increased REST protein may be having on its target genes. It is also possible that increased *REST* transcription leads to increased REST protein, but the protein is degraded by the proteasomal machinery. Finally, differential transcriptional and post-transcriptional regulation of REST may also be responsible for changes noted in REST target genes. Further experiments would be needed to distinguish between these possibilities.

We have shown that REST binds to the *RE-1* sites located -6.2 and -6.8 of TS of *REST* 5' upstream region, and represses its own transcription. Although a feed-forward loop involving β -catenin-TSC2-REST has been previously described, to our knowledge, this is the first time that REST has been shown to directly regulate its own transcription by a feedback

loop (85). The implications for our results in the context of previously described separate REST feed-forward loop are unclear as of now. It would be interesting to determine if the REST feedback loop is implicit to certain subtypes of medulloblastoma. Elevated REST protein has been previously correlated with poor patient overall survival and event free survival across multiple subtypes (28). If the REST feedback loop is functional in these tumors, increased REST transcription may be a positive prognostic indicator.

REST-HES1 co-repress *REST* transcription

The *N-box* located at -6.5 kb of the 5' *REST* upstream region is in close proximity to the -6.2 and -6.8 *RE-1* elements, and all that three sites have been validated for HES1 and REST binding respectively as shown above. Given the previously described seminal role of REST and HES1 in normal development as well as implication of both proteins in medulloblastoma pathology, we wanted to study if HES1 and REST could potentially co-regulate *REST* expression in medulloblastoma. We first assessed the presence of HES1 and REST independently at the previously validated *RE-1* sites and *N-boxes* respectively by ChIP assay, which confirmed HES1 binding to both *RE-1* sites in both cell lines, while REST occupancy was not detected at any of the *N-boxes* tested. ChIPs for HDAC1 and HDAC2 indicated occupancy of both HDACs at the *RE-1* sites, thus further corroborating our results, for both HDACs are part of the REST repressive complex, while HDAC1 is associated with the HES1 repression complex. This suggested that both REST and HES1 are potentially functional at these sites. Interestingly, despite previous HES1 binding observed at the *N-box* located at -6.5 kb from TS, no HDAC occupancy was detected, which may indicate that either that HES1 is present but not functional, or that perhaps HES1 displays differential regulation at this particular site. Indeed, presence of HDAC1, which can either associate directly with TLE-1 or can be recruited as part of the mSin3 complexes (which also associates with TLE-1), is not observed as HES1 switches to an activator (110). The activation role of HES1 is mediated by phosphorylation of several components of the HES1 complex, including HES1 itself, and dismissal of the repressive components of the complex, including TLE-1 (110). Further experiments would be necessary in order to delineate between these possibilities. Sequential ChIP to test for simultaneous co-occupancy of REST and HES1 at our sites of interest also indicated the co-occupancy of both REST and HES1 only at the *RE-1* sites, thus supporting the results of single HES1 and REST ChIPs as well as HDAC1 and HDAC2 ChIP.

Preliminary co-fractionation and co-IP experiments to determine whether the HES1 and REST could interact together in medulloblastoma cells indicated the existence of the complex. Both proteins were detected in the same fraction along with the positive controls, thus implying that at least a fraction of endogenous REST and HES1 interact with one another. Immunoprecipitation with anti-Flag antibody and western blot for HES1 and REST using DAOY expressing exogenous REST and HES1 respectively, further showed that REST and HES1 interact with one another further corroborated the findings of the co-fractionation experiment. Although preliminary, the interaction of HES1 and REST has not been shown before. Further experiments would be needed to understand the functional significance of this complex, and its contribution to regulation of *REST* expression.

Since HES1 and REST co-occupy the *RE-1* sites, and the two proteins appear to complex together, we wanted to know whether one protein was required for the binding and/or repressive activity of the other. To determine whether HES1 was required for the repressive activity of REST on the *RE-1* sites, we interfered with REST activity using REST-DBD in MB01110, a cell line with no detectable HES1. An increase in *REST* transcription was observed along with increase in other REST target genes, which is consistent with our findings in DAOY cells, where both HES1 and REST proteins are expressed. However, the change in *REST* transcription in MB01110 cells upon modulation of REST activity is greater than that observed in DAOY cells. Further experiments are needed to determine whether the greater increase in *REST* transcription in MB01110 cells as compared to DAOY cells is an artifact of two different cell lines, or a specific effect of lack of HES1 on REST transcription in MB01110. If a specific effect, it would suggest that perhaps HES1 further contributes to the repressive activity of REST in DAOY cells, thus leading to less of an increase in *REST* transcription upon modulation of REST activity, as HES1 may still be present at that site. Further experiments to determine the mechanism underlying recruitment of HES1 and REST to the *RE-1* sites, and if the presence of one protein is necessary for the other to bind would be interesting to pursue. Interestingly, a REST ChIP assay in MB01110 cells revealed no REST occupancy in this cell line, thus suggesting that perhaps HES1 is important for recruitment of REST to these sites. To conclusively determine that HES1 is indeed required for REST binding to *RE-1* sites, analysis of REST occupancy to the *RE-1* sites by ChIP assay from lysates prepared from MB01110 with ectopic expression of HES1 would be necessary. The increase in *REST* mRNA observed upon modulation of REST activity in the absence of *RE-1*

binding led us to conjecture that perhaps the effect of REST-DBD on *REST* expression is indirect. We cannot exclude the possibility that REST may still be binding to the *RE-1* site located at +0.8 downstream of TS because we were unable to amplify that specific site as previously indicated.

To determine whether HES1 and REST co-regulate *REST* expression we designed the following luciferase constructs: wildtype luciferase construct, luciferase with *RE-1* sites mutagenized, luciferase with -6.5 *N-box* mutagenized, or luciferase with all three sites mutagenized. These constructs were stably transfected into DAOY cells and a luciferase activity was measured. A greater increase in luciferase activity was observed upon simultaneously mutating both of the *RE-1* sites and *N-box* as compared to mutating either the *RE-1* site or the *N-box* alone, thus providing conclusive evidence that REST and HES1 co-repress *REST* expression and DAOY cells. It would be interesting to repeat the luciferase experiment in MB01110 cells in the presence and absence of DBD and HES1 to determine if the effect of REST-DBD on *REST* expression is indirect.

Overall, we have shown that REST and HES1 co-occupy the *RE-1* sites, and co-repress *REST* expression in medulloblastoma cells. A model summarizing our findings regarding the contribution of HES1 and REST on the transcriptional regulation of *REST* is presented below (Fig. 42). In the presence of both HES1 and REST, as is observed in DAOY cells, HES1 and REST both co-occupy *RE-1* sites, along with HDAC1 and HDAC2 (Fig. 42A). *N-boxes* are occupied by HES1 and associated HDAC1, but not REST and HDAC2, thus suggesting the occupancy of HES1 independent of REST at those sites (Fig. 42A). Our luciferase data suggests that when both HES1 and REST are present, then greater repression of *REST* expression is observed as compared with the presence of either protein alone. In the absence of HES1, observed in MB01110 cells, neither REST nor HES1 occupancy is detected at *N-boxes* or *RE-1* sites, thus indicating that HES1 may be required for REST occupancy at the *RE-1* sites (Fig. 42B). Our luciferase experiments performed in DAOY cells with simultaneous mutations in *RE-1* sites and *N-box* lead us to hypothesize that *REST* transcription should be higher in MB01110 cells, for occupancy of REST and HES1 is not detected at the *RE-1* site. Preliminary transcript data indeed shows lower levels of *REST* transcription in DAOY cells as compared to MB01110, however, further experiments are needed in order to confirm our preliminary findings. It would be interesting to determine if overexpressing HES1 in MB01110 would lead to occupancy of REST at the *RE-1* sites. Similarly, the effect of simultaneous

interference with both HES1 and REST activities in DAOY cells on *REST* expression remains to be determined. We have also shown HES1 and REST form a novel complex, and that HES1 appears to be required for REST binding to *RE-1* site, but further experiments are required to conclusively assess the requirement of HES1 for REST binding, or versa-visa. Our studies indicate that, HES1 and REST, two proteins that have been previously shown to publish in an oncogenic capacity, co-operate to repress the expression of *REST*. This may be one mechanism by which medulloblastoma cells maintain REST expression within a threshold necessary for their survival. It would be interesting to determine the contribution of post-translational regulation to the co-operative mechanism by which HES1 and REST control *REST* expression. Prognostic and therapeutic impact of this mechanism remains to be determined.

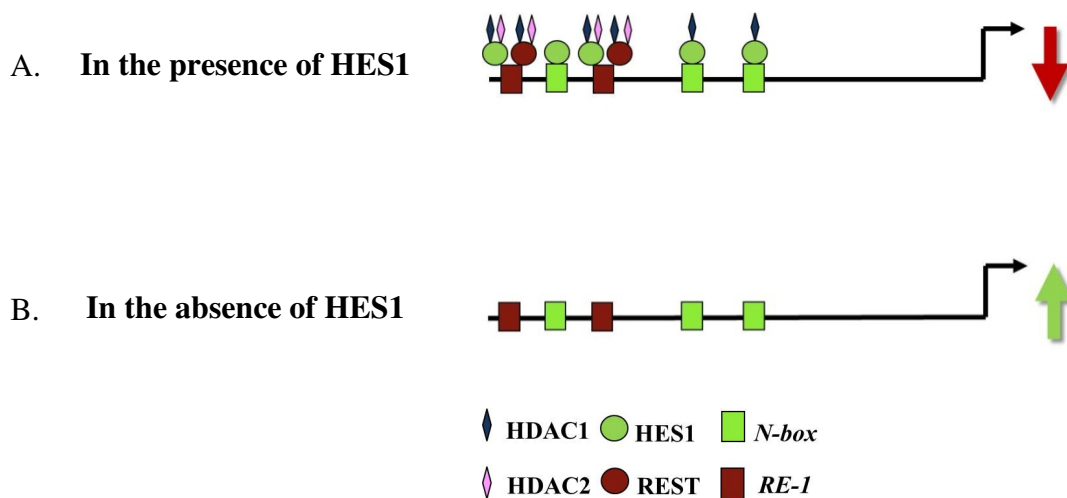


Figure 42: Model of HES1 and REST co-repression of *REST* expression.

A. In the presence of HES1 and REST (DAOY cells), *RE-1* sites are co-occupied by both REST and HES1, along with HDAC1 and HDAC2. These components function to co-repress *REST* transcription. B. In the absence of HES1 (MB01110), neither *N-boxes* nor *RE-1* sites are occupied by HES1 or REST. The lack of repression by HES1 and REST leads to up-regulation of *REST* transcription.

Retinoic acid regulates REST protein via modulation of SCF^{β-TRCP}

Neuroblastoma occurs in the sympathetic tissues, and NSCs from the developing neural crest are considered the cells of origin. Retinoic acid is a differentiating agent, and is a mainstay for neuroblastoma treatment, but the mechanism behind retinoic acid mediated differentiation remains unknown. A better understanding of this mechanism will provide

insights into the mechanism behind retinoic acid sensitivity and resistance of neuroblastoma cells lines and tumors, which can potentially translate into improved therapeutics. Given the critical role of REST in normal neurogenesis, where it suppresses neuronal differentiation, we wanted to determine if REST contributed to retinoic acid mediated differentiation of neuroblastoma cell lines.

Since the role of REST in neuroblastoma had not yet been explored, we first wanted to determine the status of REST in neuroblastoma patient samples and cell lines. Analysis of two separate sets of patient samples revealed that REST is maintained in many neuroblastoma patient samples. REST was also detected in several neuroblastoma cell lines, albeit at different levels. This is consistent with overexpression of REST observed in medulloblastoma patient samples and cell lines, another neural tumor.

To explore the mechanism behind retinoic acid mediated differentiation of neuroblastoma cell lines, all subsequent studies were done in previously published retinoic acid sensitive SK-N-SH and retinoic acid insensitive SK-N-AS cell lines (126, 127). We further characterized REST expression in these cells, and saw that while SK-N-SH cells display lower levels of REST mRNA and protein concomitant with higher levels of REST targets SynapsinI and β -tubulinIII, as compared to SK-N-AS cells. The latter is consistent with the more differentiated phenotype of SK-N-SH cells as compared to SK-N-AS cells. To assess the effect of retinoic acid treatment on REST, we treated both cell lines with retinoic acid, and analyzed REST and REST target mRNA and protein levels via qRT-PCR, Western blot, and immunofluorescence analyses. Although increase in *REST* expression upon retinoic acid treatment in both cell lines was observed, SK-N-SH cells showed a decline in REST protein, while SK-N-AS cells displayed the expected increase in REST levels (consistent with increased transcription). Protein and mRNA levels of SynapsinI and tubulin were consistent the changes in REST protein in both cell lines, with an increase in target genes observed in SK-N-SH cells, while a decrease was observed in SK-N-AS cells. Our findings are supported by a previous study which showed that unliganded RAR- α can bind to and repress *REST* transcription in cortical progenitors. It is interesting that in the presence of retinoic acid (a differentiation agent), and thereby a liganded RAR- α , an increase in *REST* transcription is observed. The same study also showed that REST is regulated by different mechanisms both transcriptionally and post-transcriptionally in cortical progenitors, thereby lending credence to our REST disparate mRNA and protein findings in response to retinoic acid treatment in SK-N-SH cells

(67). Lack of change in the Sub-G1 population of both cell lines upon retinoic acid treatment excluded apoptosis and cell cycle arrest as major contributing mechanisms.

To delineate between the transcriptional and post-transcriptional mechanisms by which retinoic acid may be regulating REST, we attempted a co-treatment of cyclohexamide and retinoic acid. However, our results were difficult to interpret, perhaps because of the limited duration of treatment (2 hours). Alternatively, to determine if proteasomal degradation may be involved in regulation of REST in response to retinoic acid, both cell lines were co-treated with MG132 and retinoic acid. A limitation of this experiment is the toxicity of cell lines to MG132 treatment, which allowed only 4 hour treatments with MG132 and retinoic acid. Since we have treated cells with retinoic acid for at least 24 hours, some of the effects of retinoic acid may be masked by the significantly decreased treatment times. Despite these limitations, analysis of REST protein in these samples showed that a block of retinoic acid mediated decline was indeed observed in SK-N-SH cells.

SCF ^{β -TRCP} has been previously shown to interact with, and ubiquitinate REST, thereby promoting its proteasomal degradation (59, 60). Since the MG132 experiment implicated the involvement of proteasome as a potential mechanism for retinoic acid mediated changes in REST, we wanted to know if retinoic acid treatment led to changes in SCF ^{β -TRCP} levels in SK-N-SH and SK-N-AS cells. Differential mRNA and protein levels of SCF ^{β -TRCP} were observed in retinoic acid treated SK-N-SH and SK-N-AS cells. Retinoic acid functions to increase SCF ^{β -TRCP} mRNA and protein which may subsequently translate into REST degradation in the retinoic acid sensitive SK-N-SH cells, but the same treatment in the retinoic acid insensitive SK-N-AS cells leads to the opposite effect of decreasing β -TRCP mRNA and protein, thereby potentially promoting the maintenance of REST levels. Ectopic expression of SCF ^{β -TRCP} in SK-N-AS cells led to increased interaction REST and SCF ^{β -TRCP} as well as increase in REST ubiquitination and degradation, concomitant with increase in SynapsinI levels.

Overall, our study has shown that REST is a key player in determining the differential response of retinoic acid sensitive and insensitive cells lines upon retinoic acid treatment. Although retinoic acid treatment leads to an increase in REST mRNA in both cell lines, retinoic-acid sensitive SK-N-SH cells up-regulate β -TRCP expression to promote degradation of REST, thus promoting differentiation. However, retinoic acid insensitive cells down-regulate β -TRCP upon retinoic acid treatment, which along with the increased REST

transcription, promotes maintenance of REST, thereby contributing to the retinoic acid insensitivity of these cells.

Conclusions

We have demonstrated that:

1. *REST* is transcriptionally mis-regulated in medulloblastoma patient samples.

This was demonstrated via qRT-PCR analysis of two separate sets of snap-frozen and paraffin embedded patient samples, where 35% and 65% of tumor samples displayed increased expression of *REST* as compared to non-tumor normal brain.

2. HES1 binds to N-boxes in *REST* 5' upstream region.

HES1 occupancy of *N-boxes* located -3.7 kb, -4.4 kb, and -6.5 kb from TS was determined by CHIP assay in DAOY and D283 cells.

3. HES1 regulates *REST* transcription.

This was demonstrated by modulating with HES1 activity via various HES1 constructs, and measuring *REST* expression via qRT-PCR. Interfering with HES1 activity in DAOY cells led to an increase in *REST* expression, while ectopic expression of HES1 in MB01110 cells led to a decrease in *REST* transcription.

4. Modulation of HES1 activity leads to change in expression of neuronal differentiation genes.

This was demonstrated by modulating HES1 activity via various HES1 mutant and wild-type constructs, and measuring *Syn1* and *SCG10* transcription via qRT-PCR. Interfering with HES1 activity in DAOY cells led to a decrease in *SCG10* expression, while ectopic expression of HES1 in MB01110 cells led to an increase in *Syn1* transcription.

5. Modulation of HES1 activity leads to altered change in survival potential of DAOY cells.

This was demonstrated by modulating HES1 activity via various HES1 mutant and wild-type constructs, and performing a competitive proliferation assay, where interfering with HES1 activity with MigR1-bHLH-OR-GFP led to an increase in the percentage of cells expressing the construct, whereas a decrease in percentage of cells expressing MigR1-HES1-GFP construct was observed.

6. *REST* binds to *RE-1* sites discovered in *REST* 5' upstream region.

REST occupancy of *RE-1* sites located -6.2 kb and -6.2 kb from TS was determined by CHIP assay in DAOY and D283 cells.

7. REST regulates its own expression in an auto-regulatory loop.

This was demonstrated by interfering with REST activity via a mutant of REST, and measuring *REST* expression via qRT-PCR. Interference with REST activity led to an increase in *REST* expression.

8. HES1 and REST co-occupy the *REST* 5' upstream region.

HES1 and REST co-occupancy of *RE-1* sites located -6.2 kb and -6.8 kb, and - was determined by CHIP assay in DAOY cells. We also found that HES1 occupancy was detected at two *RE-1* sites in HES1 CHIP samples from DAOY and D283 cells.

HDAC1 and HDAC2 were also detected at both *RE-1* sites in DAOY cells.

9. HES1 and REST interact in DAOY cells.

This was demonstrated by co-fractionation and Co-IP experiments in DAOY cells. Co-fractionation

10. REST modulates *REST* expression in the absence of HES1.

This was demonstrated by interfering with REST activity via a mutant of REST in MB01110 cells, which do not express any detectable HES1 protein, and measuring REST expression via qRT-PCR. Interference with REST activity led to an increase in *REST* expression, and this increase was greater than that noted in DAOY cells.

11. REST does not bind to *RE-1* sites in the absence of HES1.

REST occupancy of *RE-1* sites located -6.2 kb and -6.2 kb from TS in MB01110 cells, which lack any detectable HES1 protein, was determined by CHIP assay. No REST occupancy was detected at the *RE-1* sites.

12. REST is overexpressed in neuroblastoma patient samples and cell lines.

This was demonstrated by analysis of two separate set of patient samples by immunofluorescence and Western blot analyses.

13. Retinoic acid treatment leads differential regulation of REST mRNA and protein in retinoic acid sensitive SK-N-SH and retinoic acid insensitive SK-N-AS cells.

This was demonstrated by qRT-PCR, Western blot, and immunofluorescence analyses of both cell lines upon retinoic acid treatment. Retinoic acid treatment leads to an increase in *REST* transcript in both SK-N-SH and SK-N-AS cells. A decline in REST protein is observed in SK-N-SH cells, while SK-N-AS cells display increased REST levels.

14. Retinoic acid modulates REST levels in SK-N-SH and SK-N-AS cells by regulating SCF ^{β -TRCP} expression.

This was demonstrated by qRT-PCR and Western blot analyses of both cell lines upon retinoic acid treatment. SK-N-SH cells showed up-regulation of β -TRCP expression, whereas down-regulation of β -TRCP mRNA was observed in SK-N-AS cells. Inverse correlation between REST and β -TRCP was also observed in patient samples.

15. Ectopic expression of β -TRCP in SK-N-AS cells leads to increased REST- SCF ^{β -TRCP} interaction, increased REST ubiquitination, decreased REST protein, and increased Synapsin1 levels.

This was demonstrated by overexpressing β -TRCP in SK-N-AS cells, and analyzing the lysates via co-IP for REST- β -TRCP interaction and performing ubiquitin IP to detect change in REST ubiquitination. Western blot was done for REST and Synapsin1 protein levels.

Future Directions

Determining if modulation of HES1 activity translates into a change in tumorigenic potential of medulloblastoma cell lines.

We showed that interfering with HES1 activity leads to an increase in *REST* expression, while ectopic expression of HES1 leads to a decrease in *REST* transcription in medulloblastoma cell lines. Concomitant changes in *REST* target differentiation genes were also observed consistent with changes in *REST*. Furthermore, interference with HES1 using MigR1-bHLH-OR-GFP, the c-terminus deletion mutant, appears to provide a proliferative advantage over time to cells expressing the construct, while HES1 overexpression led to a decrease in proliferative potential of transgene expressing cells. We would next like to determine if modulation of HES1 in medulloblastoma cell lines would lead to an altered tumorigenic potential. Although our initial studies with the use of MB01110 have been unsuccessful in providing a clear answer because of technical problems, we continue to address these issues by use of more suitable equipment which would soon be available to the MD Anderson sorting facility. We also would like to repeat similar experiments in a different medulloblastoma cell line, DAOY. We would like to further determine if an altered tumorigenic potential upon HES1 modulation is also noted *in vivo* using xenograft models. If the technical issues are resolved, we would like to use MB01110 cells for the *in vivo* experiments, since it is a more recently derived primary cell line it may better reflect the patient tumors as compared to established cell lines. Although we have established that this cell line displays anchorage independent growth *in vivo*, we would first have to determine the tumorigenic potential of this cell line *in vivo*.

Determine the effect of HES1 modulation upon REST protein.

Although a significant change in *REST* transcription is observed upon HES1 modulation in medulloblastoma cell lines, a consistent change in REST protein is not reproducible at the same time points. The latter suggests differential mechanisms of regulating *REST* transcript and protein in these cells. We would like to determine how REST protein is regulated upon HES1 modulation. Since REST has been previously shown to be regulated via proteasomal degradation, we would first like to determine the involvement of the proteasome by treating cells expressing various HES1 construct with either cyclohexamide, which is an inhibitor of

translation, or MG-132, a proteasomal inhibitor. This would allow us to distinguish between the contributions of transcriptional and post-translational mechanisms on REST protein under our treatment conditions. If either of these possibilities is implicated, then further studies regarding mechanism regulating would be of interest.

Determine the status of REST protein in response to modulation of REST activity.

Our results show that interference with REST activity using REST DBD resulted in increased *REST* expression. Expression of other REST target genes, such as *Syn1* and *SCG10* was also observed. The latter leads us to speculate that either increased *REST* expression is not translated into increased REST protein, for the target gene expression remains low, or that the presence of REST DBD does masks the effect of increased REST protein. We would like to distinguish between these possibilities by doing a western blot for REST protein to determine if REST is indeed being expressed. Again, as proposed above, if increase in REST protein is not detected, then the contributing mechanism would be explored protein is detected.

Determine if HES1 is necessary for REST to bind to the *RE-1* sites located on the REST 5' upstream region.

We showed that REST binds to the *RE-1* site located on the REST 5' upstream region in DAOY and D283 cells, and that HES1 and REST co-occupy the two *RE-1* sites in DAOY cells. In D283 cells, although SeqChIP experiments were not performed, occupancy of HES1 was observed at the *RE-1* sites. REST ChIP experiments in MB01110, a cell line with no detectable levels of HES1 protein, did not reveal REST occupancy at the *RE-1* sites, thereby suggesting that perhaps HES1 is required REST binding to the *RE-1* sites in medulloblastoma cell lines. We would like to explore this possibility further by subjecting MB01110 cells overexpressing HES1 to ChIP assay to determine if a change in REST occupancy at the *RE-1* sites is observed. If REST is indeed binding to the *RE-1* sites under these conditions, then we would like to abrogate REST binding via REST-DBD, and determine if HES1 continues to bind, as well as the effect on REST transcription.

Determine the nature of HES1-REST complex in medulloblastoma cell lines.

Our preliminary data suggests that HES1 and REST form a complex in DAOY cells. Since both associate with co-repressor complexes with several components in common, such as mSin3, HDAC1, and HDAC2, it would be interesting to determine if REST and HES1 interact directly or via their co-repressor complexes. Co-IP and co-fractionation experiments conducted

on lysates from medulloblastoma cells expressing various domain mutants of REST, HES1, or both would be necessary to better characterize this interaction. We expect that since different domains of both proteins are associated with various complexes, deletion/mutation of these domains would abrogate HES1-REST complex. ChIP experiments with the use of these construct may further shed light on the functional significance of this interaction. Since REST has been previously implicated in an oncogenic role in medulloblastoma, and HES1 and REST appear to regulate *REST* expression, therapeutic implications of abrogating REST-HES1 interaction would also be interesting to explore.

Determine if the regulation of REST via these various mechanisms is consistent in normal neurogenesis.

We have shown different mechanisms via which *REST* expression can potentially be regulated in medulloblastoma cell lines. Since both HES1 and REST are critical for normal brain development as well as neurogenesis, perhaps the most interesting and meaningful extension of our studies in medulloblastoma cell lines would be to determine if these mechanisms are also relevant in normal neurogenesis. To this end, similar experiments to the ones we have performed in medulloblastoma cells would be repeated in NPC extracted from the cerebellum. Indeed, inconsistencies if different mechanisms are observed in NPCs, then the possibility arises that the mechanisms that we have discovered here may be contributing to the tumorigenic behavior of the medulloblastoma cell lines, and can potentially be targeted therapeutically.

Determine if overexpression of REST in SK-N-SH cells would lead to retinoic acid insensitivity

We have shown that SK-N-SH cells decrease REST protein in response to retinoic acid treatment. We would like to determine if stable ectopic expression of REST in SK-N-SH cells would lead to a retinoic acid insensitive phenotype in these cells. If shown, this would establish REST as a critical modulator of retinoic acid insensitivity in neuroblastoma cells. Therapeutic targeting of REST could potentially provide an opportunity for improved treatment.

Mechanism behind retinoic acid regulation of *SCF ^{β -TRCP}*

Our studies show that retinoic acid treatment led to change $SCF^{\beta-TRCP}$ expression in both SK-N-SH and SK-N-AS cells. It would be interesting to determine the mechanism behind regulation of $SCF^{\beta-TRCP}$ in these cell lines. Since a change in $SCF^{\beta-TRCP}$ transcription is observed, the presence of a *RARE* element in regulatory regions of $SCF^{\beta-TRCP}$. Furthermore, exploring the specific modulation of $SCF^{\beta-TRCP}$ regulation by retinoic acid sensitive and insensitive cells in response to retinoic acid treatment would further shed light on the mechanism contributing to retinoic acid insensitivity of certain cells and tumors.

Determine if ectopic $SCF^{\beta-TRCP}$ expression leads to a change in tumor forming potential of SK-N-AS cells

Our results show that ectopic expression of $SCF^{\beta-TRCP}$ leads to increased decreased REST protein levels as well as an increase in differentiation proteins. It would be interesting to know determine if this decrease in REST upon introduction of ectopic $SCF^{\beta-TRCP}$ translates into altered tumor growth potential *in vitro* and *in vivo*. To assess this anchorage independent growth assays and tumor formation via xenograft models could be done. If a decrease in tumor forming potential is indeed observed, then perhaps increase $SCF^{\beta-TRCP}$ could potentially be targeted therapeutically with agents that increase $SCF^{\beta-TRCP}$.

Chapter 8: Materials and Methods

I. Cell Culture

DAOY and D283 cell lines were purchased from American Type Culture Collection (ATCC). Both cell lines were cultured in medium containing Minimal Essential Medium (MEM), 10% fetal bovine serum (FBS), 2% L-glutamine, 1% sodium pyruvate, 1% non-essential amino acids, and 1% antibiotic solution (penicillin-streptomycin) (all from Invitrogen, Carlsbad, CA). UW426, UW228, MB01110, MB002, MB003 is a primary semi-adherent MB cell line. UW426 (from University of Washington) was cultured in DMEM with 10% FBS, 2 mM l-glutamine, 1% non-essential amino acids, and 1% PSF. UW228 (University of Washington) were cultured in the same conditions as DMEM but with 15% FBS. MB01110 (a kind gift from Dr. James Olson, Fred Hutchinson Cancer Research Center, Seattle, WA) was cultured in neurobasal media containing, 1% L-Glutamine, 1% antibiotic/antimycotic solution (PSF), supplemented with EGF (R&D, Emeryville, CA), and FGF (R&D, Emeryville, CA) (all others Invitrogen, Carlsbad, CA). MB003 and MB002 were cultured using DMEM-F12 with growth factors (EGF, FGF, LIF (Chemicon La Jolla, CA), N-2 (Invitrogen, Carlsbad, CA)) ((provided by Dennis Hughes, MD Anderson Cancer Center, Houston, TX). Dr. Zweidler-McKay (MD Anderson Cancer Center, Houston, TX) provided the HEK293-GP2 cells, are human embryonic kidney cells that have been modified to produce virus. These cells were cultured in Dulbecco's modified Eagle's medium (DMEM), 10% FBS, 5% heat inactivated horse serum (HS), 2 mM l-glutamine, 1% non-essential amino acids, and 1% PSF (all from Invitrogen, Carlsbad, CA). All cells were cultured in 5% carbon dioxide and at 37°C, and maintained at approximately 70% confluency. All neuroblastoma cell lines were kindly provided by Dr. Zweidler McKay, and cultured in RPMI media (REF) (prepared the same as MEM).

Trypsin (Invitrogen, Carlsbad, CA) was used to displace DAOY, UW426, UW228, HEK293-GP2, and all neuroblastoma cells from surface of tissue culture dishes/flasks (Becton, Dickinson, and company (BD), Franklin Lakes, NJ). D283 and MB01110 were displaced using cell scrapers (BD, Franklin Lakes, NJ) and accutase (Sigma-Aldrich, St. Louis, MO). Standard cell culture techniques were followed to thaw, maintain, and freeze all cell lines. For collection, cells were displaced as described above and pelleted via centrifugation at 1500 rpm for 3 minutes (as per the cell splitting protocol). Cell pellets were then re-suspended in D-PBS (MD Anderson Media Prep Facility, Houston, TX), and centrifuged again at 3500 rpm for 10 minutes. Supernatant was discarded, and pellets were stored at -80°C.

Retinoic acid treatment: Cells were treated with ALL-trans retinoic acid (prepared as per manufacturer's instructions) (Sigma-Aldrich, St. Louis, MO).

Cyclohexamide treatment: Cells were treated with 10 µg/ml of cyclohexamide (Sigma-Aldrich, St. Louis, MO) in the presence or absence of retinoic acid for 2 hours.

MG-132 treatment: Cells were treated with 5 µM of cyclohexamide (Sigma-Aldrich, St. Louis, MO) in the presence or absence of retinoic acid for 4 hours.

II. Infection

Producing virus: HEK293-GP2 cells were used to make all viral supernatants. Cells were plated in 10 cm² tissue culture dishes at 100% confluency in complete medium. Following manufacturer's protocol, Lipofectamine 2000 (Invitrogen, Carlsbad, CA) was used in a 1:3 DNA to Lipofectamine 2000 ratio to transfect the cells with retroviral plasmid DNA (21ug) along with pMD2G (4ug, a plasmid coat protein necessary for viral production). Cells were placed at 5% carbon dioxide and at 34°C to promote virus production. Transfection media was changed for fresh complete media 6 h post-transfection. Cells were maintained at 5% carbon dioxide and at 34°C.

Collecting viral supernatant: Media that the transfected HEK293-GP2 cells were cultured in contains the virus. It was collected in a 50 ml conical tube (Corning, Corning, NY) and centrifuged at 2450 rpm for 15 min to remove all debris (pellet). The supernatant (viral supernatant) was transferred to a new tube and stored at -80°C, while the pellet containing cellular debris was discarded. Viral supernatant was collected every 72 hours for up to 2 weeks, and was replaced by fresh media after each collection. The cells continued to be maintained at 5% carbon dioxide and at 34°C.

Cells in log phase of growth were used for retroviral infection. All infections were done in suspension in a 6 well format, and cells were plated at 30% confluency post-infection.

Cell preparation: Cells were displaced, centrifuged, and re-suspended in fresh media. A hemocytometer was used to count cells.

Infection: Viral supernatant was thawed in a 37°C water bath. To infect one well of a 6-well plate, 3x10⁴ DAOY cells and 3x10⁵ MB01110 cells were added to 750 µl of viral supernatant. 16 µg/ml and 8 µg/ml of hexadimethrine bromide (stock was 4 mg/ml, prepared as per

manufacturer's protocol (Sigma-Aldrich, St. Louis, MO) was added for DAOY and MB01110 respectively. Respective complete media were added until total volume was 2.5 ml in each well. The mix was vortexed, and added to the well, followed by centrifugation at 1000 G for 1 hour. Cells were then placed in the incubator and cultured as previously described.

Determination of appropriate hexadimethrine bromide concentration: Hexadimethrine bromide concentration for each cell line was determined empirically, by adding between 2-20 μ g/ml of hexadimethrine bromide to media or viral supernatant, and infecting cells as described above. Percent cell death and infection efficiency (as measured by GFP expression) were analyzed via flow cytometry. Lowest hexadimethrine bromide concentration with the greatest infection efficiency and least cell death was selected for each cell line.

Cell sorting: At 48 h and 72 h post-infection, cells were sorted via FACS at the MD Anderson South Campus Flow Cytometry Lab (MD Anderson Cancer Center, Houston, TX), and GFP positive were collected as described above. For further culturing of sorted cells, PSF concentration was increased to 4% for 16-72 hours to avoid contamination, and standard cell culture techniques described above were followed.

III. Transfections:

Lipofectamine 2000 (Invitrogen, Carlsbad, CA): DAOY cells were transfected according to manufacturer's instructions with either control MigR1-GFP vector or MigR1-DBD-GFP using a DNA to reagent ratio of 1:2 in MEM. Media was changed to complete MEM media after 6 hours.

Fugene HD (Roche, San Francisco, CA): SK-N-AS cells were transfected according to manufacturer's instructions with either control vector pQCXIP or the plasmid pQCXIP-SCF β -TRCP (kindly provided by Dr. Thomas Westbrook, Baylor College of Medicine, Houston, TX) using a DNA to reagent ratio of 3:2 in MEM. Media was changed to complete RPMI media after 6 hours.

IV. Competitive Proliferation Assay

MigR1-GFP control and plasmid infected medulloblastoma cells were cultured as normal, and analyzed by flow cytometry for GFP expression. Percentage of positive cells was calculated for all samples, and normalized as per the first day of flow analysis (usually 3 or 4 days).

V. Anchorage Independent Growth Assay

Bottom layer was composed of 0.4% low-melting agarose, while top layer contained 0.3% low melting agarose. The assay was done in a 24 well format. Untreated and treated MB01110 cells (500-100000) were plated in the top layer, and maintained at??. Colonies were visualized by a Gelcount scanner, counted using Gelcount software starting at 7 days after plating, and visualized every other day until day 27. We would like to thank Dr. Oliver Bogler for allowing us to use his equipment, and Laura Gibson, B.S. for the technical advice and guidance.

VI. Western blot analysis (WBA):

Making extract: Pellets were taken out of -80°C and thawed on ice. They were re-suspended in 50µl-100µl western blot (WB) lysis buffer (50mM potassium chloride (KCL), 10mM 4-(2-hydroxyethyl)-1-piperazineethanesulfonic acid (HEPES) (pH 7.5), 5mM Tris-Chloride (Tris-Cl) (pH 7.5), 10% glycerol, 2mM ethylenediaminetetraacetic acid (EDTA), 1mM DTT, 1% Triton X-100, 0.4% octylphenoxypolyethoxyethanol (Igepal), 1% protease inhibitors (Halt, Thermo Scientific, Rockford, IL) diluted in water), and sonicated for 1 min at a power setting of 0.5 every 2 seconds (Misonix Sonicator 3000, Misonix Incorporated, Farmingdale, NY). Samples were submerged in iced ethanol while sonication to prevent protein denaturation. Sonicated samples were then centrifuged at 14000 rpm for 10 min at 4°C to pellet debris. The supernatant was transferred to a new 1.7 ml eppendorf tube (Corning, Corning, NY) on ice, while the pellet was discarded. Protein concentration was determined using a 1x Commassie blue reagent (6x stock was diluted 1:6 in water) (Bio-Rad Protein Assay Dye-Reagent concentrate, Bio-Rad Laboratories, Hercules, CA) by mixing 995 µl of 1:6 diluted Commassie blue reagent with 5 µl of protein extract and measuring the OD by spectrophotometric analysis at 600 nm (Genesys 10-S, Thermo Electron Corporation, Waltham, MA). Equation used to calculate protein concentration from the OD was determined by doing a standard curve for protein concentration using protein Albumin.

Preparation of samples for loading: Total volume of each sample to be loaded was 15 μ l. Equal μ g of protein extract were added across treatments to 2.5 μ l of 6x loading dye (final concentration of the dye was 1x) and water was added for a total volume of 15 μ l. The samples were heated at 100°C for 3 min, followed by brief centrifugation at 14000 rpm.

SDS-PAGE electrophoresis: Samples were loaded on to a pre-cast gradient denaturing sodium dodecyl sulfate (SDS) polyacrylamide gel (Bio-Rad, Hercules, CA) for electrophoresis (PAGE). The gel was electrophoresed in running buffer (10x Tris/SDS (Bio-Rad, Hercules, CA) diluted 1:10 in water) at 100 V until the loading dye ran off the gel or until the desired separation was attained. Electrophoresed proteins were transferred to a Hybond-P membrane (GE Healthcare, Little Chalfont, UK) in transfer buffer (3.03 g tris, 14.4 g glycine, 100 ml methanol, and 900 ml water) at 100 volts (V) for 1 hour (all from Sigma-Aldrich, St. Louis, MO). Membranes were incubated in blocking buffer (5% nonfat dry milk (Nestle HealthCare Nutrition, Florham, NJ) prepared in D-PBS with 0.1% Tween (Bio-Rad, Hercules, CA) (PBS-T)) for 1 hour at RT while shaking. Primary antibody were diluted in blocking buffer as follows: Rabbit anti-REST (1:1000, Millipore, Waltham, MA), Rabbit anti-HES1 (1:2000 Millipore, Waltham, MA), anti-ActinHRP (1:20,000 Cell Signaling, Danvers, MA), anti-GAPDH HRP (Abcam, Cambridge, MA), anti- synapsin (1:2000 Millipore, Waltham, MA), anti-RAR- α (1: 1000 Santa Cruz Biotechnology, Santa Cruz, CA), N-Myc (1:1000 Santa Cruz Biotechnology, Santa Cruz, CA), anti-TUJ-1 (1:2000 Covance, Princeton, NJ), anti- β -TRCP (1:2000 Invitrogen, Carlsbad, CA); Ki-67 (1:500 BD Biosciences, San Jose, CA) The membrane was incubated overnight at 4°C while shaking with primary antibodies. Membrane was washed 5 times with blocking buffer for 10 minutes at RT while shaking, followed by incubation with peroxidase conjugated secondary antibodies (also prepared in blocking buffer) against rabbit immunoglobulins (IgGs) (1:10000) or against mouse IgGs (1:5000) for 1 hour at RT. Membranes were then washed 5 times with PBS-T for 10 minutes at RT while shaking, and immunocomplexes were visualized using Super Signal West Dura Enhanced Chemiluminescence (ECL) reagent (Thermo Scientific Pierce, Rockford, IL), Film (thermocientific) and a Kodak film developer (Eastman Kodak). Exposure time of the film varied for each antibody.

VII. SYBR Green qRT-PCR

RNA preparation:

Patient samples: RNA was extracted using FFPE RNA mini kit following manufacturer's protocol (Qiagen, Valencia, CA).

Cell lines: RNA was extracted using RNA mini kit following manufacturer's protocol (Qiagen, Valencia, CA).

RT-PCR: RNA was converted to cDNA using cDNA synthesis kit (Bio-Rad, Hercules, CA) following manufacturer's protocol. $\leq 1\mu\text{g}$ of RNA was added.

Preparing Mix: SYBR Green mix (2x Sensimix, Bioline, Taunton, MA) was used for qRT-PCR and qPCR analyses. cDNA was diluted 1:10, and the reaction was set up as described below in the 96 well PCR plates (Midsci, St. Louis, MO). All primers were ordered from Integrated DNA Technologies (IDT, Coralville, Iowa), and listed in Table 4 . All preparations were done on ice. The PCR mix was made as follows, and total volume was 15 μl /well:

Table 2: Syber Green PCR mix

Mix	1X (15 μl)
SYBR Green PCR master mix	7.5 μl
FWD primer (10 μM)	1 μl
REV primer (10 μM)	1 μl
Water	3.5 μl
Total	13.00 μl
Add to each well	
Mix	13 μl
DNA or water	2 μl
Total	15 μl

A master mix, consisting of all components except the DNA, for each primer set was prepared in a 1.7 ml eppendorf tube (Corning, Corning, NY), and 13 μl of the master mix was loaded

into the appropriate well of the PCR plate. 2 μ l of 1:10 dilution of cDNA was then added to the appropriate well, while 2 μ l of water was added to the blank wells. Each sample was loaded thrice on the PCR plate to assess pipetting error. The Microamp Optical Adhesive Film B was placed over the plate, and the plate was centrifuged at 2000rpm for 1 minute. Plate was loaded into the iCycler (Bio-Rad, Hercules, CA).

Data Analysis: Data was analyzed using Microsoft excel (Microsoft, Redmond, WA). Cycle threshold (CT) values that are greater than one cycle different from others in the triplicate were considered outliers, and removed from analysis. $\Delta\Delta$ ct method was used to analyze the data (REF). *RPS18* served as the internal control for all experiments. All values were first normalized to the internal control *RPS18* by subtracting the average CT (average of three CT values) for *RPS18* from the average CTs of other genes for the corresponding samples. Relative mRNA expression was determined calculating the power of the normalized values using the formula =power(1.9, -normalized value). Samples were scaled from 0 to 1 relative to the highest value. Experiments were done in triplicate.

Table 3: List of qRT-PCR Primers

Gene	Forward Primer	Reverse Primer
RPS18	5'- GTGGTGTTGAGGAAAGCAGA CATTG -3'	5'- CATCCTTCTGTCTGTTCAAGAAC CAGT C -3'
REST	5'- GTAGGAGCAGAAGAGGCAGA TGAGAG -3'	5'- GCTTCACGTTCTTCTACTGCTGA AGG -3'
p27	5'- TCTCTGCAGTGCTTCTCCAA - 3'	5'- AGATGTCAAACGTGCGAGTC -3'
SYN1	5'- GTCTGACAGATAACAAGCTGTG GGTG -3'	5'- GACCACGAGCTCTACGATGAGC TG -3'
HES1 total	5'- CAGCATCTGAGCACAGAAAG TCATCAAAGC -3'	5'- GGAATGCCGCGAGCTATCTTTCT TCAG -3'
HES1 endogeno us	5'- CAGGGACTTGCCTCACTGTGT CC -3'	5'- CTGATCAGGAGGCTTGCAAACC - 3'
TUBB3	5'- GGAAGGAGTGTGAAAACCTGC GACTG -3'	5'- CACGACGCTGAAGGTGTTTCATG ATG -3'
RAR- α	5'- CATCCCCAGCCACCATTGAGA C -3'	5'- GACAGACAAAGCAAGGCTTGTA GATG -3'

VIII. Chromatin Immunoprecipitation (ChIP)

Cross-linking and sonication: 1 million cells were used for ChIP assay. Cells were pelleted as described before by centrifugation at 3500 rpm for 10 minutes. Cells were re-suspended in

crosslinking and homogenization buffer (50 mM HEPES pH 8.0, 140 mM NaCl, 1 mM EDTA pH 8.0, 0.8% Iqpel CA-630, 0.4% Triton X-100, 10% protease inhibitors (HALT, Thermo Scientific, Rockford, IL) diluted in water) and cross-linked by addition of 1% formaldehyde, followed by inverting the tube to mix 10 times, and a 10 minute incubation at RT while shaking. 1/10 of the total volume of 1.4 M glycine was added to neutralize the crosslinking, and incubated for 5 minutes while shaking at RT. Nuclei were pelleted via centrifugation at 14000 rpm for 1 minute at 4°C, followed by re-suspension in crosslinking and homogenization buffer and another 4°C centrifugation at 14000 rpm for 1 minute. Next, the pellet was washed twice with nuclear wash buffer (20 mM Tris-Cl pH 8, 150 mM NaCl, 1 mM EDTA pH 8, and 1% protease inhibitors diluted in water) interspersed by 4°C centrifugation at 14000 rpm for 1 minute. Nuclei were prepared for sonication by re-suspending them in sonication buffer (50 mM Tris-Cl pH 8, 10 mM EDTA pH 8, 1% SDS, 10% protease inhibitors), and sonicated at 1.5 power level setting as per instructions. Sonicated extract was centrifuged two times at 14000 rpm for 1 minute at 4°C to remove debris.

Pre-clearing and immunoprecipitation: 10% of each set of IgG and specific pull-down was saved as input DNA and the remaining 90% was diluted 10 fold using ChIP dilution buffer (16.7 mM Tris-Cl pH 8, 1.2 mM EDTA pH 8, 16.7 mM NaCl, 1.1% Triton X-100, 10% protease inhibitors diluted in water). Lysates were pre-cleared using Protein G magnetic beads (DAOY and D283) for 2 hours at 4°C with shaking

Magnetized stand was used to pellet the magnetic beads, whereas beads were collected via centrifugation at 3000 rpm for 1 minute at 4°C. The pre-cleared supernatant was incubated with either 5µg of specific antibody (REST, HES1) or 5µg control IgG for 12 hours at 4°C with shaking. Simultaneously, beads were incubated with 4.4 µg of salmon sperm DNA. Beads incubated with salmon sperm DNA were then incubated with lysates immunoprecipitated with control or specific antibody for 2 hours while shaking at 4°C. Magnetized stand was used to pellet the magnetic beads, whereas protein A/G beads were collected via centrifugation at 1000 rpm for 1 minute at 4°C.

DNA elution and purification: Beads were then subjected to two low salt washes (20 mM Tris-Cl, pH 8, 2 mM EDTA pH 8, 150 mM NaCl, 0.10% SDS, 1% Triton X-100, 10% protease inhibitors diluted in water), two high salt washes (20 mM Tris-Cl, pH 8, 2 mM EDTA pH 8,

500 mM NaCl, 0.10% SDS, 1% Triton X-100, 10% protease inhibitors diluted in water) , two lithium chloride (LiCl) washes (10 mM Tris-Cl, pH 8, 1 mM EDTA pH 8, 250 mM LiCl, 1% Igepal CA630, 1% sodium deoxycholate, 10% protease inhibitors diluted in water), and two washes with TE interspersed by centrifugation at 1000 rpm for 1 minute at 4°C. To elute the immunoprecipitated DNA from beads by adding 2x elution buffer (EB) (2% SDS, 0.2 M sodium bicarbonate diluted in water) followed by vortexing for 10 minutes, and centrifugation at 14000 rpm at RT for 2 minutes. Supernatant was moved to a new tube, and the beads were re-eluted with 1X EB (1% SDS, 0.1 M sodium bicarbonate diluted in water) followed by vortexing for 15 seconds, and centrifugation at 14000 rpm at RT for 2 minutes. The supernatant was added to the previous eluent, and centrifuged at 14000 rpm at RT for 2 minutes to remove all beads. Supernatant was moved to a new tube, and equal volume of 2x dilution buffer (20 mM Tris-Cl, pH 8, 2 mM EDTA pH 8 diluted in water) is added to the eluents. 135 µl of 1x EB was added to inputs, and volume was adjusted with 2x dilution buffer so that the total volume of inputs is equal to the eluent volume. DNA was extracted by adding 0.3 M NaCl to all samples followed by an overnight incubation in a 65°C water bath. Qiaquick PCR purification columns were used to purify DNA as per manufacturer's instructions (Qiagen).

SeqChIP: Similar protocol was used as described above. First ChIP was done as before with anti-HES1 or IgG and eluted with elution buffer (50 mM Tris-Cl pH 8.0, 10 mM EDTA pH 8.0, 1% SDS, 1% protease inhibitors diluted in water). Elution1 was adjusted to concentrations of IP buffer1. Second ChIP was done with anti-REST or IgG, followed by elution with EB as described in the ChIP protocol.

Analysis of samples: Samples were analyzed using SYBR green qPCR. Mix was prepared using the same protocol as described for qRT-PCR. ChIP and DNA were diluted 1:10. Primers used are indicated in Table 5.

Data Analysis: Data was analyzed using Microsoft excel (Microsoft, Redmond, WA). We first searched each set of three CT values for each sample for outliers and removed them from the analysis. The average of input CT values was subtracted from the average of corresponding sample (specific antibody) and control (IgG) CT values. Relative binding was determined calculating the power of the latter values using the formula =power(1.9, -((sample or control)-

input). Samples values were then compared to control values, and scaled from 0 to 1 relative to the highest value. Experiments were done in triplicate.

Validating primers: To validate primer sets, a serial dilution was prepared by combining several cDNA samples for a standard curve (1:10, 1:100, 1:1 000, 1:10 000).

Table 4: List of ChIP primers.

Site	Forward Primer	Reverse Primer
<i>REST N-box</i> -3.7 kb	5'- CTGATGCGTGAAATCAGGA ATGTGC -3'	5'- CTGCCTCCTTGAATCTCCCTAATAAC TAC -3'
<i>REST N-box</i> -4.4 kb	5'- GAGTCATGGGTCCTACCTCC ATCTGTG -3'	5'- GCCTCTCTTCTCTGGCCTTTACCAT TG -3'
<i>REST RE-1</i> -6.2 kb	5'- GTCGTACATGTAGTCCCAGC TACTCG -3'	5'- CAATGCGACAAAGATACTGAGCACC -3'
<i>REST N-box</i> -6.5 kb	5'- GACACCTCCCATTTGGGTCT TTAGG -3'	5'- GAACCGCCTGCCTAGCCTATG -3'
<i>REST RE-1</i> -6.8 kb	5'- GAGGTTGTGGTGAGCCAAG ATCATG -3'	5'- CCATGTTCAAGCGATTCTTCTGCCTC -3'
<i>p27</i> (positive control)	5'- GTGCAATGGCATGATCATA GCTCACTG -3'	5'- GTCAGAGTCCTTGCCTGTGGG -3'
<i>p27</i> (negative control)	5'- GAGCTTCAGGATCCGGAAA CTGAAGAG -3'	5'- CTTCAGCCCATGTGTGATGAAGATGC AG -3'
<i>Syn1</i>	5'- CAACACTACAAACCGAGTA TCTGC -3'	5'- GCCTCATCCTGGTCCTAAAA -3'

IX. Immunoprecipitation

Lysates from transfected SK-N-AS cells were denatured by heating at 95°C for 5 minutes. Lysates were pre-cleared as described above with protein G magnetic beads (Millipore, Billerica, MA), followed by immunoprecipitation with mouse anti-ubiquitin antibody (Abcam, Cambridge, MA), as described above. Immunoprecipitated proteins were eluted using 2x sodium SDS buffer. Immunoprecipitants as well as inputs (1% and 3%) were then subjected to western blot analysis as described before (anti-REST 1:1000).

X. Co-immunoprecipitation

Lysates from transfected DAOY or SK-N-AS cells were pre-cleared and immunoprecipitated with specific antibodies or IgGs described above (rabbit anti-Flag or mouse anti- β -TRCP respectively), followed by elution as described above (immunoprecipitation protocol). Immunoprecipitated proteins and input material (1% or 3%) were then subjected to Western blot analysis for detection of REST (anti-REST 1:1000), HES1 (anti-HES1 1:2000, Abcam, Cambridge, MA), and β -TRCP (anti- β -TRCP Cell Signaling, Danvers, MA)

XI. Co-fractionation

DAOY cells were lysed by sonication in sedimentation lysis buffer (5 mM Tris-Cl pH 7.5, 2 mM EDTA pH 8.0, 50 mM KCl, 10 mM HEPES pH 7.5, 10% glycerol, 1% Triton X-100, 0.4% Igepal CA-630, 1% protease inhibitors diluted in water). Sonicated extract was then subjected to centrifugation at 14000 rpm for 1 minute, and supernatant was transferred to a new tube, while the pellet was discarded. Protein concentration was determined via spectrophotometric analysis as described before. The Superdex200 column (GE Healthcare Biosciences, Pittsburgh, PA) was equilibrated with lysis buffer. 2 mg of protein was loaded onto the column which was run with a pump flow rate of 0.45. Eluents were collected in 1.7 ml eppendorf tubes containing protease inhibitors every 5.5 minutes. Reference standards for the column are F22-668 kDa and F29-232 kDa. Samples were combined in 2X2 samples and analyzed by Western blot analysis.

XII. Immunofluorescence Assay

Cells were plated in Lab-Tek II Chamber Slides (Thermo Fisher Scientific, Rochester, NY), fixed using 2% buffered paraformaldehyde, and followed by three 1 minute PBS washes. After blocking, the cells were incubated anti-REST (1:500), TujI (1:1000), and SCF β -TRCP (1:1000) overnight at 4°C. Next, the samples were subjected to three 3 minute washes with D-PBS. Next, the fixed cells were incubated with fluorophore-conjugated secondary antibodies for 1h while shaking, followed by three 3 minute D-PBS washes. Slides were then covered with 40,6-diamidino-2-phenylindole (1 μ g/mL), and observed under a Nikon fluorescence microscope (Nikon Inc., Melville, NY). Data was analyzed via MetaMorph software (Molecular Devices, Downingtown, Pa). Initial deparaffinization preceded the procedure described above for staining patient samples.

XIII. Statistical Analysis:

Criteria for statistical significance for all analyses is as follows: * $p \leq 0.05$, ** $p \leq 0.01$, *** $p \leq 0.001$)

Patient samples: Non-parametric T-test was used to analyze patient samples and non-tumor normal brain tissue using GraphPad Prism5 (GraphPad Software, La Jolla, CA). Scatter plots were generated using GraphPad Prism5, while Microsoft Excel was used to make the bar graphs.

Interference experiments: One way analysis of variance (ANOVA), and Fisher LSD post-hoc test were conducted for statistical analyses using Statistica 6.0 (Statsoft, Tulsa, OK). Relative transcripts (*REST*, *p27*, *Syn1*, *SCG10* normalized to *RPS18*) of cells specific construct (mutant HES1 constructs, full-length HES1 construct, or REST-DBD construct) were compared to those of control MigR1 infected cells.

ChIP: One way analysis of variance (ANOVA), and Fischer least significant difference post-hoc test (LSD) was conducted for statistical analyses using Statistica 6.0. Control (IgG) values (normalized to input) were compared to control values (normalized to input).

XIV. Cloning: Overview

1. PCR 2. agarose gel electrophoresis 3. cut and purify band of interest 4. TOPO ligation 5. bacterial transformation 6. picking colonies 7. miniprep I 8. restriction digest 9. miniprep II 10. sequencing 11. cutting out of TOPO vector 12. ligation into vector of interest 13. bacterial transformation 14. picking colonies 15. miniprep I 16. restriction digest 17. midiprep 18. sequence

REST-DBD:

The DNA binding domain of REST (REST-DBD) was cloned out of previously published pcDNA3.1-DBD, and cloned into retroviral vector MigR1-GFP and MigR1-mKate. REST-DBD was flanked with XhoI and EcoR1 on 5' and 3' end respectively, and stop codons were introduced to the 3' end. The following primers were used: DBD FWD and DBD REV (Table 6). PCR was done using PFU Turbo was used as per manufacturer's protocol (Roche, San Francisco, CA)

All subsequent cloning steps were followed as described above.

REST luciferase:

5' upstream region of *REST*

Genomic DNA was extracted from DAOY and D283 cells using genomic extraction kit as per manufacturer's protocol (Qiagen, Valencia, CA). Several attempts were made to clone -7 kb of 5 upstream region of *REST* relative to TS, using numerous PCR reagents with DAOY, D283 genomic DNA, and fosmids as template, as well as fosmid digestion, but the attempts were unsuccessful.

5' upstream region of *REST* ranging from -6.8 kb to -6.2 kb relative to TS was amplified from DAOY genomic DNA. NheI and XhoI restriction sites were introduced into 5' and 3' ends respectively using the following primers: REST -7 FWD and REST -6 REV

5'-

Advantage GC Genomic LA Polymerase Mix (Clontech, Mountain View, CA) was used to amplify genomic DNA, and the reaction was set up as per manufacturer's instructions.

All subsequent cloning steps were done as described above to ensure the presence and validity of the cloned region. The piece was then digested with NheI and XhoI and ligated into

pGL4.15-sv40 (described below) as previously described to generate pGL4.15-sv40-hREST-6.8 to -6.2. All subsequent cloning steps were followed as described above to ensure the presence and validity of the cloned region.

pGL4.15-sv40:

Fragment containing sv40 minimal promoter, was cut out of pGL3 promoter vector using BglII and HindIII, and was then ligated into pGL4.15 as described above to generate pGL4.15-sv40. The new construct was sequenced to ensure the presence and validity of the sv40 promoter.

Mutating *REST* luciferase:

RE-1 sites located -6.8 and -6.2 kb from TS and *N-box* located -6.5 kb from TS were mutated as follows in pGL4.15-sv40-hREST-6.8 to -6.2. SacII and MluI restriction sites were introduced in the middle of mutated *RE-1* and *N-box* sequences respectively. NheI was introduced at -7 kb and BglII and XhoI sites were introduced at -6 kb to facilitate further cloning. pGL4.15sv40-WT as template for all PCRs unless otherwise specified.

The following PCR reactions using PFU Turbo (Roche, San Francisco, CA) were carried out as per manufacturer's protocol

To mutate *RE-1* located -6.8 kb upstream of TS:

PCR1: from -6.8 mutated *RE-1* to -6

PCR2: from -7 to -6.8 mutated *RE-1*

PCR products were ligated into TOPO vector, and all subsequent cloning steps were followed as described above to ensure the validity of the piece. Digestion with XhoI and SacII, followed by ligation as described below was done to mutate the *RE-1* site located at -6.8 kb upstream of TS. All subsequent cloning steps were followed as described above to ensure the validity of the piece

Similarly, *RE-1* located at -6.2 kb upstream of TS:

PCR1: from -6.2 kb mutated *RE-1* to -6 kb

PCR2: from -7 kb to -6.8 kb mutated *RE-1*

PCR products were ligated into TOPO vector, and all subsequent cloning steps were followed as described above to ensure the validity of the piece. Digestion with XhoI and SacII, followed

by ligation as described below was done to mutate the *RE-1* site located at -6.2 kb upstream of TS. All subsequent cloning steps were followed as described above to ensure the validity of the piece

Similarly, *N-box* located at -6.5 kb upstream of TS:

PCR1: from -6.5 kb mutated *N-box* to -6 kb

PCR2: from -7 kb to -6.5 kb mutated *N-box*

PCR products were ligated into TOPO vector, and all subsequent cloning steps were followed as described above to ensure the validity of the piece. Digestion with MluI and XhoI, followed by ligation as described below was done to mutate the *N-box* site located at -6.5 kb upstream of TS. All subsequent cloning steps were followed as described above to ensure the validity of the piece.

To mutate both *RE-1* sites:

Both constructs were digested with NheI and HpaI, followed by ligation as described below. All subsequent cloning steps were followed as described above to ensure the validity of the piece.

To mutate both *RE-1* sites and *N-box* located -6.5 kb upstream of TS:

PCR1: From -6.5 kb mutated *N-box* to -6 kb with -6.2 kb mutated *RE-1* construct as template

PCR2: from -7 kb to -6.5 kb mutated *N-box* with -6.8 kb mutated *RE-1* construct as template

Both constructs were digested with NheI and HpaI, followed by ligation as described below.

All subsequent cloning steps were followed as described above to ensure the validity of the piece.

Table 5: List of Cloning Primers

Primer	Forward Sequence	Reverse Sequence
REST-DBD	REST-DBD 5'- CATCGTCTCGAGAAGGATGA CGACGATAAGATGGCAGAAC TGATGCCGGTTGGGGATAAC - 3'	REST-DBD 5'- CCGCGCGAATTCTCATCACTATCATC ATTTTGTGGAAGATTCCTCATCATTCA CAGGAC -3'
hREST-6.8 to -6.2	<i>REST -7</i> 5'- AGT AGA GCT AGC GGA GAT GCG GAG GTT GTG GTG AGC CAA GAT CAT GCC GTT GCA TTT CAA -3'	<i>REST -6</i> 5'- CCG TGC CTC GAG CAA TGC GAC AAA GAT ACT GAG CAC CTG GAA TTC TCT CTC TCT TTT CC -3'
hREST-6.8 Mut PCR1	<i>REST -6.8mut</i> GAATATGCTAGCCAGTTAA <u>A</u> ACCGCGGTTAATTCGCCTGTA GTCCCAGCTACTCAGGAGG	<i>REST -6</i> 5'- CCG TGC AGATCT CTC GAG CAA TGC GAC AAA GAT ACT GAG CAC CTG GAA TTC TCT CTC TCT TTT CC -3'
hREST-6.8 Mut PCR2	<i>REST -7</i> AGT AGA GCT AGC GGA GAT GCG GAG GTT GTG GTG AGC CAA GAT CAT GCC GTT GCA TTT CAA	<i>REST -6.8mut</i> GCGGGCAGATCTAATTAACCGCGGTT TTAACTGTTTTTGTGTTTTTTGTGTTTT TTGAGATGAAGT
hREST-6.2 Mut PCR1	<i>REST -6.2mut</i> GAATATGCTAGCCAGTTAA <u>A</u>	<i>REST -6</i> 5'- CCG TGC AGATCT CTC GAG CAA

	ACCGCGGTTAATTGGGGGAG GATCGCTTGAGTCCAGGAGG	TGC GAC AAA GAT ACT GAG CAC CTG GAA TTC TCT CTC TCT TTT CC -3'
hREST-6.2 Mut PCR2	<i>REST -7</i> 5'- AGT AGA GCT AGC GGA GAT GCG GAG GTT GTG GTG AGC CAA GAT CAT GCC GTT GCA TTT CAA -3'	<i>REST -6.2mut</i> 5'- TCGCGGAGATCTAATTAACCGCGGTT TTAACTGGACTACATGTACGACCTAC CACACCCA -3'
hREST-6.5 Mut PCR1	<i>REST -6.5mut</i> TGGCCCGCTAGCACGCGTTAA ATATCTAGGAATGTGATGACT GGATTATATGCTAAGTGT	<i>REST -6</i> CCGTGCAGATCTCTCGAGCAATGCCA CAAAGATACTGAGCACCTGGAATTCT CTCTCTC -3'
hREST-6.5 Mut PCR2	<i>REST -7</i> AGT AGA GCT AGC GGA GAT GCG GAG GTT GTG GTG AGC CAA GAT CAT GCC GTT GCA TTT CAA	<i>REST -6.5mut</i> 5'- TCCGTGAGATCTACGCGTAGAACTGA AAACCTGTGGTACCTAAAGACCCAAA TGGGAGGT -3'

Common Cloning Protocols

Agarose gel electrophoresis:

Gel preparation: Appropriate percentage agarose gel was prepared by dissolving xg of agarose in 100ml of 0.5x Tris Boric acid Ethylenediaminetetraacetic (EDTA) (TBE) buffer in a weight to volume ratio (5x TBE stock (56 g tris-Cl, 27.5 g Boric, 20 ml 0.5M EDTA pH 8 diluted in water) was diluted 1:10 in water to make 0.5x). The mix poured into the agarose gel electrophoresis apparatus, and 10 µl of ethidium bromide was added and mixed to uniformity. A comb was placed in the gel to form the appropriately sized wells, and the mix was allowed to polymerize for 1 hour. The samples were prepared by adding appropriate amount of 6x loading buffer (bromophenol blue, xylene cyanol, glycerol in water), and electrophoresed in 0.5x TBE

buffer at 100 volts (V) until desired separation was attained. The bands were visualized under UV light using Chemidoc.

Purification of product from agarose gel:

The band of interest was cut out using a blade and purified using a gel extraction kit following manufacturer's protocol.

Bacterial transformation via heat-shock:

NEB10 competent cells were thawed on ice. The DNA was placed on ice and allowed to cool before the transformation. In a cool 1.7 ml microcentrifuge tube, 1 µg of DNA were mixed with 40 µl of competent cells, and incubated on ice for 20-45 minutes. The mix was then placed into a 42°C water bath for 20-25 seconds, and then placed back on ice for 1-2 minutes. 250 µl of SOC, prepared as per manufacturer's instructions, was added to the transformation reaction followed by 1 hour incubation at 37°C in a bacterial incubator while shaking. 10 µl of the transformation reaction was plated on an agar plate containing the appropriate antibiotic, and placed at 37°C in the bacterial incubator overnight (12-16 hours). For transforming the ligations, the entire 250 µl SOC culture was centrifuged at 1500 rpm for 15 minutes to pellet the bacteria. The supernatant is discarded, and cells are re-suspended in 50 µl of LB and plated on the appropriate antibiotic plate. Ampicillin was used at 100 µg/ml concentration (Sigma, prepared as per manufacturer's instructions), while kanamycin concentration was 50 µg/ml (Sigma prepared as per manufacturer's instructions).

Picking bacterial colonies from agar plates:

Colonies were picked using sterilized toothpicks, and allowed to grow in 2 ml of LB broth (Invitrogen, prepared as per manufacturer's instructions), containing the appropriate antibiotic at 37°C overnight. The cultures were pelleted via centrifugation at 3500 rpm for 20 minutes. The supernatant was discarded, and pellet was either stored at -80°C or used for further experiments.

Miniprep I:

Colonies were picked using sterile toothpicks into 2 ml of LB with appropriate antibiotic, and allowed to grow overnight at 37°C overnight while shaking. 1 ml of the culture was transferred

in to a 1.7 ml eppendorf tube, and the bacteria were pelleted by centrifugation at 3500 rpm for 20 minutes. The supernatant was removed and discarded, while the pellet was re-suspended in 300 μ l of STET. To release the plasmid from the bacteria, 25 μ l of lysozyme (10 mg/ml in 1x Tris-Cl EDTA (TE) (10mM Tris-Cl pH 8, 1mM EDTA pH8 diluted in water)) was added to the sample and incubated for 3 min, followed by heating the samples at 100°C for 1 minute 20 seconds. The samples were then centrifuged at 14000 rpm for 10 min, and the pellets containing the lysed bacterial particles were removed with a toothpick. The samples were then incubated with 325 μ l of isopropanol at room temperature (RT) for 5 minutes to precipitate the DNA, followed by centrifugation at 14000 rpm for 10 minutes to pellet the plasmid DNA. The supernatant was discarded and the tube was allowed to air dry for 15 minutes. The pellet was then re-suspended in 50-100 μ l of 1xTE.

Restriction digest:

All restriction enzymes were purchased from New England Biolabs (NEB). The following components were added together in a 1.7 ml eppendorf tube, and incubated in a 37°C water bath for 1 hour: 1/10 of the total reaction volume was the appropriate buffer, 1/20 of the total volume of restriction enzyme, appropriate amount of DNA (typically, 1 μ g for 50 μ l reaction or 5 μ l of miniprep (miniprep I) DNA in 10 μ l reaction), and water to make up the remaining volume. The digests were subjected to agarose gel electrophoresis using an appropriate percentage gel.

Sequencing:

1 μ g of DNA (diluted to 100 ng/ μ l as per the core facility's instructions) was sent for sequencing to MD Anderson DNA core facility to verify the presence and validity of the insert. Some common sequencing primes were provided by the core facility, and any specific sequencing primers were sent to them (10 pmol/ μ l as per core facility's instructions).

Ligations

For ligation, 1 μ g of vector and 5 μ g of plasmid containing insert were subjected to restriction digests with the appropriate restriction enzymes in a 50 μ l reaction. The cut vector was then treated with 1 μ l of calf-intestine phosphatase for 1 hour incubation 37°C. The reactions were subjected to agarose electrophoresis, and band of interest was cut and purified. Ligations were

then set up using T4 ligase as per manufacturer's instructions in the following vector to insert ratios based on size and intensity ratios of the digested pieces: 1:0, 1:1, 1:3, 1:6, 1:maximum. The ligations were incubated either at RT for 1 h or 14°C overnight in iCycler.

Midiprep: A 50 ml bacterial culture was grown overnight (or grown to the recommended optical density (OD)) while shaking at 37°C under appropriate antibiotic selection. Bacteria were pelleted via centrifugation at 3500 rpm for 20 min at 4°C. Supernatant was discarded, and pellets were either stored at -80°C, or midiprepmed using Plasmid plus midi kit (Qiagen, Valencia, CA) following manufacturer's protocol.

References

1. Guessous, F., Y. Li, and R. Abounader. 2008. Signaling pathways in medulloblastoma. *J Cell Physiol* 217:577-583.
2. Pfister, S. M., A. Korshunov, M. Kool, M. Hasselblatt, C. Eberhart, and M. D. Taylor. 2010. Molecular diagnostics of CNS embryonal tumors. *Acta Neuropathol* 120:553-566.
3. Gilbertson, R. J., and D. W. Ellison. 2008. The origins of medulloblastoma subtypes. *Annu Rev Pathol* 3:341-365.
4. Gibson, P., Y. Tong, G. Robinson, M. C. Thompson, D. S. Curre, C. Eden, T. A. Kranenburg, T. Hogg, H. Poppleton, J. Martin, D. Finkelstein, S. Pounds, A. Weiss, Z. Patay, M. Scoggins, R. Ogg, Y. Pei, Z. J. Yang, S. Brun, Y. Lee, F. Zindy, J. C. Lindsey, M. M. Taketo, F. A. Boop, R. A. Sanford, A. Gajjar, S. C. Clifford, M. F. Roussel, P. J. McKinnon, D. H. Gutmann, D. W. Ellison, R. Wechsler-Reya, and R. J. Gilbertson. 2010. Subtypes of medulloblastoma have distinct developmental origins. *Nature* 468:1095-1099.
5. Jakacki, R. I. 2005. Treatment strategies for high-risk medulloblastoma and supratentorial primitive neuroectodermal tumors. Review of the literature. *J Neurosurg* 102:44-52.
6. Kool, M., J. Koster, J. Bunt, N. E. Hasselt, A. Lakeman, P. van Sluis, D. Troost, N. S. Meeteren, H. N. Caron, J. Cloos, A. Mrcic, B. Ylstra, W. Grajkowska, W. Hartmann, T. Pietsch, D. Ellison, S. C. Clifford, and R. Versteeg. 2008. Integrated genomics identifies five medulloblastoma subtypes with distinct genetic profiles, pathway signatures and clinicopathological features. *PLoS One* 3:e3088.
7. Northcott, P. A., A. Korshunov, H. Witt, T. Hielscher, C. G. Eberhart, S. Mack, E. Bouffet, S. C. Clifford, C. E. Hawkins, P. French, J. T. Rutka, S. Pfister, and M. D. Taylor. 2011. Medulloblastoma comprises four distinct molecular variants. *J Clin Oncol* 29:1408-1414.
8. Cho, Y. J., A. Tsherniak, P. Tamayo, S. Santagata, A. Ligon, H. Greulich, R. Berhoukim, V. Amani, L. Goumnerova, C. G. Eberhart, C. C. Lau, J. M. Olson, R. J. Gilbertson, A. Gajjar, O. Delattre, M. Kool, K. Ligon, M. Meyerson, J. P. Mesirov, and

- S. L. Pomeroy. 2011. Integrative genomic analysis of medulloblastoma identifies a molecular subgroup that drives poor clinical outcome. *J Clin Oncol* 29:1424-1430.
9. Hatten, M. E., and M. F. Roussel. 2011. Development and cancer of the cerebellum. *Trends Neurosci* 34:134-142.
 10. Ramaswamy, V., P. A. Northcott, and M. D. Taylor. 2011. FISH and chips: the recipe for improved prognostication and outcomes for children with medulloblastoma. *Cancer Genet* 204:577-588.
 11. Wang, V. Y., and H. Y. Zoghbi. 2001. Genetic regulation of cerebellar development. *Nat Rev Neurosci* 2:484-491.
 12. Roussel, M. F., and M. E. Hatten. 2011. Cerebellum development and medulloblastoma. *Curr Top Dev Biol* 94:235-282.
 13. Ruiz i Altaba, A., V. Palma, and N. Dahmane. 2002. Hedgehog-Gli signalling and the growth of the brain. *Nat Rev Neurosci* 3:24-33.
 14. Wetmore, C., D. E. Eberhart, and T. Curran. 2001. Loss of p53 but not ARF accelerates medulloblastoma in mice heterozygous for patched. *Cancer Res* 61:513-516.
 15. Marino, S. 2005. Medulloblastoma: developmental mechanisms out of control. *Trends Mol Med* 11:17-22.
 16. Rossi, A., V. Caracciolo, G. Russo, K. Reiss, and A. Giordano. 2008. Medulloblastoma: from molecular pathology to therapy. *Clin Cancer Res* 14:971-976.
 17. Luger, K., A. W. Mader, R. K. Richmond, D. F. Sargent, and T. J. Richmond. 1997. Crystal structure of the nucleosome core particle at 2.8 Å resolution. *Nature* 389:251-260.
 18. Kouzarides, T. 2007. Chromatin modifications and their function. *Cell* 128:693-705.
 19. Bannister, A. J., and T. Kouzarides. 2011. Regulation of chromatin by histone modifications. *Cell Res* 21:381-395.
 20. Bannister, A. J., and T. Kouzarides. 2005. Reversing histone methylation. *Nature* 436:1103-1106.
 21. Lindsey, J. C., J. A. Anderton, M. E. Lusher, and S. C. Clifford. 2005. Epigenetic events in medulloblastoma development. *Neurosurg Focus* 19:E10.
 22. Sonnemann, J., K. S. Kumar, S. Heesch, C. Muller, C. Hartwig, M. Maass, P. Bader, and J. F. Beck. 2006. Histone deacetylase inhibitors induce cell death and enhance the

- susceptibility to ionizing radiation, etoposide, and TRAIL in medulloblastoma cells. *Int J Oncol* 28:755-766.
23. Furchert, S. E., C. Lanvers-Kaminsky, H. Juurgens, M. Jung, A. Loidl, and M. C. Fruhwald. 2007. Inhibitors of histone deacetylases as potential therapeutic tools for high-risk embryonal tumors of the nervous system of childhood. *Int J Cancer* 120:1787-1794.
 24. Canettieri, G., L. Di Marcotullio, S. Coni, A. Greco, and A. Gulino. 2010. Turning off the switch in medulloblastoma: the inhibitory acetylation of an oncogene. *Cell Cycle* 9:2047-2048.
 25. Lawinger, P., R. Venugopal, Z. S. Guo, A. Immaneni, D. Sengupta, W. Lu, L. Rastelli, A. Marin Dias Carneiro, V. Levin, G. N. Fuller, Y. Echelard, and S. Majumder. 2000. The neuronal repressor REST/NRSF is an essential regulator in medulloblastoma cells. *Nat Med* 6:826-831.
 26. Fuller, G. N., X. Su, R. E. Price, Z. R. Cohen, F. F. Lang, R. Sawaya, and S. Majumder. 2005. Many human medulloblastoma tumors overexpress repressor element-1 silencing transcription (REST)/neuron-restrictive silencer factor, which can be functionally countered by REST-VP16. *Mol Cancer Ther* 4:343-349.
 27. Su, X., V. Gopalakrishnan, D. Stearns, K. Aldape, F. F. Lang, G. Fuller, E. Snyder, C. G. Eberhart, and S. Majumder. 2006. Abnormal expression of REST/NRSF and Myc in neural stem/progenitor cells causes cerebellar tumors by blocking neuronal differentiation. *Mol Cell Biol* 26:1666-1678.
 28. Taylor, P., Fangusaro, J., Rajaram, V., Goldman, S., Helenowski, I.B., Radenecker, A. W., MacDonald, T., Hasselblatt, M., Riedemann, L., Laureano, A., Cooper, L., and Gopalakrishnan, V. 2012. REST is a Novel Prognostic Factor and Therapeutic Target for Medulloblastoma *Mol Cancer Ther*.
 29. Goodrich, L. V., L. Milenkovic, K. M. Higgins, and M. P. Scott. 1997. Altered neural cell fates and medulloblastoma in mouse patched mutants. *Science* 277:1109-1113.
 30. Huse, J. T., and E. C. Holland. 2010. Targeting brain cancer: advances in the molecular pathology of malignant glioma and medulloblastoma. *Nat Rev Cancer* 10:319-331.
 31. Hallahan, A. R., J. I. Pritchard, S. Hansen, M. Benson, J. Stoeck, B. A. Hatton, T. L. Russell, R. G. Ellenbogen, I. D. Bernstein, P. A. Beachy, and J. M. Olson. 2004. The

- SmoA1 mouse model reveals that notch signaling is critical for the growth and survival of sonic hedgehog-induced medulloblastomas. *Cancer Res* 64:7794-7800.
32. Hatton, B. A., E. H. Villavicencio, J. Pritchard, M. LeBlanc, S. Hansen, M. Ulrich, S. Ditzler, B. Pullar, M. R. Stroud, and J. M. Olson. 2010. Notch signaling is not essential in sonic hedgehog-activated medulloblastoma. *Oncogene* 29:3865-3872.
 33. Kawauchi, D., G. Robinson, T. Uziel, P. Gibson, J. Rehg, C. Gao, D. Finkelstein, C. Qu, S. Pounds, D. W. Ellison, R. J. Gilbertson, and M. F. Roussel. 2012. A mouse model of the most aggressive subgroup of human medulloblastoma. *Cancer Cell* 21:168-180.
 34. Pei, Y., C. E. Moore, J. Wang, A. K. Tewari, A. Eroshkin, Y. J. Cho, H. Witt, A. Korshunov, T. A. Read, J. L. Sun, E. M. Schmitt, C. R. Miller, A. F. Buckley, R. E. McLendon, T. F. Westbrook, P. A. Northcott, M. D. Taylor, S. M. Pfister, P. G. Febbo, and R. J. Wechsler-Reya. 2012. An animal model of MYC-driven medulloblastoma. *Cancer Cell* 21:155-167.
 35. Dakubo, G. D., C. J. Mazerolle, and V. A. Wallace. 2006. Expression of Notch and Wnt pathway components and activation of Notch signaling in medulloblastomas from heterozygous patched mice. *J Neurooncol* 79:221-227.
 36. Mueller, S., and K. K. Matthay. 2009. Neuroblastoma: biology and staging. *Curr Oncol Rep* 11:431-438.
 37. Maris, J. M. 2010. Recent advances in neuroblastoma. *N Engl J Med* 362:2202-2211.
 38. Westermarck, U. K., M. Wilhelm, A. Frenzel, and M. A. Henriksson. 2011. The MYCN oncogene and differentiation in neuroblastoma. *Semin Cancer Biol* 21:256-266.
 39. Brodeur, G. M. 2003. Neuroblastoma: biological insights into a clinical enigma. *Nat Rev Cancer* 3:203-216.
 40. Janoueix-Lerosey, I., G. Schleiermacher, E. Michels, V. Mosseri, A. Ribeiro, D. Lequin, J. Vermeulen, J. Couturier, M. Peuchmaur, A. Valent, D. Plantaz, H. Rubie, D. Valteau-Couanet, C. Thomas, V. Combaret, R. Rousseau, A. Eggert, J. Michon, F. Speleman, and O. Delattre. 2009. Overall genomic pattern is a predictor of outcome in neuroblastoma. *J Clin Oncol* 27:1026-1033.
 41. Janoueix-Lerosey, I., and O. Delattre. 2009. [ALK, a key gene in the pathogenesis of neuroblastoma]. *Med Sci (Paris)* 25:330-332.

42. Weiss, W. A., K. Aldape, G. Mohapatra, B. G. Feuerstein, and J. M. Bishop. 1997. Targeted expression of MYCN causes neuroblastoma in transgenic mice. *EMBO J* 16:2985-2995.
43. Schonherr, C., K. Ruuth, S. Kamaraj, C. L. Wang, H. L. Yang, V. Combaret, A. Djos, T. Martinsson, J. G. Christensen, R. H. Palmer, and B. Hallberg. 2012. Anaplastic Lymphoma Kinase (ALK) regulates initiation of transcription of MYCN in neuroblastoma cells. *Oncogene*.
44. Schulte, J. H., S. Lindner, A. Bohrer, J. Maurer, K. De Preter, S. Lefever, L. Heukamp, S. Schulte, J. Molenaar, R. Versteeg, T. Thor, A. Kunkele, J. Vandesompele, F. Speleman, H. Schorle, A. Eggert, and A. Schramm. 2012. MYCN and ALKF1174L are sufficient to drive neuroblastoma development from neural crest progenitor cells. *Oncogene*.
45. Maris, J. M., M. D. Hogarty, R. Bagatell, and S. L. Cohn. 2007. Neuroblastoma. *Lancet* 369:2106-2120.
46. Beckwith, J. B., and E. V. Perrin. 1963. In Situ Neuroblastomas: A Contribution to the Natural History of Neural Crest Tumors. *Am J Pathol* 43:1089-1104.
47. Huang, X., and J. P. Saint-Jeannet. 2004. Induction of the neural crest and the opportunities of life on the edge. *Dev Biol* 275:1-11.
48. Decock, A., M. Ongenaert, J. Vandesompele, and F. Speleman. 2011. Neuroblastoma epigenetics: from candidate gene approaches to genome-wide screenings. *Epigenetics* 6:962-970.
49. Chong, J. A., J. Tapia-Ramirez, S. Kim, J. J. Toledo-Aral, Y. Zheng, M. C. Boutros, Y. M. Altshuller, M. A. Frohman, S. D. Kraner, and G. Mandel. 1995. REST: a mammalian silencer protein that restricts sodium channel gene expression to neurons. *Cell* 80:949-957.
50. Mori, N., C. Schoenherr, D. J. Vandenberg, and D. J. Anderson. 1992. A common silencer element in the SCG10 and type II Na⁺ channel genes binds a factor present in nonneuronal cells but not in neuronal cells. *Neuron* 9:45-54.
51. Schoenherr, C. J., and D. J. Anderson. 1995. Silencing is golden: negative regulation in the control of neuronal gene transcription. *Curr Opin Neurobiol* 5:566-571.
52. Ballas, N., E. Battaglioli, F. Atouf, M. E. Andres, J. Chenoweth, M. E. Anderson, C. Burger, M. Moniwa, J. R. Davie, W. J. Bowers, H. J. Federoff, D. W. Rose, M. G.

- Rosenfeld, P. Brehm, and G. Mandel. 2001. Regulation of neuronal traits by a novel transcriptional complex. *Neuron* 31:353-365.
53. Chen, Z. F., A. J. Paquette, and D. J. Anderson. 1998. NRSF/REST is required in vivo for repression of multiple neuronal target genes during embryogenesis. *Nat Genet* 20:136-142.
54. Maue, R. A., S. D. Kraner, R. H. Goodman, and G. Mandel. 1990. Neuron-specific expression of the rat brain type II sodium channel gene is directed by upstream regulatory elements. *Neuron* 4:223-231.
55. Kraner, S. D., J. A. Chong, H. J. Tsay, and G. Mandel. 1992. Silencing the type II sodium channel gene: a model for neural-specific gene regulation. *Neuron* 9:37-44.
56. Wuenschell, C. W., N. Mori, and D. J. Anderson. 1990. Analysis of SCG10 gene expression in transgenic mice reveals that neural specificity is achieved through selective derepression. *Neuron* 4:595-602.
57. Li, L., T. Suzuki, N. Mori, and P. Greengard. 1993. Identification of a functional silencer element involved in neuron-specific expression of the synapsin I gene. *Proc Natl Acad Sci U S A* 90:1460-1464.
58. Ooi, L., and I. C. Wood. 2007. Chromatin crosstalk in development and disease: lessons from REST. *Nat Rev Genet* 8:544-554.
59. Guardavaccaro, D., D. Frescas, N. V. Dorrello, A. Peschiaroli, A. S. Multani, T. Cardozo, A. Lasorella, A. Iavarone, S. Chang, E. Hernando, and M. Pagano. 2008. Control of chromosome stability by the beta-TrCP-REST-Mad2 axis. *Nature* 452:365-369.
60. Westbrook, T. F., G. Hu, X. L. Ang, P. Mulligan, N. N. Pavlova, A. Liang, Y. Leng, R. Maehr, Y. Shi, J. W. Harper, and S. J. Elledge. 2008. SCFbeta-TRCP controls oncogenic transformation and neural differentiation through REST degradation. *Nature* 452:370-374.
61. Shimojo, M., J. H. Lee, and L. B. Hersh. 2001. Role of zinc finger domains of the transcription factor neuron-restrictive silencer factor/repressor element-1 silencing transcription factor in DNA binding and nuclear localization. *J Biol Chem* 276:13121-13126.

62. Lee, J. H., Y. G. Chai, and L. B. Hersh. 2000. Expression patterns of mouse repressor element-1 silencing transcription factor 4 (REST4) and its possible function in neuroblastoma. *J Mol Neurosci* 15:205-214.
63. Shimojo, M. 2006. Characterization of the nuclear targeting signal of REST/NRSF. *Neurosci Lett* 398:161-166.
64. Bruce, A. W., I. J. Donaldson, I. C. Wood, S. A. Yerbury, M. I. Sadowski, M. Chapman, B. Gottgens, and N. J. Buckley. 2004. Genome-wide analysis of repressor element 1 silencing transcription factor/neuron-restrictive silencing factor (REST/NRSF) target genes. *Proc Natl Acad Sci U S A* 101:10458-10463.
65. Johnson, D. S., A. Mortazavi, R. M. Myers, and B. Wold. 2007. Genome-wide mapping of in vivo protein-DNA interactions. *Science* 316:1497-1502.
66. Otto, S. J., S. R. McCorkle, J. Hover, C. Conaco, J. J. Han, S. Impey, G. S. Yochum, J. J. Dunn, R. H. Goodman, and G. Mandel. 2007. A new binding motif for the transcriptional repressor REST uncovers large gene networks devoted to neuronal functions. *J Neurosci* 27:6729-6739.
67. Ballas, N., C. Grunseich, D. D. Lu, J. C. Speh, and G. Mandel. 2005. REST and its corepressors mediate plasticity of neuronal gene chromatin throughout neurogenesis. *Cell* 121:645-657.
68. Ariano, P., P. Zamburlin, R. D'Alessandro, J. Meldolesi, and D. Lovisolo. 2010. Differential repression by the transcription factor REST/NRSF of the various Ca²⁺ signalling mechanisms in pheochromocytoma PC12 cells. *Cell Calcium* 47:360-368.
69. Lv, H., G. Pan, G. Zheng, X. Wu, H. Ren, Y. Liu, and J. Wen. 2010. Expression and functions of the repressor element 1 (RE-1)-silencing transcription factor (REST) in breast cancer. *J Cell Biochem* 110:968-974.
70. Kehayova, P., K. Monahan, W. Chen, and T. Maniatis. 2011. Regulatory elements required for the activation and repression of the protocadherin-alpha gene cluster. *Proc Natl Acad Sci U S A* 108:17195-17200.
71. Qureshi, I. A., and M. F. Mehler. 2009. Regulation of non-coding RNA networks in the nervous system--what's the REST of the story? *Neurosci Lett* 466:73-80.
72. Rossbach, M. 2011. Non-Coding RNAs in Neural Networks, REST-Assured. *Front Genet* 2:8.

73. Singh, S. K., M. N. Kagalwala, J. Parker-Thornburg, H. Adams, and S. Majumder. 2008. REST maintains self-renewal and pluripotency of embryonic stem cells. *Nature* 453:223-227.
74. Jorgensen, H. F., Z. F. Chen, M. Merckenschlager, and A. G. Fisher. 2009. Is REST required for ESC pluripotency? *Nature* 457:E4-5; discussion E7.
75. Watanabe, Y., S. Kameoka, V. Gopalakrishnan, K. D. Aldape, Z. Z. Pan, F. F. Lang, and S. Majumder. 2004. Conversion of myoblasts to physiologically active neuronal phenotype. *Genes Dev* 18:889-900.
76. Abramovitz, L., T. Shapira, I. Ben-Dror, V. Dror, L. Granot, T. Rousso, E. Landoy, L. Blau, G. Thiel, and L. Vardimon. 2008. Dual role of NRSF/REST in activation and repression of the glucocorticoid response. *J Biol Chem* 283:110-119.
77. Palm, K., N. Belluardo, M. Metsis, and T. Timmusk. 1998. Neuronal expression of zinc finger transcription factor REST/NRSF/XBR gene. *J Neurosci* 18:1280-1296.
78. Palm, K., M. Metsis, and T. Timmusk. 1999. Neuron-specific splicing of zinc finger transcription factor REST/NRSF/XBR is frequent in neuroblastomas and conserved in human, mouse and rat. *Brain Res Mol Brain Res* 72:30-39.
79. Tapia-Ramirez, J., B. J. Eggen, M. J. Peral-Rubio, J. J. Toledo-Aral, and G. Mandel. 1997. A single zinc finger motif in the silencing factor REST represses the neural-specific type II sodium channel promoter. *Proc Natl Acad Sci U S A* 94:1177-1182.
80. Shimojo, M. 2008. Huntingtin regulates RE1-silencing transcription factor/neuron-restrictive silencer factor (REST/NRSF) nuclear trafficking indirectly through a complex with REST/NRSF-interacting LIM domain protein (RILP) and dynactin p150 Glued. *J Biol Chem* 283:34880-34886.
81. Shimojo, M., and L. B. Hersh. 2003. REST/NRSF-interacting LIM domain protein, a putative nuclear translocation receptor. *Mol Cell Biol* 23:9025-9031.
82. Abderrahmani, A., G. Niederhauser, V. Lenain, R. Regazzi, and G. Waeber. 2005. The hairy and enhancer of split 1 is a negative regulator of the repressor element silencer transcription factor. *FEBS Lett* 579:6199-6204.
83. Nishihara, S., L. Tsuda, and T. Ogura. 2003. The canonical Wnt pathway directly regulates NRSF/REST expression in chick spinal cord. *Biochem Biophys Res Commun* 311:55-63.

84. Ravanpay, A. C., S. J. Hansen, and J. M. Olson. 2010. Transcriptional inhibition of REST by NeuroD2 during neuronal differentiation. *Mol Cell Neurosci* 44:178-189.
85. Tomasoni, R., S. Negrini, S. Fiordaliso, A. Klajn, T. Tkatch, A. Mondino, J. Meldolesi, and R. D'Alessandro. 2011. A signaling loop of REST, TSC2 and beta-catenin governs proliferation and function of PC12 neural cells. *J Cell Sci* 124:3174-3186.
86. Calarco, J. A., S. Superina, D. O'Hanlon, M. Gabut, B. Raj, Q. Pan, U. Skalska, L. Clarke, D. Gelinias, D. van der Kooy, M. Zhen, B. Ciruna, and B. J. Blencowe. 2009. Regulation of vertebrate nervous system alternative splicing and development by an SR-related protein. *Cell* 138:898-910.
87. Raj, B., D. O'Hanlon, J. P. Vessey, Q. Pan, D. Ray, N. J. Buckley, F. D. Miller, and B. J. Blencowe. 2011. Cross-regulation between an alternative splicing activator and a transcription repressor controls neurogenesis. *Mol Cell* 43:843-850.
88. D'Alessandro, R., and J. Meldolesi. 2010. In PC12 cells, expression of neurosecretion and neurite outgrowth are governed by the transcription repressor REST/NRSF. *Cell Mol Neurobiol* 30:1295-1302.
89. Yu, M., L. Cai, M. Liang, Y. Huang, H. Gao, S. Lu, J. Fei, and F. Huang. 2009. Alteration of NRSF expression exacerbating 1-methyl-4-phenyl-pyridinium ion-induced cell death of SH-SY5Y cells. *Neurosci Res* 65:236-244.
90. Coulson, J. M., J. L. Edgson, P. J. Woll, and J. P. Quinn. 2000. A splice variant of the neuron-restrictive silencer factor repressor is expressed in small cell lung cancer: a potential role in derepression of neuroendocrine genes and a useful clinical marker. *Cancer Res* 60:1840-1844.
91. Coulson, J. M. 2005. Transcriptional regulation: cancer, neurons and the REST. *Curr Biol* 15:R665-668.
92. Majumder, S. 2006. REST in good times and bad: roles in tumor suppressor and oncogenic activities. *Cell Cycle* 5:1929-1935.
93. Kitchens, D. L., E. Y. Snyder, and D. I. Gottlieb. 1994. FGF and EGF are mitogens for immortalized neural progenitors. *J Neurobiol* 25:797-807.
94. Kageyama, R., T. Ohtsuka, and K. Tomita. 2000. The bHLH gene Hes1 regulates differentiation of multiple cell types. *Mol Cells* 10:1-7.
95. Kageyama, R., T. Ohtsuka, J. Hatakeyama, and R. Ohsawa. 2005. Roles of bHLH genes in neural stem cell differentiation. *Exp Cell Res* 306:343-348.

96. Ishibashi, M., K. Moriyoshi, Y. Sasai, K. Shiota, S. Nakanishi, and R. Kageyama. 1994. Persistent expression of helix-loop-helix factor HES-1 prevents mammalian neural differentiation in the central nervous system. *EMBO J* 13:1799-1805.
97. Fan, X., I. Mikolaenko, I. Elhassan, X. Ni, Y. Wang, D. Ball, D. J. Brat, A. Perry, and C. G. Eberhart. 2004. Notch1 and notch2 have opposite effects on embryonal brain tumor growth. *Cancer Res* 64:7787-7793.
98. Julian, E., R. K. Dave, J. P. Robson, A. R. Hallahan, and B. J. Wainwright. 2010. Canonical Notch signaling is not required for the growth of Hedgehog pathway-induced medulloblastoma. *Oncogene* 29:3465-3476.
99. Ingram, W. J., K. I. McCue, T. H. Tran, A. R. Hallahan, and B. J. Wainwright. 2008. Sonic Hedgehog regulates Hes1 through a novel mechanism that is independent of canonical Notch pathway signalling. *Oncogene* 27:1489-1500.
100. Schreck, K. C., P. Taylor, L. Marchionni, V. Gopalakrishnan, E. E. Bar, N. Gaiano, and C. G. Eberhart. 2010. The Notch target Hes1 directly modulates Gli1 expression and Hedgehog signaling: a potential mechanism of therapeutic resistance. *Clin Cancer Res* 16:6060-6070.
101. Zhang, C., Z. Zhang, H. Shu, S. Liu, Y. Song, K. Qiu, and H. Yang. 2010. The modulatory effects of bHLH transcription factors with the Wnt/beta-catenin pathway on differentiation of neural progenitor cells derived from neonatal mouse anterior subventricular zone. *Brain Res* 1315:1-10.
102. Sasai, Y., R. Kageyama, Y. Tagawa, R. Shigemoto, and S. Nakanishi. 1992. Two mammalian helix-loop-helix factors structurally related to *Drosophila* hairy and Enhancer of split. *Genes Dev* 6:2620-2634.
103. Campos-Ortega, J. A. 1990. Mechanisms of a cellular decision during embryonic development of *Drosophila melanogaster*: epidermogenesis or neurogenesis. *Adv Genet* 27:403-453.
104. Campos-Ortega, J. A., and E. Knust. 1990. Molecular analysis of a cellular decision during embryonic development of *Drosophila melanogaster*: epidermogenesis or neurogenesis. *Eur J Biochem* 190:1-10.
105. Campos-Ortega, J. A., and E. Knust. 1990. Genetics of early neurogenesis in *Drosophila melanogaster*. *Annu Rev Genet* 24:387-407.

106. Davis, R. L., and D. L. Turner. 2001. Vertebrate hairy and Enhancer of split related proteins: transcriptional repressors regulating cellular differentiation and embryonic patterning. *Oncogene* 20:8342-8357.
107. Klambt, C., E. Knust, K. Tietze, and J. A. Campos-Ortega. 1989. Closely related transcripts encoded by the neurogenic gene complex enhancer of split of *Drosophila melanogaster*. *EMBO J* 8:203-210.
108. Rushlow, C. A., A. Hogan, S. M. Pinchin, K. M. Howe, M. Lardelli, and D. Ish-Horowicz. 1989. The *Drosophila* hairy protein acts in both segmentation and bristle patterning and shows homology to N-myc. *EMBO J* 8:3095-3103.
109. Kannan, S., W. Fang, G. Song, C. G. Mullighan, R. Hammit, J. McMurray, and P. A. Zweidler-McKay. 2011. Notch/HES1-mediated PARP1 activation: a cell type-specific mechanism for tumor suppression. *Blood* 117:2891-2900.
110. Ju, B. G., D. Solum, E. J. Song, K. J. Lee, D. W. Rose, C. K. Glass, and M. G. Rosenfeld. 2004. Activating the PARP-1 sensor component of the groucho/ TLE1 corepressor complex mediates a CaMKinase II δ -dependent neurogenic gene activation pathway. *Cell* 119:815-829.
111. Paroush, Z., R. L. Finley, Jr., T. Kidd, S. M. Wainwright, P. W. Ingham, R. Brent, and D. Ish-Horowicz. 1994. Groucho is required for *Drosophila* neurogenesis, segmentation, and sex determination and interacts directly with hairy-related bHLH proteins. *Cell* 79:805-815.
112. Grbavec, D., and S. Stifani. 1996. Molecular interaction between TLE1 and the carboxyl-terminal domain of HES-1 containing the WRPW motif. *Biochem Biophys Res Commun* 223:701-705.
113. Kageyama, R., and T. Ohtsuka. 1999. The Notch-Hes pathway in mammalian neural development. *Cell Res* 9:179-188.
114. Strom, A., P. Castella, J. Rockwood, J. Wagner, and M. Caudy. 1997. Mediation of NGF signaling by post-translational inhibition of HES-1, a basic helix-loop-helix repressor of neuronal differentiation. *Genes Dev* 11:3168-3181.
115. Jin, Y. H., H. Kim, H. Ki, I. Yang, N. Yang, K. Y. Lee, N. Kim, H. S. Park, and K. Kim. 2009. Beta-catenin modulates the level and transcriptional activity of Notch1/NICD through its direct interaction. *Biochim Biophys Acta* 1793:290-299.

116. Fan, X., W. Matsui, L. Khaki, D. Stearns, J. Chun, Y. M. Li, and C. G. Eberhart. 2006. Notch pathway inhibition depletes stem-like cells and blocks engraftment in embryonal brain tumors. *Cancer Res* 66:7445-7452.
117. Solecki, D. J., X. L. Liu, T. Tomoda, Y. Fang, and M. E. Hatten. 2001. Activated Notch2 signaling inhibits differentiation of cerebellar granule neuron precursors by maintaining proliferation. *Neuron* 31:557-568.
118. Takebayashi, K., Y. Sasai, Y. Sakai, T. Watanabe, S. Nakanishi, and R. Kageyama. 1994. Structure, chromosomal locus, and promoter analysis of the gene encoding the mouse helix-loop-helix factor HES-1. Negative autoregulation through the multiple N box elements. *J Biol Chem* 269:5150-5156.
119. Hirata, H., S. Yoshiura, T. Ohtsuka, Y. Bessho, T. Harada, K. Yoshikawa, and R. Kageyama. 2002. Oscillatory expression of the bHLH factor Hes1 regulated by a negative feedback loop. *Science* 298:840-843.
120. Julian, E., A. R. Hallahan, and B. J. Wainwright. 2010. RBP-J is not required for granule neuron progenitor development and medulloblastoma initiated by Hedgehog pathway activation in the external germinal layer. *Neural Dev* 5:27.
121. Murata, K., M. Hattori, N. Hirai, Y. Shinozuka, H. Hirata, R. Kageyama, T. Sakai, and N. Minato. 2005. Hes1 directly controls cell proliferation through the transcriptional repression of p27Kip1. *Mol Cell Biol* 25:4262-4271.
122. Pear, W. S., J. P. Miller, L. Xu, J. C. Pui, B. Soffer, R. C. Quackenbush, A. M. Pendergast, R. Bronson, J. C. Aster, M. L. Scott, and D. Baltimore. 1998. Efficient and rapid induction of a chronic myelogenous leukemia-like myeloproliferative disease in mice receiving P210 bcr/abl-transduced bone marrow. *Blood* 92:3780-3792.
123. Schoch, S., G. Cibelli, and G. Thiel. 1996. Neuron-specific gene expression of synapsin I. Major role of a negative regulatory mechanism. *J Biol Chem* 271:3317-3323.
124. Singh, A., C. Rokes, M. Gireud, S. Fletcher, J. Baumgartner, G. Fuller, J. Stewart, P. Zage, and V. Gopalakrishnan. 2011. Retinoic acid induces REST degradation and neuronal differentiation by modulating the expression of SCF(beta-TRCP) in neuroblastoma cells. *Cancer* 117:5189-5202.
125. Richards, K. N., P. A. Zweidler-McKay, N. Van Roy, F. Speleman, J. Trevino, P. E. Zage, and D. P. Hughes. 2010. Signaling of ERBB receptor tyrosine kinases promotes neuroblastoma growth in vitro and in vivo. *Cancer* 116:3233-3243.

126. Preis, P. N., H. Saya, L. Nadasdi, G. Hochhaus, V. Levin, and W. Sadee. 1988. Neuronal cell differentiation of human neuroblastoma cells by retinoic acid plus herbimycin A. *Cancer Res* 48:6530-6534.
127. Cohen, P. S., J. J. Letterio, C. Gaetano, J. Chan, K. Matsumoto, M. B. Sporn, and C. J. Thiele. 1995. Induction of transforming growth factor beta 1 and its receptors during all-trans-retinoic acid (RA) treatment of RA-responsive human neuroblastoma cell lines. *Cancer Res* 55:2380-2386.

VITA

Akanksha Singh was born in New Delhi, India on January 24, 1985, the Daughter of Jitendra Singh and Indira Singh. After completing her work at L.V. Hightower High School, Missouri City, Texas in 2002, she entered The University of Saint Thomas in Houston, Texas. She received the degree of Bachelor of Arts with a major in biology and psychology in May, 2007. In August of 2007 she entered The University of Texas Health Science Center at Houston Graduate School of Biomedical Sciences.

Permanent address:

1014 Hayden Creek Drive

Sugar Land, Texas 77479